ABSTRACT

Title of Document: THE EFFECT OF TRIFOLIRHIZIN AND RESVERATROL ON HUMAN PROSTATE CELLS

Junjun Zhang, Ph.D., 2008

Directed By: Professor David Kai Y. Lei, Department of Nutrition and Food Science

Trifolirhizin is a potent polycyclic flavonoid with anticarcinogenic effects. The treatment of 25 μM trifolirhizin in human derived prostate cancer LNCaP cells for 6 days decreased cell proliferation by 40%. Higher dosages caused the proliferation inhibition effect to be manifested in as early as 3 days. Another prostate cancer cell line, PC-3, was not affected by trifolirhizin till 125 μM resulting in about 45 % reduction in cell proliferation after 4 to 6 days of incubation. Most importantly, for normal human prostate epithelial (NHPrE) cells, trifolirhizin was effective only at the highest concentration of 200 μM. The proliferation inhibition in trifolirhizin-treated LNCaP and PC-3 cells was associated with cell cycle arrest at the G0/G1 and G2/M phase, respectively. Moreover, the expression of cyclin E was unchanged but that of cyclin D1, p53, p21 and p-Rb was suppressed in 50 μM trifolirhizin-treated LNCaP cells.

To evaluate the influence of resveratrol on cellular zinc status, NHPrE cells were treated with 6 levels of resveratrol (0, 0.5, 1, 2.5, 5 and 10 μM) and 4 levels of

zinc [0, 4, 16 and 32 μM representing zinc deficient (ZD), zinc normal (ZN), zinc adequate (ZA) and zinc supplemented (ZS), respectively]. Among each zinc treatment, a progressive reduction in cell growth or increase in cellular total zinc was observed with increases of resveratrol from 2.5, 5 and 10 μM or from 5 and 10 μM, respectively. In ZS cells a much higher increase in cellular total zinc was observed as early as 1 μM resveratrol. The resveratrol (10 μM) induced G2/M arrest was found to be responsible for the depressed cell proliferation. An *in vitro* experiment demonstrated complex formation between resveratrol and zinc ion. Fluorescent spectrofluorimetry and microscope imaging revealed that intracellular free labile zinc decreased in resveratrol-treated ZD and ZN NHPrE cells but increased in high zinc (ZA and ZS) cells. Furthermore, increases in cellular zinc status induced reactive oxygen species (ROS) generation as well as senescence in cells treated with 2.5 or 10 μM resveratrol, especially in ZA and ZS cells. Thus, increase in free labile zinc may induce ROS and senescence.

# THE EFFECT OF TROFOLIRHIZIN AND RESVERATROL ON HUMAN PROSTATE CELLS

By

Junjun Zhang

Dissertation submitted to the Faculty of the Graduate School of the
University of Maryland, College Park, in partial fulfillment
of the requirements for the degree of
Doctor of Philosophy
2008

Advisory Committee:
Professor David Kai Y. Lei, Chair
Professor Robert T. Jackson
Professor Liangli (Lucy) Yu
Professor Wen-Hsing Cheng
Professor Yang Tao

# Acknowledgements

First of all, I sincerely thank my advisor, Prof. David K. Y. Lei for offering me the most precious experience in my career. During the past 3 years, he has never stopped giving me his greatest support and invaluable instruction on my research. His magnificent personality, precise scientific thinking and dedicative spirit impress me deeply and will be a model I look up to for the rest of my life. For me to say that I am greatly grateful to have him as my advisor is a definite understatement.

Secondly, I would like to express my appreciation to the other members of my dissertation committee, Prof. Robert T. Jackson, Prof. Liangli (Lucy) Yu, Prof. Wen-Hsing Cheng and Prof. Yang Tao for their insightful advice and comments. Especially, I thank Prof. Yu for providing the trifolirhizin samples and Dr. Thomas Wang from USDA for letting me use his lab and teaching me the quantitative real-time PCR technology.

My heartfelt thanks go to Dr. Norberta Schoene and Mrs. Noella Bryden from USDA for their technical assistance on flow cytometry and atomic absorption spectrophotometry for zinc analysis. Ms. Min Wu, a Ph.D. student in Dr. Cheng's lab, also earns my special gratitude for helping me with most of the tedious and repetitive work in the resveratrol project.

I am deeply grateful to my wife Mrs. Yuan Zhou, who gave up so much accompanying me here in the USA over the last 3 years and provided me with endless spiritual encouragement and delicate care. Without her, I would have never been able to finish my Ph.D. so smoothly.

Lastly, I would like to thank many friends and the staff in our department for their incessant concern and support. I really enjoy the time I spent with them, which will be one of the most unforgettable recollections in my life.

# Table of Contents

# List of Tables

**CHPTER II**



**CHAPTER III**

# List of Figures

# CHAPTER I: INTRODUCTION

## *1.1 General Introduction*

Nature produces a large pool of organic natural products including polyketides, terpenoids, amino acids, proteins, carbohydrates, lipids, nucleic acid bases, RNA and DNA. These materials, which are derived from a variety of living creatures such as plants, animals, marine organisms and microorganisms (Mukherjee et al., 2001), reflect directly on the impact of evolution on the self-defense system employed by living creatures to repel or destroy their predators or archenemies and represent an enormous resource for medical treatments. Since most plants have limited mobility, the chemical diversity has helped them develop sophisticated defensive mechanisms including delicate chemical arsenal of toxic substances, such as terpenes and alkaloids, that exert growth inhibition effect on other plants and keep predators away (da Rocha et al., 2001). Plant based natural products have been used for traditional medicine worldwide ever since ancient eras. Even today, although a large portion of drugs are synthesized or processed by medicinal chemistry, drugs derived from plant based natural products continue to contribute significantly to modern medication.

This dissertation includes results from two projects concerning two phytochemicals originated from plants with potential beneficial effect for human health, trifolirhizin and resveratrol, will be presented. The trifolirhizin project was mainly focused on elucidating the anticancer mechanism of this phytochemical. The effect of trifolirhizin on cell cycle progression, expression of tumor suppressor genes

and apoptosis induction on human prostate cancer cell lines as well as on normal prostate cells in primary cultures was examined. Data generated from this project will contribute to the understanding of the molecular mechanism(s) of trifolirhzin. Specifically the results may aid in the discovery of new effective compounds as potential anticancer chemopreventive and chemotherapeutic agents of plant origin.

The resveratrol project was initiated in response to a large volume of reports on the health-promoting effect but lack of data on undesired aspects of resveratrol, specifically, the prooxidant activity coming from its interaction with divalent metal ion, e.g. Cu. The NHPrE cells were selected as our model system because they represent normal prostate tissue and accumulate high levels of zinc. Data generated will not only contribute to the development of biomarkers for the measurement of health outcomes of the bioactive resveratrol, together with its interactions with the essential trace metal, zinc, but also aid in providing updated information for the setting of dietary reference intakes for resveratrol and zinc, as well as in the design of clinical studies for further exploration of the interaction between resveratrol and zinc in human subjects.

## *1.2 References*

**da Rocha, A. B., R. M. Lopes, & G. Schwartsmann.** (**2001).** Natural products in anticancer therapy. *Curr Opin Pharmacol* **1**:364-369.

**Mukherjee, A. K., S. Basu, N. Sarkar, & A. C. Ghosh.** (**2001).** Advances in cancer therapy with plant based natural products. *Curr Med Chem* **8**:1467-1486.

# CHAPTER II: LITERATURE REVIEW

## *2.1 Prostate and Prostate Cancer*

The prostate is a sexual organ comprised of branched glands, with ducts lined by secretory epithelial cells and basal cells (McNeal, 1988). The major function of prostate in human body is to produce seminal fluid to facilitate sperm motility. There are four major zones within the normal prostate: the peripheral zone, which constitutes about 70% of glandular tissue, the central zone (20%), the transition zone (5%) and the anterior fibromuscular stroma (5%) (McNeal, 1981). Prostate carcinoma most commonly develops in the peripheral zone (McNeal et al., 1988).

In the United States, prostate cancer is the second leading cause of cancer-related deaths in men (Jemal et al., 2006). More than 10% of men over the age of 65 are diagnosed with prostate cancer (Bosland et al., 2002; Jemal et al., 2006). Morbidities are mainly caused by the cancer cell progression from androgen-dependent state to androgen-independent state, which fails to respond to hormone ablation therapy (Dong, 2006; Kopper and Timar, 2005; Tang and Porter, 1997; Denmeade et al., 1996). Several key regulatory genes in the cellular program that determine cell proliferation, programmed cell death and cellular processes against environmental agents including GSTP1, PTEN, p53 and androgen receptor (AR) have been found to be associated with prostate cancer development (Dong, 2006; Kopper and Timar, 2005; Simard et al., 2003). As there are only few options in surgery and chemotherapy, identification and development of alternative chemopreventive and chemotherapeutic strategies are in great need.

## *2.2 Cell Cycle Progression, Apoptosis and Cancer*

Deregulation of cell cycle and destruction of normal cellular proliferation can lead to uncontrolled cell proliferation and eventually cancer. Cellular cell cycle or cell division cycle is referred to as a series of events in eukaryotic cells taking place between one division and the next. Generally, human cell cycle consists of four phases including G1, S, G2, and M. When there is cell proliferation, cell enters G1 phase during which new nucleosides and proteins are synthesized for the preparation of DNA synthesis that usually occurs in the S phase, a phase following G1. A cell at G1 phase can either proceed to S phase smoothly with a green signal from a molecular surveillance system at the checkpoint between G1 and S or enter a state of quiescence, G0 phase, where cell division has temporarily or semi-permanently stopped and the cell carries out its ordinary role for the organism. The next phase, G2 phase, follows successful completion of DNA synthesis and chromosomal replication, and then mainly focuses on preparing other structures imperative for mitosis, the M phase, where two daughter cells are produced. Between the G2 and M phase, the G2/M checkpoint which monitors cellular fitness of proceeding to enter mitosis, prevents cells with damaged DNA from carrying out mitosis, and provides an opportunity for DNA repair and puts a stop to the proliferation of genetically damaged cells (Morgan, 2007; Lodish et al., 2004).

Apoptosis, also known as programmed cell death, plays a vital role in the regulation of cellular activities in eukaryotes and is highly conserved in evolution (Wyllie et al., 1980). Basically, cells undergoing apoptosis exhibit phenomena including reduced cell volume, condensed chromatin, DNA fragmentation, loss of

membrane integrity and generation of apoptotic bodies (Van and Van Den, 2002). There are two major apoptotic pathways: the extrinsic pathway that favors the activation of the TNA/Fas death receptor family and involves caspases 8 as a downstream signal mediator and the intrinsic pathway involving the mitochondria and caspases 9. The caspase proteins, the major executioners of this process, are generally considered imperative in either pathway of apoptosis (Nicholson, 1999). Disturbance of apoptosis, especially the interruption of the expression of genes involved in apoptosis regulation, is highly related to cancer occurrence.

Cancer begins to initiate when normal cells, supposed to differentiate into various specialized subsets required for specific tissue function or chemical production after a period of proliferation, are mutated or damaged genetically. These cells escape from the systematic surveillance, survive the programmed cell death and proliferate inappropriately without any control. Since many cancer cell lines are resistant to cell death, apoptosis induction has recently become a popular idea in cancer treatment. Many anticancer drugs used clinically in chemotherapy nowadays have been demonstrated to share a common anticancer mechanism of cell cycle inhibition or apoptosis induction.

## *2.3 Zinc*

Zinc is an integral component of a wide variety of functional proteins such as enzymes and transcription factors, where it exerts specific actions over a wide range of physiological processes such as growth, development, and functioning of the endocrine, immune, and nervous systems (Prasad, 1983; Vallee and Falchuk, 1993; Wallwork and Sandstead, 1993), and may contribute to the development of tumors.

Epidemiological studies have reported dietary zinc deficiency as a factor strongly associated with an increased incidence of esophageal carcinoma in men (Barch, 1989). Concentrations of tissue copper and zinc, as well as copper/zinc ratio are increased in human pancreatic cancer from 1.40 to 2.70 (Ebadi and Swanson, 1988). In addition, serum zinc levels were shown to be low and urinary zinc excretion to be high in patients with significantly reduced and increased, respectively, in patients with bronchial carcinoma as abnormal zinc metabolism. Interestingly, the inductions of certain types of cancer including esophagus, liver, kidney, and small intestine cancer by known carcinogens have been found to be enhanced by zinc deficiency (Fong et al., 1978). Moreover, reductions of zinc status may promote apoptosis in certain cell types (Franker and Telford, 1997) and depress G1/S cell type progression in HepG2 cells (Cui et al., 2002). In contrast, supplementation of zinc has been shown to depressed G2/M progression in normal human bronchial epoithelial cells (Shih et al., 2006). Similarly, G2/M arrest has been observed in zinc supplemented human prostate carcinoma cell lines, LNCaP (p53+/+) and PC-3 (p53-/-) cells, indicating that the impared cell cycle progression may be independent of p53, since the existence of p53 gene in these cell lines does not affect the manifestation of the cell cycle arrest effect (Liang et al., 1999). Thus zinc deficiency and supplementation may depress normal cell cycle progression and functions.

### 2.3.1 Functions of zinc in normal prostate

Prostate has been known to contain remarkably high zinc content since as early as the 1920s by Bertrand and Vladesco (1921). It was reported that normal prostate is able to accumulate 10-fold higher zinc as compared to other organs, such

as liver and kidney; and the glandular epithelial cells in the peripheral zone of prostate accumulate the highest levels of total intracellular zinc (Suzuki et al., 1991; Costello et al., 2004). Low zinc content in seminal plasma may cause infertility in men by mitigating the mobility of sperm (Koca et al., 2003; Pant 2003; Pant and Srivastava, 2003). The major essential functions of prostate secretary epithelial cells are accumulation of cellular zinc and secretion of zinc into the prostatic fluid by the prostate glands (Sorensen et al., 1997). The zinc-accumulating function of secretary epithelial cells has been connected to the inhibitory effect of high cellular zinc on net citrate production via Kreb cycle (Costello et al., 1997). In these cells, zinc was shown to inhibit the mitochondrial aconitase activity and prevent the oxidation of citrate accumulated in mitochodria and secreted into prostatic fluid, while in other mammalian cells, the inhibition of m-aconitase activity and citrate oxidation is lethal.

There are reports indicating that intracellular zinc levels in malignant prostate epithelial cells are 70%-80% lower than the surrounding normal epithelial cells (Zaichick et al., 1997; Feustel and Wennrich, 1984). Moreover, a strong, inverse correlation between plasma zinc levels and various prostatic diseases was reported, with 83% rise in benign prostatic hyperplasia (BPH) and 37% fall in patients with malignancy as compared to normal patients (Goel and Sankhwar, 2006). In accordance with plasma level, the whole blood zinc levels in prostate cancer patients were 25% lower than the controls (Picurelli et al., 1991; Ozmen et al., 2006).

## *2.4 Phytochemicals*

'Phytochemicals' is a term refering to as a group of bioactive, plant-derived, non-nutrient compounds linked to reducing the risk of major chronic diseases.

Phytochemicals, characterized as a highly sustainable, easily obtainable and large-scale plantable resource, became potent candidates for drug development targeting the treatment and prevention of prostate cancer. They appeared to be promising because of their chemopreventive and chemotherapeutic actions reported in epidemiologic and experimental studies (Hong and Sporn, 1997; Kucuk, 2002; Barnes, 2001).

### 2.4.1 Proposed anticancer mechanisms of dietary phytochemicals

Research on the anticancer activity of numerous phytochemicals has demonstrated that phytochemicals in common fruits, vegetable as well as medicinal plants possess complementary and overlapping mechanisms of action (Table 1). These mechanisms that have been reported include antioxidant activity and free radical scavenging; inhibition of cell proliferation, oncogene expression and signal transduction pathways; regulation of gene expression in cell differentiation and proliferation; induction of oncogene expression, cell cycle arrest and apoptosis; modulation of enzyme activities in detoxification, oxidation, and reduction; stimulation of the immune system; regulation of hormone metabolism; as well as antibacterial and antiviral effects (Liu, 2004).

**Table 1: Proposed mechanisms by which dietary phytochemicals may prevent cancer**

| |
|---|
| Antioxidant activity |
| Scavenge free radicals and reduce oxidative stress |
| Inhibition of cell proliferation |
| Induction of cell differentiation |
| Inhibition of oncogene expression |
| Induction of tumor suppress gene expression |
| Induction of cell-cycle arrest |
| Induction of apoptosis |
| Inhibition of signal transduction pathways |
| Enzyme induction and enhancing detoxification |
| Phase II enzyme |
| Glutathione peroxidase |
| Catalase |
| Superoxide dismutase |
| Enzyme inhibition |
| Phase I enzyme (block activation of carcinogens) |
| Cyclooxygenase-2 |
| Inducible nitric oxide synthase |
| Xanthine oxide |
| Enhancement of immune functions and surveillance |
| Antiangiogenesis |
| Inhibition of cell adhesion and invasion |
| Inhibition of nitrosation and nitration |
| Prevention of DNA binding |
| Regulation of steroid hormone metabolism |
| Regulation of estrogen metabolism |
| Antibacterial and antiviral effects |

*Source: Liu, 2004*

### 2.4.2 Anticancer roles of Asian phytochemicals (*In vitro* evidence)

In this section, plant natural products have been shown to exert their anticancer functions by antiproliferation, induction of apoptosis, inhibition of DNA synthesis and DNA damage. Although many phytochemicals exert their anticancer activities through multiple mechanisms, antiproliferation and induction of apoptosis appear to be a common mechanism. Nearly every effective component listed in the table 2 and 3 is cytotoxic to cancer cells in a dosage and time dependent manner to different extent in their own experimental system. Exceptions include a 60kd protein isolated from the *Acanthopanax gracilistylus* extract, which can only inhibit the proliferation of cancer cells such as MT-2, Raji, HL-60, TMK-1 and HSC-2 but not induce cell death at the highest concentration of 10μg/ml (Shan et al., 2000). In addition, several bioactive anthraquinones, of which anti-tumor activity is not mediated by cytotoxic mechanism, as exemplified by the fact that more than 75% of the CNS and colon cancer cells remained viable after 48h of treatment with the anthraquinones at their GI50 concentrations (Cichewicz et al., 2004. The broad-spectrum antiproliferative activity of these bioactive compounds is indicative of their potential as chemopreventive drug candidates.

#### *Favored apoptosis pathway: intrinsic pathway*

With all the available information about the molecular events listed in table 2 and 3, it is not difficult to find out that most of the phytochemicals included favor the intrinsic apoptosis pathway, which involves the mitochondria and caspase 9. In the intrinsic apoptosis model, a group of proto-oncogene, tumor suppressor genes and genes involved in growth and differentiation, such as p53, and the Bcl-2 superfamily

proteins, transfers signals leading to a change in mitochondria membrane permeability and the release of cytochrome c during the initial phase of apoptosis. Members of the Bcl-2 family either promote cell survival (e.g., Bcl-2 and Bcl-XL) or induce apoptosis (e.g. Bax) (Gross, 2001; Crompton, 2000). The ratio of Bax/Bcl-2 is critical for the induction of apoptosis and determines whether cells will undergo apoptosis (Reed, 1995). An increase in the Bax/Bcl-2 ratio indicates cells are stimulated to release cytochrome c from mitochondria into the cytosol, where an apoptosis complex 'apopsome' is formed by cytochrome c and Apaf-1 and then activates the caspase 9 and other execution caspases of the cascade, which turn on the irreversible apoptotic signaling pathway (Hoffman and Liebermann, 1994). However, not all the intrinsic apoptosis pathways induced by these compounds are through caspase activation. There is evidence indicating that the apoptosis induction by magnolol treatment in U937 Cells is caspase-independent and mediated by the release of AIF from mitochondria (Ikai et al., 2006). Another case of caspase-independent apoptosis was reported in trofolirhizin and maackiain treated HL-60 cells and the apoptosis was mediated by generation of active oxidants by these two compounds (Aratanechemuge et al., 2004). Whether the apoptosis was intrinsic or extrinsic still requires further experimentation. The extrinsic apoptotic pathway was also reported in a very low frequency. In one case, shikonin from Lithospermum erythrorhizon induced apoptosis in HeLa cells by activation of caspase-8, not caspase-9, which triggers the mitochondrial pathway-independent caspase cascades, leading to activation of caspase-3 and DNA fragmentation simultaneously (Wu et al., 2004). Surprisingly, in another case, the induction of apoptosis in human hepatoblastoma

cells by tetrandrine from Stephania tetrandra involved both caspases-8 and -9 activation. The findings of caspase -8 activation preceded by that of caspase-9, the release of cytochrome c, cleavage of Bid and downregulation of Bcl-XL, however, suggested that the mitochondrial pathway was primarily involved in the tetrandrine-induced apoptosis (Oh and Lee, 2003).

### *Cell cycle arrest dependency on compounds and cell types*

Interestingly, berberine can not only induce G0/G1 cell cycle arrest in human prostate cancer DU145 cells (Mantena et al., 2006), but also induce G2/M cell cycle arrest in human gastric carcinoma SNU-5 cells (Lin et al., 2006). More intriguingly, berberine treatment at the comparable dosage induced apoptosis with G0/G1 and G2/M cell cycle arrests in murine leukemia L1210 cells (Jantova et al., 2003) but exerted no cell cycle arrest effect in Ehrlich ascites carcinoma cells (Letasiova et al., 2006). These findings suggested that the berberine induction of cell cycle arrest may be dependent on cell types. Another compound, shikonin, induced G1/S blockage in A375-S2 cells through the activation of caspase 9 and a typical intrinsic apoptotic pathway (Wu et al., 2004). However, in HeLa cells, shikonin acted through the activation of caspase 8, a hallmark of extrinsic apoptotic pathway (Wu et al., 2004). The shikonin treatment can also induce apoptosis without cell cycle arrest in COLO 205 cells while exhibiting similar molecular events favoring the intrinsic apoptotic pathway (Hsu et al., 2004). Therefore, the anticancer effects of these compounds may be exerted through different mechanisms in different cell types. Even if the same natural product causes the same cell cycle arrest, the mechanism may not be the same as well. The treatment with magnolol, a compound isolated from Magnolia officinalis,

arrested the COLO-205 cells at the G0/G1 phase of the cell cycle (Lin et al., 2002). In contrast, it was not reported to influence the cell cycle in CH27 cells (Yang et al., 2003). One common finding for both studies was that magnolol was able to induce apoptosis in these two kinds of cells. Careful examination of these two papers reveals that it is possible that cell cycle arrest also exits in CH27 cells treated with magnolol but the flow cytometric periment was not carried out because these investigators focused their interests mainly on the molecular pathway of apoptosis.

From the aspect of cell types, prostate cancer cells including both androgen-unresponsive (DU-145 and PC-3) as well as androgen-responsive (LNCaP) types tend to be arrested at G1 phase when treated with ducursin (Yim et al., 2005), berberine (Mantena et al., 2006) and ginsenoside Rg3 (Liu et al., 2000). In contrast, the cell cycle arrest effects on the tsFT210 and K562 cells are more drug-dependent, showing a G0/G1 arrest with the treatment of labdane-type diterpenes (Li et al., 2005) and a G2/M arrest with the treatment of flavonoids (Li et al., 2005), although both types of compound are isolated from the same medicinal plant, Vitex trifolia.

### *With normal cells as control*

The majority of the experimental studies that we have discussed above were concentrated on the anticancer effects of these bioactive compounds on cancer cells, while lacking the cytotoxic effects on normal cells. Only a very small portion of studies have included normal cells in their experimental system to address this cytotoxic effect issue (Table 3). In 1999, Lee et al. reported that water or organic solvent extract fractions from Selaginella tamariscina exhibited significant tumoricidal effects against cultured human leukemia cells but did not affect normal

human lymphocytes (Lee et al., 1999). Recently, in a prostate cancer model, three cancer cell lines including DU145, PC-3 and LNCaP and nonneoplastic human prostate epithelial PWR-1E cells were tested against a novel anticancer agent, decursin from Angelica gigas, for its anticancer effects. For the first time, decursin (25-100 μM) treatment for 24 to 96 hours was found to strongly inhibit growth by causing a strong G1 arrest, and induce cell death in these three carcinoma cell lines. Comparatively, decursin was nontoxic to PWR-1E cells and only moderately inhibited their growth and showed slight G1 arrest. Further molecular examination revealed that there were no significant changes of the level of proteins between drug-treated and non-treated PWR-1E cells (Yim et al., 2005). Berberine from Berberis poiretii and Mahonia bealei was applied to the same cell model system and similar results were observed. The treatment of PWR-1E with berberine, under identical conditions, significantly inhibited proliferation and induced cell death associated with G1-phase cell cycle arrest in DU145, PC-1 and LNCaP cell lines, but did not affect the viability and cell cycle progression of PWR-1E cells (Mantena et al., 2006). In another study, magnolol, a hydroxylated biphenyl compound isolated from Magnolia officinalis, at very low concentrations (3-10 μM) inhibited DNA synthesis and cell growth in cultured human COLO-205 and HepG2 hepatoblastoma cells in a dose-dependent manner, but not in human untransformed cells such as keratinocytes, fibroblasts, and human umbilical vein endothelial cells (HUVEC). However, magnolol did not show any effect on cell death or cell cycle arrest in both cancer cells and normal cells, probably due to these low concentrations (Lin et al., 2002). The treatment of Maackiain and trifolirhizin, two phytochemicals from Sophora

Subprostrate, significantly induced apoptosis in leukemia HL-60 cells, whereas no induction of apoptosis was observed in normal lymphocytes treated with the same concentration. In sum, the tested compounds or extracts are selectively effective for cancer cells but not for normal cells. They exerted nontoxic and/or moderate growth inhibition effects on normal cells while significantly inhibited the growth and induced cell death in cancer cell lines.

**Table 2. Plant natural products with anticancer and cell cycle arrest effects.**

| Cancer type | Plant latin name | Cell line used | Normal cells used | Effective component | Mechanism | Molecular events | Cell cycle arrested | References |
|---|---|---|---|---|---|---|---|---|
| Human leukemia, stomach cancer squamous cell carcinoma | *Acanthopanax gracilistylus* | MT-2,HL-60 and TMK-1, HSC-2 | N/A | 60kd protein | Antiproliferation | ↓ CDK2, 4 and phosphorylated Rb | G0/G1 | (Shan et al. 2000) |
| Human prostate cancer | *Angelica gigas* | DU145, PC-3 and LNCaP | PWR-1E | Decursin | Antiproliferation and apoptosis induction | ↓ cyclin D1, CDK 2, 4 and 6; ↑ p21, p27, CDKI/CDK interaction, caspase-3, -9 and PARP | G1 | (Yim et al. 2005) |
| Gastric carcinoma | *Berberis poiretii and Mahonia bealei* | SNU-5 | N/A | Berberine | Antiproliferation, apoptosis induction and release of calcium | ↓ cyclin B, Bcl-2, ↑ p53, Wee1 and CDK1, Bax protein | G2/M | (Lin et al. 2006) |
| Human cervical cancer and murine leukemia | *Berberis poiretii and Mahonia bealei* | L1210 and HeLa | N/A | Berberine | Antiproliferation, Induction of intercalation with DNA, dsDNA damage and apoptosis | N/A | G0/G1, G2/M | (Janova et al. 2003) |
| Human prostate cancer | *Berberis poiretii and Mahonia bealei* | DU145, PC-3 and LNCaP | PWR-1E | Berberine | Antiproliferation, apoptosis induction and DNA damage | ↓ cyclin D1, D2, E, CDK 2, 4 and 6, ↑ p21, p27, p21/cdk, p27/CDK interaction, Bax/Bcl-2 ratio, destruction of mictochodria membrane and release of cytochrome c | G1 | (Mantena et al. 2006) |
| Rat glioma | *Gardenia jasminoides* | rat C6 glioma cells | N/A | Penta-acetyl geniposide, (Ac)5-GP | Antiproliferation and apoptosis induction | ↓ cyclin D1, cyclin D1/CDK 4, the phosphorylation of Rb; ↑ p53, p21, | G0/G1 | (Chang et al. 2004) |
| Human cervical cancer, leukemia and breast cancer | *Gleditsia sinensis* | Bel-7402, BGC-823, HeLa, HL-60 and MCF-7 | N/A | Gleditsioside E | Antiproliferation and apoptosis induction | N/A | G2/M | (Zhong et al. 2003) |
| Human malignant melanoma | *Lithospermum erythrorhizon* | A375-S2 | N/A | Shikonin | Antiproliferation and apoptosis induction | ↓ Bcl-2, CDK4; ↑ p53, Bax, caspase-9 activity | G1 | (Wu et al. 2004a) |
| Human cervical cancer, malignant melanoma and mouse fibrosarcoma | *Lithospermum erythrorhizon* | HeLa A375-S2 L929 | N/A | Shikonin | Antiproliferation, apoptosis induction and blockage of DNA synthesis | ↑ caspase3 and 8 activity | G1/S | (Wu et al. 2004b) |
| Human colon and liver cancer | *Magnolia officinalis* | Colo-205, HT-29, HepG2 and Hep-3B | Keratinocytes and fibroblasts HUVEC | Magnolol | Antiproliferation, apoptosis induction and inhibition of DNA synthesis | ↓ cyclin A, E and CDK 2 ; ↑ p21 and p21/CDK; stable cyclin D1 and D3, CDK 4, p27 and PCNA | G0/G1 | (Lin et al. 2002) |
| Human prostate cancer and mouse fibrosarcoma | *Panax ginseng* | LNCaP L929 | N/A | Ginsenoside Rg3 | Antiproliferation and apoptosis induction | ↓ cyclin D1 Bcl-2; ↑ p21, p27 caspase3 mRNA | G1 | (Liu et al. 2000) |
| Human breast carcinoma | *Poria cocos* | MCF-7 | N/A | Beta-glucan PCM3-II | Antiproliferation and apoptosis induction | ↓ cyclin D1 and E; ↑ Bax/Bcl-2 ratio | G1 | (Zhang et al. 2006) |
| Human leukemia, ovarian and colon cance | *Selaginella tamariscina* | U937, A2780 and HT-29 | Human lymphocytes | Water and organic solvent extracts | Antiproliferation | ↑ p53 mRNA | G1 | (Lee et al. 1999) |
| Human cervical cancer, lung adenocarcinoma and neuroblastoma | *Sinopodophyllum emodi* | HeLa, A2 and SH-SY5Y | N/A | 4DPG | Antiproliferation and apoptosis induction | Stable Bcl-2; ↑ p53 and Bax, Bax/Bcl-2 ratio | G2/M | (Zhang et al. 2005) |
| Human colon carcinoma | *Stephania tetrandra* | HT-29 | N/A | Tetradrine | Antiproliferation and apoptosis induction | ↓ E2F1; ↑ p53 and p21 | G1 | (Meng et al. 2004) |
| Mouse temperature-sensitive p34cdc2 mutant and human myeloid leukemia | *Vitex trifolia* | tsFT210 and K562 | N/A | Flavonoids | Antiproliferation and apoptosis induction | N/A | G2/M | (Li et al. 2005a) |
| Mouse temperature-sensitive p34cdc2 mutant and human myeloid leukemia | *Vitex trifolia* | tsFT210 and K562 | N/A | Labdane-type diterpenes | Antiproliferation and apoptosis induction | N/A | G0/G1 | (Li et al. 2005b) |
| Human promyelocytic leukemia and erythroleukemia | *Salvia miltiorrhiza BUNGE* | HL60 and K562 | N/A | Tanshinoni IIA | Antiproliferation, induction of apoptosis and internucleosomal DNA fragmentation | ↑ cleaved PARP increase caspase-3; stable caspase-1 | G2/M | (Sung et al. 1999) |

Note: CDK, cyclin-dependent kinase; CDKI cyclin-dependent kinase inhibitor; N/A, not applicable; PARP, poly ADP-ribose polymerase; PCNA, proliferating cell nuclear antigen; Rb, retinoblastoma protein; 4DPG, 4-Demethyl-picropodophyllotoxin 7'-o-β-D-glucopyranoside.

Table 3. Plant natural products with anticancer effects but without cell cycle arrest effects.

| Cancer type | Plant latin name | Cell line used | Effective component | Mechanism | Molecular events | References |
|---|---|---|---|---|---|---|
| Human T lymphoma and leukemia | *Atractylodes macrocephala* | Jurkat, U937, HL-60 | Methanol extract | Apoptosis induction | ↑ intracellular ROS | (Huang et al. 2005) |
| Ehrlich ascites carcinoma | *Berberis poireti and Mahonia bealei* | EAC | Berberine | Antiproliferation, induction of intercalation with DNA, dsDNA damage and apoptosis | N/A | (Letasiova et al. 2006) |
| Human lung, colon, melanoma, renal, ovarian, brain, and leukemia | *Chrysanthemum morifolium* | 60 human tumor cell lines | Taraxastanes and oleanares | Antiproliferation | N/A | (Ukiya et al. 2002) |
| Human leukemia, lung cancer, colon cancer, and melanoma | *Euphorbia kansui* | 35 cancer cell lines | Kansuiphorin A and B | Antiproliferation | N/A | (Wu et al. 1991) |
| Human promyelocytic leukemia and erythroleukemia | *Gleditsia sinensis* | HL-60 and K562 | Saponin | Antiproliferation and apoptosis induction | N/A | (Chow et al. 2003) |
| Human breast, lunt and colon cancer | *Hemerocallis fulva* | MCF-7, SF-268, NCI-H460 and HCT-116 | Anthraquinones | Antiproliferation | N/A | (Cichewicz et al. 2004) |
| Human gastric adenocarcinoma, uterus carcinoma and mouse melanoma | *Inula helenium* | MK-1, HeLa and B16F10 | Sesquiterpenes | Antiproliferation | N/A | (Konishi et al. 2002) |
| Human small cell lung cancer | *Lindera strychnifolia* | SBC-3 | Sesquiterpene lactones | Antiproliferation | N/A | (Ohno et al. 2005) |
| Human colon adenocarcinoma and promyeloid leukemia | *Lithospermum erythrorhizon* | COLO 205, HT-29 and HL-60 | Shikonin | Antiproliferation | ↓ Bcl-2 and Bcl-Xl; ↑ p53, p27 and Bad, caspase-3 and -9 | (Hsu et al. 2004) |
| Human lung squamous carcinoma | *Magnolia officinalis* | CH27, H460, H1299 and WI38 | Magnolol | Antiproliferation and caspase-independent apoptosis induction | ↓ Bcl-XL; ↑ Bad and Bcl-Xs proteins, caspase-9, -3 and -6 activity release of cytochrome c | (Yang et al. 2003) |
| Human leukemia | *Magnolia obovata.* | U937 | Magnolol | Antiproliferation and apoptosis induction | Transient ↓ of phosphorylated ERK, release of AIF, ↓ membrane potential; unchanged p38, phosphor-p38, Akt and phosphor-Akt, pan-caspase inhibitors have no effect | (Ikai et al. 2006) |
| Human hepatoma | *Paris polyphylla* | HepG2 | Polyphyllin D | Antiproliferation,and apoptosis induction | Release of cytochrom c, AIF and ROS | (Cheung et al. 2005) |
| Human breast carcinoma | *Paris polyphylla* | MCF-7 and MDA-MB-231 | Polyphyllin D | Antiproliferation,and apoptosis induction | ↑ Bax/Bcl- ratio ↓ pro-caspase-9 activity | (Lee et al. 2003a) |
| Human gastric cancer | *Pharbitis nil and Saussurea lappa* | AGS | 80% ethanol extract | Antiproliferation and apoptosis induction | ↑ P53, P21, Bax and cleaved caspase-3 activity, stable Bcl-2 | (Ko et al. 2004) |
| Human promyeloid leukemia | *Pheilodendron amurense and Cynomorium songaricum* | HL-60 | 70% ethanol extract | Antiproliferation and apoptosis induction | ↑ caspase-3 activity | (Nishida et al. 2003) |
| Human rectal colon and liver cancer, | *Platycodon grandiflorum* | HT-29, HRT-18 and HepG2 | Petroleum ether extract | Antiproliferation | N/A | (Lee et al. 2004) |
| Human colon, cervix, liver and stomach cancer | *Polyporus umbellatus* | Hep3B, HT-29, Hela229 and AGS | Ergone | Antiproliferation | N/A | (Lee et al. 2005b) |
| Human sarcoma and gastric carcinoma | *Poria cocos* | Sarcoma 180, MKN-45 and SGC-7901 | Derivatives of a beta-glucan | Antiproliferation | N/A | (Wang et al. 2004) |
| Human prostate cancer | *poria cocos* | LNCaP,DU145 | Pachymic acid | Antiproliferation | ↑ p21, caspase -9 and -3 activity and Bcl-2 phosphorylation; ↓ bad phosphorylation, | (Gapter et al. 2005) |
| Mouse leukemia | *Sanguisorba officinalis* | L1210 | Methanol extract | Antiproliferation | N/A | (Goun et al. 2002) |
| Human leukemia | *Scutellaria barbata* | U937 | Methylene chloride fraction | Antiproliferation, apoptosis induction and inhibition of DNA synthesis | ↑ PARP cleaved, Bax/Bcl-2 ratio, release of cytochrome c, caspase -9 and -3 activity. | (Cha et al. 2004) |
| Human colon adenocarcinoma | *Scutellaria barbata* | LoVo | Methanol extract | Antiproliferation and apoptosis induction | Several proteins exhibit two fold changes detected by tandem mass spectrometry | (Goh et al. 2005) |
| Human lung cancer | *Scutellaria barbata* | A549 | Ethanol extract | Antiproliferation and apoptosis induction | ↑ caspase -3/7 activity, 16 genes undergo more than 5 fold change | (Yin et al. 2004) |
| Human leukemia | *Sophora Subprostrate* | HL-60 and normal human lymphocytes | Maackiain trifolirhizin and | Antiproliferation and caspase-independent apoptosis induction mediated by active oxidant through | Caspase inhibitors, Z-VAD-FMK, Ac-DEVD-CHO and Z-Asp-CH2 have no effect; N-acetyl-L-cystein suppressed DNA fragmentation | (Arataneche muge et al 2004d) |
| Human hepatoma | *Stephania tetrandra* | HepG2 | Tetrandrine | Antiproliferation and apoptosis induction | ↑ p53 ,caspases -9, -3, and -8 activity, cleavage of Bax and bid, and release of cytochrome c; ↓ Bcl-XL | (Oh and Lee 2003) |

Note: AIF, apoptosis-inducing factor; CDK, cyclin-dependent kinase; N/A, not applicable; PARP, poly ADP-ribose polymerase; Rb, retinoblastoma protein; ROS, reactive oxygen species;

### 2.4.3 Anticancer roles of Asian phytochemicals (*In vivo* evidence)

Experiments in animals, especially in mice, were conducted to explore the anticancer effects of interested plant natural products (Table 4). Several compounds, including decursinol angelate and decursin from Angelica gigas (Lee et al., 2003), cordycepin from Cordyceps sinensis (Yoshikawa et al., 2004), euscaphic acid from Eriobotrya japonica (Banno et al., 2005), glycosides from Prunus persica (Fukuda et al., 2003), magnolol from Magnolia officinalis (Lin et al., 2002) and [6]-gingerol from Zingiber officinale (Park et al., 1998; Katiyar et al., 1996) have been explored for their in vivo anti-tumor activities. These compounds tested for potential biopotency seem to share the same mechanism by inhibiting skin tumor initiation and growth in the mice system. Treatment with these bioactive compounds can significantly reduce the average number of tumor bearing mice, as well as incidence of tumor formation in mouse skin when compared with the control treated only with tumor initiator and promoter. As far as the molecular basis was concerned, p21 level of the tumor cells implanted subcutaneously into nude mice was found elevated by the treatment of magnolol (Lin et al., 2002). This finding suggests the inhibition of the progression of cell cycle activity was involved in the magnolol induced tumor regression, which coincided with the in vitro experimental results. Therefore, the validity of the results of in vitro system in this study was supported by similar data from in vivo system.

*One agent with multiple anticancer mechanisms*

Park et al, 1998 and Katiyar et al. 1996 reported that the ethanol extract and pure compound [6]-gingerol exert their anticancer effect on mice skin papilloma by inhibition of TPA induction of epidermal ornithine decarboxylase (ODC) activity. ODC is a rate-limiting enzyme in the biosynthesis of polyamines, a prerequisite for cell proliferation, differentiation, and neoplastic transformation. The induction of ODC has been suggested to be highly correlated with tumor promotion; while the inhibition of ODC has shown promising results for screening inhibitors of tumorigenesis. However, these two studies could not establish whether the compounds inhibited the action of the tumor promoter and/or the enzymatic pathway(s). Several years later, the same group of scientists found that [6]-gingerol reduces COX-2 expression by blocking the activation of p38 MAP kinase and NFκB in TPA-stimulated mouse skin, demonstrating modulation of abnormal upregulation of these intracellular signaling molecules could be the mechanism of chemopreventive activity exerted by some phytochemicals (Kim et al., 2005). Interestingly, in another study, [6]-gingerol was shown to inhibit the sprouting of endothelial cells in the rat aorta *ex vivo* and formation of new blood vessel in the mouse cornea in response to VEGF, as well as reduce the number of lung metastasis in mice receiving i.v. injection of B16F10 melanoma cells, suggesting strong anti-angiogenic activity may be employed in the treatment of tumors and other angiogenesis-dependent diseases (Kim et al., 2005). The evidence cited above along with the ones in the in vitro experiments about [6]-gingerol suggest that one chemopreventive agent may exert its anticancer activity in different organs or cell

types through different mechanisms, which may be highly specifc to particular cell type.

**Table 4. *In vivo* anticancer effects of Plant natural products.**

| Cancer type | Plant latin name | Model | Effective component | Mechanism | Molecular events | References |
|---|---|---|---|---|---|---|
| Sarcoma | Angelica gigas | ICR mice | Decursinol Angelate and Decursin | Inhibition of tumor growth and initiation | N/A | (Lee et al. 2003) |
| Mouse melanoma | Cordyceps sinensis | C57BL/6Cr mice | Cordycepin | Inhibition of tumor growth and initiation | N/A | (Yoshikawa et al. 2004) |
| Mouse skin papilloma | Eriobotrya japonica | ICR mice | Euscaphic acid | Inhibition of tumor growth and initiation | N/A | (Banno et al. 2005) |
| COLO-205 subcutaneous injection | Magnolia officinalis | Nude mice | Magnolol | Inhibition of tumor growth | ↑ p21 | (Lin et al. 2002) |
| Mouse skin papilloma | Prunus persica | ICR mice | Glycosides | Inhibition of tumor growth and initiation | N/A | (Fukuda et al. 2003) |
| Mouse skin papilloma | Zingiber officinale | ICR mice | [6]-gingerol | inhibition of tumor growth and initiation | Inhibition of epidermal ODC | (Park et al. 1998) |
| Mouse skin papilloma | Zingiber officinale | SENCAR mice | Ethanol extract | Inhibition of tumor growth and initiation | Inhibition of epidermal ODC, cycloxygenase and lipoxygenase activities | (Katiyar et al. 1996) |
| Mouse melanoma | Zingiber officinale | C57BL/6 mice | [6]-gingerol | Inhibition of angiogenesis | N/A | (Kim et al. 2005a) |
| N/A | Zingiber officinale | ICR mice | [6]-gingerol | Inhibition of TPA-induced COX-2 expression by blocking the p38 MAP kinase-NF-κB signaling pathway | ↓TPA induced COX-2, NF-κB, p65, pIκBα, p-p65-(Ser-536) total p38, p-p38, p-ATF2 | (Kim et al. 2005b) |

Note: ICR, Institute of Cancer Research; N/A, not applicable; ODC, ornithine decarboxylase; TPA, 12-*O*-tetradecanoylphorbol-13 acetate.

### 2.4.4 A proposed molecular model for Asian phytochemicals

Despite the diversity of compounds, extracts and medicinal plants discussed above, a scrutinized examination of the molecular events involved in the anticancer actions exerted by these materials reveals a common pattern (Figure 1) that accounts for the similarity exhibited in the functionary mechanisms. Although there might be slight divergence or incompleteness in some cases, in general, treatment of various cancer cells with these natural plant products markedly elevated the p53 expression. On one hand, the increase in p53 caused decrease of cyclins and CDKs, increase of expression of CDK inhibitor p21 and p27 as well as enhanced CDK/CDK inhibitor interaction, resulting in cell cycle arrest. On the other hand, the elevated p53 decreased mitochondrial membrane potential; and promoted cytochrome c release by generating reactive oxygen species (ROS) and elevating the Bax/Bcl-2 ratio; as well as further activated caspase 9 and downstream caspase cascade leading to intrinsic apoptosis. Cautions must be applied about the pivot role of p53 in this model. There has been evidence indicating that p21 can function as a tumor suppressor in a p53 independent manner (Chen et al., 2004), suggesting p53 may not be the only regulator of these CDK inhibitors.

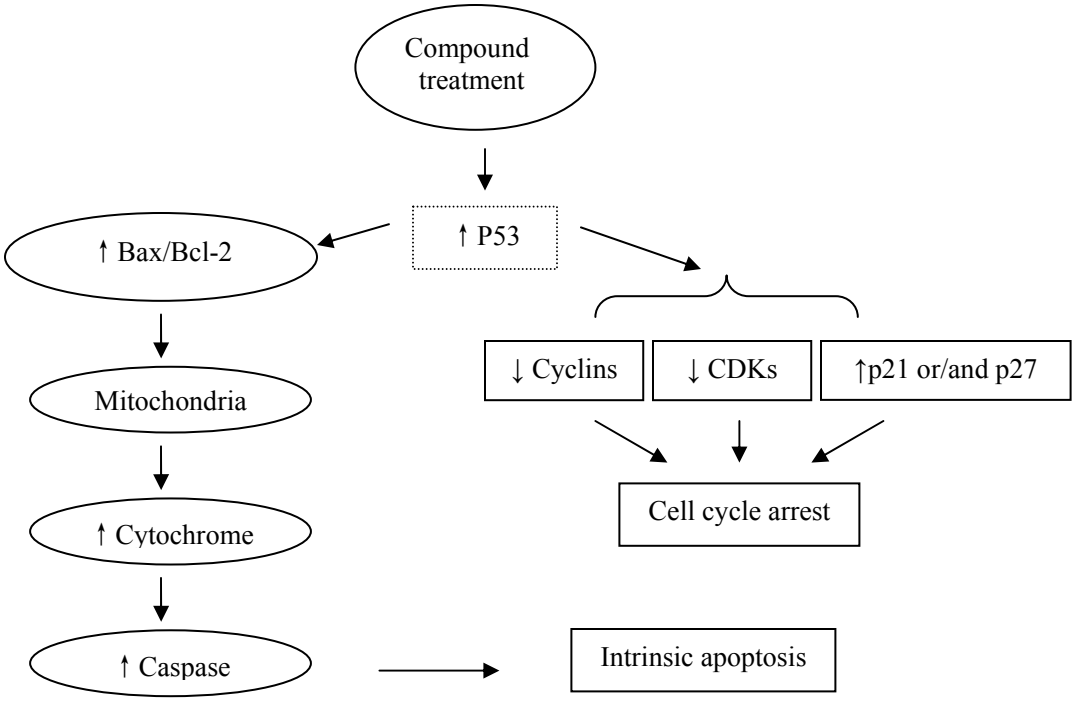


**Figure 1. Proposed anticancer mechanism of Asian plant natural products.** Dotted square represents signal transitions that might be by-passed. CDK, cyclin-dependent kinase.

## *2.5 Trifolirhizin*

Trifolirhzin is a naturally occurring polycyclic flavonoid in Sophorae Radix, derived from the roots of *Sophora flavescens*, a traditional Asian medicinal plant that has been used as a diuretic, stomachic, antipyretic, and anthelmintic for centuries (Zhao and Xiao, 2006). Although alkaloids and flavonoids from *Sophora flavescens* have exhibited a wide spectrum of antitumoral effects (Zhang et al., 2001; Sun et al., 2007; Han et al., 2007), the research on the application of trifolirhizin on cancer prevention and treatment was not well documented.

### 2.5.1 Anticancer activity of trifolirhizin

Trifolirhizin has been shown to inhibit cell proliferation of several tumor cell lines, which include A549 (non small cell lung), SK-OV-3 (ovary), SK-MEL-2 (skin), XF498 (central nerve system) and HCT-15 (colon) with the ED50 from 33.6-84.8 μM (Ryu et al., 1997). In human promyelotic HL-60 leukemia cells, trifolirhizin exerts its anticancer activity by growth inhibition and apoptosis induction mediated by change in oxidation stress in a concentration and time dependent manner (Aratanechemuge et al., 2004). A recent article reported trifolirhizin also possess tyrosinase inhibitory activity and can markedly inhibit (>50%) tyrosinase-dependent melanin biosynthesis at 50 μM in cultured B16 melanoma cells (Hyun et al., 2008). However, most of these reports did not contrast the effects of trifolirhizin on cancer cell lines and on their respective normal human cells in primary culture.

## *2.6 Resveratrol*

Resveratrol (3, 4', 5-trihydroxystilbene) is a phytoalexin synthesized in the fruits of a wide variety of plants (which include grapes, peanuts and mulberries) in response to environmental stress, injury, UV irradiation, and fungal infection (Hammerschmidt, 1999). The pioneering work of Hain et al. 1993 demonstrated that resistance to Botrytis cinerea infection was found to be enhanced in transgenic tobacco plant with the addition of stilbene synthase genes from grapevine. Resveratrol is also the active compound found in the roots of Polygonum species for the preparation of "kojokon", a traditional Asian medicine for the treatment of several diseases, in particular, lipid disorders (Kimura et al., 1983; Kimura et al., 1985). In the grapevine, resveratrol is synthesized as a trans-isomer mainly at the skin of grape berries and is found at much higher levels in red than white wines (Jeandet et al., 1991; Jeandet et al., 1993). Red wine contains 1 to 10 mg of resveratrol per L (4 to 40 μM) (Goldberg et al., 1996). In the US and Europe, resveratrol is commercially available as a nutraceutical, ranging from 50 μg to 100 mg per dosage. Oral intakes of resveratrol at 50 mg/kg body weight in rats can attain plasma resveratrol concentration of as high as 10 μM (Marier et al., 2002). A recent human study reported single dose intakes of up to 5 gram of resveratrol resulted in peak plasma level of 2.4 μM at 1.5 h post-dose (Boocock et al., 2007). Moreover, peak levels of two monoglucuronides and resveratrol-3-sulfate were 3- and 8-fold higher, respectively. These levels are close to the systemic concentration of about 5 μM, suggested by mechanistic in vitro cellular studies, to be required to elicit bio-activities relevant to chemoprevention (Gescher and Steward, 2003; Clement et al., 1998);

Delmas et al., 2002; Jang et al., 1997; Sale et al., 2005; Soleas et al., 2001). However, concentrations needed to elicit bioactivities in studies in vitro may only be a rough estimate of levels required for efficacy in vivo. Thus, future human studies are needed to establish if repeated or continuous dosing schedules may attain higher systemic concentrations of resveratrol and if the glucocuronide and sulfate metabolites, which are abundantly synthesized after resveratrol consumption, may possess bioactivities by themselves.

The interest in resveratrol was initiated by the "French paradox", the relatively low prevalence of coronary heart disease in Southern France, despite high dietary saturated fat intake (Renaud and de, 1993). This finding is correlated with the region's moderate intake of red wine that contains resveratrol, which has been identified as the major component responsible for the health benefits. Relevant to its widely considered cardiovascular protective properties, resveratrol has been shown to exert a number of anti-inflammatory (Jang et al., 1997), antiangiogenic (Cao et al., 2005; Tseng et al., 2004) and anti-mutagenic (Uenobe et al., 1997) effects, as well as to function as an estrogen receptor agonist (Gehm et al., 1997). Similar to other polyphenolic compounds, resveratrol is redox active and has been identified as an antioxidant (Li et al., 2006; Orallo, 2006) capable of quenching highly reactive free radicals via their donation of a hydrogen atom to form less reactive phenoxyl radicals (Mitchell et al., 1998). This interception of free radicals by resveratrol and phenolic compounds suppresses destructive self-propagating chain reactions, such as lipid peroxidation, thereby sparing α-tocopherol. In addition, phenolic compounds may suppress free-radical reactions via their chelation of catalytic metal ions, notably iron

and copper (Iwahashi et al., 1990; Brown et al., 1998). In deed, the inhibition of LDL oxidation by resveratrol (Frankel et al., 1993) was attributed to its ability to chelate Cu ions as well as by free radical scavenging mechanism (Belguendouz et al., 1997). Resveratrol was established as the most potent chelator of Cu but not of iron (Fe).

Studies of cells in culture and isolated subcellular models *in vitro* implicate a number of mechanisms for the pharmacologic function of resveratrol (Gescher & Steward, 2003). These mechanisms involve the induction of p53 (Soleas et al., 2001), cyclin A, cyclin B1, CDK1 and 2 (Delmas et al., 2002), and Fas/Fas ligand-mediated apoptosis (Clement et al., 1998). In addition, resveratrol has been demonstrated to suppress the expression and activity of cyclooxygenase enzymes (Sale et al., 2005), androgen actions (Bhat et al., 2001), activation of SIRT1 (Howitz et al., 2003), NF-κB (Banerjee et al., 2002), and cytochrome P-450 isoenzyme 1A1 (Ciolino and Yeh, 1999). Moreover, resveratrol has been implicated to delay the development of colonic aberrant crypt foci (Tessitore et al., 2000), esophageal (Li et al., 2006) and mammary malignancies (Bhat et al., 2001) as well as inhibit solid hepatoma growth and metastasis in rats (Miura et al., 2003). Furthermore, in the LNCaP prostate cancer cells, limited available data suggested that resveratrol inhibits growth (Hsieh and Wu, 1999), cell cycle progression into the S phase, and DNA synthesis (Kuwajerwala et al., 2002), as well as increases apoptosis (Lin et al., 2002). The inhibitory effect of resveratrol on cell growth may be due to the associated increases in p53 expression and serine phosphorylation of p53 (Narayanan et al., 2003). Thus, the activation of p53 dependent pathway may contribute to the growth inhibitory effect of resveratrol. Others have found resveratrol treatment can lead to decrease in prostate-specific

antigen (PSA) (Hsieh and Wu, 1999). However, the molecular mechanisms exerted by resveratrol on these changes remain unclear. Nevertheless, in-vitro data generally support a beneficial effect for resveratrol on prostate cancer. Currently, very limited data are available on the influence of resveratrol on normal human prostate cells or other normal human cell types, which make this proposed project highly relevant and timely.

### 2.6.1 Interactions between resveratrol and Cu

Many studies have reported potential harmful pro-oxidant properties of polyphenolic compounds at high concentrations because of their ease of oxidation in the presence of metal ions. The DNA cleaving prooxidant activity of resveratrol in the presence of Cu ions was first reported by Fukuhara and Miyata, 1998. Thereafter, the mechanism of DNA cleaving prooxident activity of resveratrol was found to involve the formation of resveratrol-Cu(II) complex resulting in the reduction of Cu ions and the formation of ROS (Ahmad et al., 2000). This prooxidant activity of resveratrol was acompanied by its ability to inactivate bacteriophage λ by the DNA cleavage mechanism. Resveratrol has been shown to cause oxidative single strand breakage in DNA either alone or in the presence of transition metal ion like copper. In the chromatin, copper the most redoxactive metal ion is associated with DNA bases, particularly guanine (Kagawa et al., 1991). Resveratrol and other polyphenols have been shown to induce apoptotic cell death in various cancer cell lines but not for normal cells (Clement et al., 1998). The cytotoxic effect has been proposed to involve mobilization of copper ions and their subsequent prooxidant action. Resveratrol in the

presence of Cu (II) has been confirmed to cause DNA degradation in peripheral lymphocytes derived from human blood. Moreover, the inhibition of DNA degradation in lymphocytes by scavengers of reactive oxygen and by neocuproine, a Cu(I) specific sequester, demonstrated that the DNA breakage is induced by reactive oxygen species (ROS) derived from the reduction of Cu(II)–Cu(I) by these polyphenols (Azmi et al., 2006).

### 2.6.2 Possible interactions between resveratrol and Zn

Resveratrol has been shown to extend the lifespan of diverse species, including S. cerevisiae, C. elegans and D. melanogaster, and was found to be dependent on the Sir2 protein, which belongs to the sirtuin/Sir2 family of NAD+-dependent deacetylases (Howitz et al., 2003; Wood et al., 2004; Viswanathan et al., 2005). Seven mammalian sirtuin genes, SIRT1 to 7, have been identified and implicated in genomic stability, transcriptional regulation, mitochondrial regulation and life span extension (Blander and Guarente, 2004). They catalyse the removal of acetyl groups from lysine amino acids of histones and transcription factors (p53 and forkhead transcription factors). In mammalian cells, resveratrol induces SIRT1 expression, which modulates glucose and insulin production, fat metabolism, and cell survival (Kolthur-Seetharam et al., 2006; Frescas et al., 2005). Recently, dietary intakes of 5.2 and 22.4 mg/kg/day of resveratrol, which were considered to be feasible daily doses for humans by the reporting researchers, were shown to shift the physiology of middle-age mice on a high caloric diet towards that of mice on a standard diet as well as markedly enhanced their lifespan and insulin sensitivity (Baur

et al., 2006). In addition, reduced insulin-like growth factor-1 level as well as enhanced AMP-activated protein kasinase and PPAR-γ coactivator 1α activity were observed. The authors specified that the dosages used are feasible daily doses for human. Within the SIRT protein, a novel zinc ribbon motif that binds zinc was found to be essential for catalytic activity. Thus, an increase in zinc ion concentration would enhance enzyme activity for a pool of SIRT proteins lacking this required zinc ions. Interestingly, a recent study demonstrated that the sirtuin pathway is involved in Zn(II) toxicity in mice cortical neuron cells in culture (Cai et al., 2006). Other cellular damages that have been shown to be Zn(II) mediated may also involve the sirtuin pathway.

## *2.7 References*

**Ahmad, A., Farhan, A. S., Singh, S. & Hadi, S. M. (2000).** DNA breakage by resveratrol and Cu(II): reaction mechanism and bacteriophage inactivation. *Cancer Lett* **154,** 29-37.

**Aratanechemuge, Y., Hibasami, H., Katsuzaki, H., Imai, K. & Komiya, T. (2004).** Induction of apoptosis by maackiain and trifolirhizin (maackiain glycoside) isolated from sanzukon (Sophora Subprostrate Chen et T. Chen) in human promyelotic leukemia HL-60 cells. *Oncol Rep* **12,** 1183-1188.

**Azmi, A. S., Bhat, S. H., Hanif, S. & Hadi, S. M. (2006).** Plant polyphenols mobilize endogenous copper in human peripheral lymphocytes leading to oxidative DNA breakage: a putative mechanism for anticancer properties. *FEBS Lett* **580,** 533-538.

**Banerjee, T., Valacchi, G., Ziboh, V. A. & van, d., V (2002).** Inhibition of TNFalpha-induced cyclooxygenase-2 expression by amentoflavone through suppression of NF-kappaB activation in A549 cells. *Mol Cell Biochem* **238,** 105-110.

**Banno, N., Akihisa, T., Tokuda, H. et al. (2005).** Anti-inflammatory and antitumor-promoting effects of the triterpene acids from the leaves of Eriobotrya japonica. *Biol Pharm Bull* **28,** 1995-1999.

**Barch, D. H. (1989).** Esophageal cancer and microelements. *J Am Coll Nutr* **8,** 99-107.

**Barnes, S. (2001).** Role of phytochemicals in prevention and treatment of prostate cancer. *Epidemiol Rev* **23,** 102-105.

**Baur, J. A., Pearson, K. J., Price, N. L. et al. (2006).** Resveratrol improves health and survival of mice on a high-calorie diet. *Nature* **444,** 337-342.

**Belguendouz, L., Fremont, L. & Linard, A. (1997).** Resveratrol inhibits metal ion-dependent and independent peroxidation of porcine low-density lipoproteins. *Biochem Pharmacol* **53,** 1347-1355.

**Bhat, K. P. L., Kosmeder, J. W. & Pezzuto, J. M. (2001).** Biological effects of resveratrol. *Antioxid Redox Signal* **3,** 1041-1064.

**Blander, G. & Guarente, L. (2004).** The Sir2 family of protein deacetylases. *Annu Rev Biochem* **73,** 417-435.

**Boocock, D. J., Patel, K. R., Faust, G. E. et al. (2007).** Quantitation of trans-resveratrol and detection of its metabolites in human plasma and urine by high performance liquid chromatography. *J Chromatogr B Analyt Technol Biomed Life Sci* **848,** 182-187.

**Bosland, M. C., McCormick, D. L., Melamed, J., Walden, P. D., Zeleniuch-Jacquotte, A. & Lumey, L. H. (2002).** Chemoprevention strategies for prostate cancer. *Eur J Cancer Prev* **11 Suppl 2,** S18-S27.

**Brown, J. E., Khodr, H., Hider, R. C. & Rice-Evans, C. A. (1998).** Structural dependence of flavonoid interactions with Cu2+ ions: implications for their antioxidant properties. *Biochem J* **330 ( Pt 3),** 1173-1178.

**Cai, A. L., Zipfel, G. J. & Sheline, C. T. (2006).** Zinc neurotoxicity is dependent on intracellular NAD levels and the sirtuin pathway. *Eur J Neurosci* **24,** 2169-2176.

**Cao, Y., Fu, Z. D., Wang, F., Liu, H. Y. & Han, R. (2005).** Anti-angiogenic activity of resveratrol, a natural compound from medicinal plants. *J Asian Nat Prod Res* **7,** 205-213.

**Cha, Y. Y., Lee, E. O., Lee, H. J., Park, Y. D., Ko, S. G., Kim, D. H., Kim, H. M., Kang, I. C. & Kim, S. H. (2004).** Methylene chloride fraction of Scutellaria barbata induces apoptosis in human U937 leukemia cells via the mitochondrial signaling pathway. *Clin Chim Acta* **348,** 41-48.

**Chang, Y. C., Chou, F. P., Huang, H. P., Hsu, J. D. & Wang, C. J. (2004).** Inhibition of cell cycle progression by penta-acetyl geniposide in rat C6 glioma cells. *Toxicol Appl Pharmacol* **198,** 11-20.

**Chen, T., Turner, J., McCarthy, S., Scaltriti, M., Bettuzzi, S. & Yeatman, T. J. (2004).** Clusterin-mediated apoptosis is regulated by adenomatous polyposis coli and is p21 dependent but p53 independent. *Cancer Res* **64,** 7412-7419.

**Cheung, J. Y., Ong, R. C., Suen, Y. K., Ooi, V., Wong, H. N., Mak, T. C., Fung, K. P., Yu, B. & Kong, S. K. (2005).** Polyphyllin D is a potent apoptosis inducer in drug-resistant HepG2 cells. *Cancer Lett* **217,** 203-211.

**Chow, L. M., Chui, C. H., Tang, J. C. et al. (2003).** Gleditsia sinensis fruit extract is a potential chemotherapeutic agent in chronic and acute myelogenous leukemia. *Oncol Rep* **10,** 1601-1607.

**Cichewicz, R. H., Zhang, Y., Seeram, N. P. & Nair, M. G. (2004).** Inhibition of human tumor cell proliferation by novel anthraquinones from daylilies. *Life Sci* **74,** 1791-1799.

**Ciolino, H. P. & Yeh, G. C. (1999).** Inhibition of aryl hydrocarbon-induced cytochrome P-450 1A1 enzyme activity and CYP1A1 expression by resveratrol. *Mol Pharmacol* **56,** 760-767.

**Clement, M. V., Hirpara, J. L., Chawdhury, S. H. & Pervaiz, S. (1998).** Chemopreventive agent resveratrol, a natural product derived from grapes, triggers CD95 signaling-dependent apoptosis in human tumor cells. *Blood* **92,** 996-1002.

**Costello, L. C., Feng, P., Milon, B., Tan, M. & Franklin, R. B. (2004).** Role of zinc in the pathogenesis and treatment of prostate cancer: critical issues to resolve. *Prostate Cancer Prostatic Dis* **7,** 111-117.

**Costello, L. C., Liu, Y., Franklin, R. B. & Kennedy, M. C. (1997).** Zinc inhibition of mitochondrial aconitase and its importance in citrate metabolism of prostate epithelial cells. *J Biol Chem* **272,** 28875-28881.

**Crompton, M. (2000).** Bax, Bid and the permeabilization of the mitochondrial outer membrane in apoptosis. *Curr Opin Cell Biol* **12,** 414-419.

**Cui, L., Schoene, N. W., Zhu, L., Fanzo, J. C., Alshatwi, A. & Lei, K. Y. (2002).** Zinc depletion reduced Egr-1 and HNF-3beta expression and apolipoprotein A-I promoter activity in Hep G2 cells. *Am J Physiol Cell Physiol* **283,** C623-C630.

**da Rocha, A. B., Lopes, R. M. & Schwartsmann, G. (2001).** Natural products in anticancer therapy. *Curr Opin Pharmacol* **1,** 364-369.

**Delmas, D., Passilly-Degrace, P., Jannin, B., Cherkaoui, M. M. & Latruffe, N. (2002).** Resveratrol, a chemopreventive agent, disrupts the cell cycle control of human SW480 colorectal tumor cells. *Int J Mol Med* **10,** 193-199.

**Denmeade, S. R., Lin, X. S. & Isaacs, J. T. (1996).** Role of programmed (apoptotic) cell death during the progression and therapy for prostate cancer. *Prostate* **28,** 251-265.

**Dong, J. T. (2006).** Prevalent mutations in prostate cancer. *J Cell Biochem* **97,** 433-447.

**Ebadi, M. & Swanson, S. (1988).** The status of zinc, copper, and metallothionein in cancer patients. *Prog Clin Biol Res* **259,** 161-175.

**Feustel, A. & Wennrich, R. (1984).** Determination of the distribution of zinc and cadmium in cellular fractions of BPH, normal prostate and prostatic cancers of different histologies by atomic and laser absorption spectrometry in tissue slices. *Urol Res* **12,** 253-256.

**Fong, L. Y., Sivak, A. & Newberne, P. M. (1978).** Zinc deficiency and methylbenzylnitrosamine-induced esophageal cancer in rats. *J Natl Cancer Inst* **61,** 145-150.

**Fraker, P. J. & Telford, W. G. (1997).** A reappraisal of the role of zinc in life and death decisions of cells. *Proc Soc Exp Biol Med* **215,** 229-236.

**Frankel, E. N., Waterhouse, A. L. & Kinsella, J. E. (1993).** Inhibition of human LDL oxidation by resveratrol. *Lancet* **341,** 1103-1104.

**Frescas, D., Valenti, L. & Accili, D. (2005).** Nuclear trapping of the forkhead transcription factor FoxO1 via Sirt-dependent deacetylation promotes expression of glucogenetic genes. *J Biol Chem* **280,** 20589-20595.

**Fukuda, T., Ito, H., Mukainaka, T., Tokuda, H., Nishino, H. & Yoshida, T. (2003).** Anti-tumor promoting effect of glycosides from Prunus persica seeds. *Biol Pharm Bull* **26,** 271-273.

**Fukuhara, K. & Miyata, N. (1998).** Resveratrol as a new type of DNA-cleaving agent. *Bioorg Med Chem Lett* **8,** 3187-3192.

**Gapter, L., Wang, Z., Glinski, J. & Ng, K. Y. (2005).** Induction of apoptosis in prostate cancer cells by pachymic acid from Poria cocos. *Biochem Biophys Res Commun* **332,** 1153-1161.

**Gehm, B. D., McAndrews, J. M., Chien, P. Y. & Jameson, J. L. (1997).** Resveratrol, a polyphenolic compound found in grapes and wine, is an agonist for the estrogen receptor. *Proc Natl Acad Sci U S A* **94,** 14138-14143.

**Gescher, A. J. & Steward, W. P. (2003).** Relationship between mechanisms, bioavailibility, and preclinical chemopreventive efficacy of resveratrol: a conundrum. *Cancer Epidemiol Biomarkers Prev* **12,** 953-957.

**Goel, T. & Sankhwar, S. N. (2006).** Comparative study of zinc levels in benign and malignant lesions of the prostate. *Scand J Urol Nephrol* **40,** 108-112.

**Goh, D., Lee, Y. H. & Ong, E. S. (2005).** Inhibitory effects of a chemically standardized extract from Scutellaria barbata in human colon cancer cell lines, LoVo. *J Agric Food Chem* **53,** 8197-8204.

**Goldberg, D. M., Tsang, E., Karumanchiri, A., Diamandis, E., Soleas, G. & Ng, E. (1996).** Method to assay the concentrations of phenolic constituents of biological interest in wines. *Anal Chem* **68,** 1688-1694.

**Goun, E. A., Petrichenko, V. M., Solodnikov, S. U., Suhinina, T. V., Kline, M. A., Cunningham, G., Nguyen, C. & Miles, H. (2002).** Anticancer and antithrombin activity of Russian plants. *J Ethnopharmacol* **81,** 337-342.

**Gross, A. (2001).** BCL-2 proteins: regulators of the mitochondrial apoptotic program. *IUBMB Life* **52,** 231-236.

**Hain, R., Reif, H. J., Krause, E. et al. (1993).** Disease resistance results from foreign phytoalexin expression in a novel plant. *Nature* **361,** 153-156.

**Hammerschmidt, R. (1999).** PHYTOALEXINS: What Have We Learned After 60 Years? *Annu Rev Phytopathol* **37,** 285-306.

**Han, J., Sun, M., Cui, Y. et al. (2007).** Kushen flavonoids induce apoptosis in tumor cells by inhibition of NF-kappaB activation and multiple receptor tyrosine kinase activities. *Phytother Res* **21,** 262-268.

**Hoffman, B. & Liebermann, D. A. (1994).** Molecular controls of apoptosis: differentiation/growth arrest primary response genes, proto-oncogenes, and tumor suppressor genes as positive & negative modulators. *Oncogene* **9,** 1807-1812.

**Hong, W. K. & Sporn, M. B. (1997).** Recent advances in chemoprevention of cancer. *Science* **278,** 1073-1077.

**Howitz, K. T., Bitterman, K. J., Cohen, H. Y. et al. (2003).** Small molecule activators of sirtuins extend Saccharomyces cerevisiae lifespan. *Nature* **425,** 191-196.

**Hsieh, T. C. & Wu, J. M. (1999).** Differential effects on growth, cell cycle arrest, and induction of apoptosis by resveratrol in human prostate cancer cell lines. *Exp Cell Res* **249,** 109-115.

**Hsu, P. C., Huang, Y. T., Tsai, M. L., Wang, Y. J., Lin, J. K. & Pan, M. H. (2004).** Induction of apoptosis by shikonin through coordinative modulation of the Bcl-2 family, p27, and p53, release of cytochrome c, and sequential activation of caspases in human colorectal carcinoma cells. *J Agric Food Chem* **52,** 6330-6337.

**Huang, H. L., Chen, C. C., Yeh, C. Y. & Huang, R. L. (2005).** Reactive oxygen species mediation of baizhu-induced apoptosis in human leukemia cells. *J Ethnopharmacol* **97,** 21-29.

**Hyun, S. K., Lee, W. H., Jeong, d. M., Kim, Y. & Choi, J. S. (2008).** Inhibitory effects of kurarinol, kuraridinol, and trifolirhizin from Sophora flavescens on tyrosinase and melanin synthesis. *Biol Pharm Bull* **31,** 154-158.

**Ikai, T., Akao, Y., Nakagawa, Y., Ohguchi, K., Sakai, Y. & Nozawa, Y. (2006).** Magnolol-induced apoptosis is mediated via the intrinsic pathway with release of AIF from mitochondria in U937 cells. *Biol Pharm Bull* **29,** 2498-2501.

**Iwahashi, H., Ishii, T., Sugata, R. & Kido, R. (1990).** The effects of caffeic acid and its related catechols on hydroxyl radical formation by 3-hydroxyanthranilic acid, ferric chloride, and hydrogen peroxide. *Arch Biochem Biophys* **276,** 242-247.

**Jang, M., Cai, L., Udeani, G. O. et al. (1997).** Cancer chemopreventive activity of resveratrol, a natural product derived from grapes. *Science* **275,** 218-220.

**Jantova, S., Cipak, L., Cernakova, M. & Kost'alova, D. (2003).** Effect of berberine on proliferation, cell cycle and apoptosis in HeLa and L1210 cells. *J Pharm Pharmacol* **55,** 1143-1149.

**Jeandet, P., Bessis, R. & Gautheron, B. (1991).** The production of resveratrol (3,5,4'- trihydroxystilbene) by grape berries in different developmental stages. *Am J Enol Vitic* **42,** 41-46.

**Jeandet, P., Bessis, R., Maume, B. & Sbaghi, M. (1993).** Analysis of resveratrol in Burgundy wines. *J Wine Res* **4,** 79-85.

**Jemal, A., Siegel, R., Ward, E., Murray, T., Xu, J., Smigal, C. & Thun, M. J. (2006a).** Cancer statistics, 2006. *CA Cancer J Clin* **56,** 106-130.

**Kagawa, T. F., Geierstanger, B. H., Wang, A. H. & Ho, P. S. (1991).** Covalent modification of guanine bases in double-stranded DNA. The 1.2-A Z-DNA structure of d(CGCGCG) in the presence of CuCl2. *J Biol Chem* **266,** 20175-20184.

**Katiyar, S. K., Agarwal, R. & Mukhtar, H. (1996).** Inhibition of tumor promotion in SENCAR mouse skin by ethanol extract of Zingiber officinale rhizome. *Cancer Res* **56,** 1023-1030.

**Kim, E. C., Min, J. K., Kim, T. Y., Lee, S. J., Yang, H. O., Han, S., Kim, Y. M. & Kwon, Y. G. (2005a).** [6]-Gingerol, a pungent ingredient of ginger, inhibits angiogenesis in vitro and in vivo. *Biochem Biophys Res Commun* **335,** 300-308.

**Kim, S. O., Kundu, J. K., Shin, Y. K., Park, J. H., Cho, M. H., Kim, T. Y. & Surh, Y. J. (2005b).** [6]-Gingerol inhibits COX-2 expression by blocking the activation of p38 MAP kinase and NF-kappaB in phorbol ester-stimulated mouse skin. *Oncogene* **24,** 2558-2567.

**Kimura, Y., Ohminami, H., Okuda, H., Baba, K., Kozawa, M. & Arichi, S. (1983).** Effects of Stilbene Components of Roots of Polygonum ssp. on Liver Injury in Peroxidized Oil-fed Rats. *Planta Med* **49,** 51-54.

**Kimura, Y., Okuda, H. & Arichi, S. (1985).** Effects of stilbene derivatives on arachidonate metabolism in leukocytes. *Biochim Biophys Acta* **837,** 209-212.

**Ko, S. G., Koh, S. H., Jun, C. Y., Nam, C. G., Bae, H. S. & Shin, M. K. (2004).** Induction of apoptosis by Saussurea lappa and Pharbitis nil on AGS gastric cancer cells. *Biol Pharm Bull* **27,** 1604-1610.

**Koca, Y., Ozdal, O. L., Celik, M., Unal, S. & Balaban, N. (2003).** Antioxidant activity of seminal plasma in fertile and infertile men. *Arch Androl* **49,** 355-359.

**Kolthur-Seetharam, U., Dantzer, F., McBurney, M. W., de, M. G. & Sassone-Corsi, P. (2006).** Control of AIF-mediated cell death by the functional interplay of SIRT1 and PARP-1 in response to DNA damage. *Cell Cycle* **5,** 873-877.

**Konishi, T., Shimada, Y., Nagao, T., Okabe, H. & Konoshima, T. (2002).** Antiproliferative sesquiterpene lactones from the roots of Inula helenium. *Biol Pharm Bull* **25,** 1370-1372.

**Kopper, L. & Timar, J. (2005).** Genomics of prostate cancer: is there anything to "translate"? *Pathol Oncol Res* **11,** 197-203.

**Kucuk, O. (2002).** Chemoprevention of prostate cancer. *Cancer Metastasis Rev* **21,** 111-124.

**Kuwajerwala, N., Cifuentes, E., Gautam, S., Menon, M., Barrack, E. R. & Reddy, G. P. (2002).** Resveratrol induces prostate cancer cell entry into s phase and inhibits DNA synthesis. *Cancer Res* **62,** 2488-2492.

**Lee, I. S., Nishikawa, A., Furukawa, F., Kasahara, K. & Kim, S. U. (1999).** Effects of Selaginella tamariscina on in vitro tumor cell growth, p53 expression, G1 arrest and in vivo gastric cell proliferation. *Cancer Lett* **144,** 93-99.

**Lee, J. Y., Hwang, W. I. & Lim, S. T. (2004).** Antioxidant and anticancer activities of organic extracts from Platycodon grandiflorum A. De Candolle roots. *J Ethnopharmacol* **93,** 409-415.

**Lee, M. S., Yuet-Wa, J. C., Kong, S. K., Yu, B., Eng-Choon, V. O., Nai-Ching, H. W., Chung-Wai, T. M. & Fung, K. P. (2005a).** Effects of polyphyllin D, a steroidal saponin in Paris polyphylla, in growth inhibition of human breast cancer cells and in xenograft. *Cancer Biol Ther* **4,** 1248-1254.

**Lee, S., Lee, Y. S., Jung, S. H., Shin, K. H., Kim, B. K. & Kang, S. S. (2003).** Anti-tumor activities of decursinol angelate and decursin from Angelica gigas. *Arch Pharm Res* **26,** 727-730.

**Lee, W. Y., Park, Y., Ahn, J. K., Park, S. Y. & Lee, H. J. (2005b).** Cytotoxic Activity of Ergosta-4,6,8(14),22-tetraen-3-one from the Sclerotia of Polyporus umbellatus. *Bull Korean Chem Soc* **26,** 1464-1466.

**Letasiova, S., Jantova, S., Miko, M., Ovadekova, R. & Horvathova, M. (2006).** Effect of berberine on proliferation, biosynthesis of macromolecules, cell cycle and induction of intercalation with DNA, dsDNA damage and apoptosis in Ehrlich ascites carcinoma cells. *J Pharm Pharmacol* **58,** 263-270.

**Li, W. X., Cui, C. B., Cai, B., Wang, H. Y. & Yao, X. S. (2005a).** Flavonoids from Vitex trifolia L. inhibit cell cycle progression at G2/M phase and induce apoptosis in mammalian cancer cells. *J Asian Nat Prod Res* **7,** 615-626.

**Li, W. X., Cui, C. B., Cai, B. & Yao, X. S. (2005b).** Labdane-type diterpenes as new cell cycle inhibitors and apoptosis inducers from Vitex trifolia L. *J Asian Nat Prod Res* **7,** 95-105.

**Li, Y., Cao, Z. & Zhu, H. (2006).** Upregulation of endogenous antioxidants and phase 2 enzymes by the red wine polyphenol, resveratrol in cultured aortic smooth

muscle cells leads to cytoprotection against oxidative and electrophilic stress. *Pharmacol Res* **53,** 6-15.

**Liang, J. Y., Liu, Y. Y., Zou, J., Franklin, R. B., Costello, L. C. & Feng, P. (1999).** Inhibitory effect of zinc on human prostatic carcinoma cell growth. *Prostate* **40,** 200-207.

**Lin, H. Y., Shih, A., Davis, F. B., Tang, H. Y., Martino, L. J., Bennett, J. A. & Davis, P. J. (2002a).** Resveratrol induced serine phosphorylation of p53 causes apoptosis in a mutant p53 prostate cancer cell line. *J Urol* **168,** 748-755.

**Lin, J. P., Yang, J. S., Lee, J. H., Hsieh, W. T. & Chung, J. G. (2006).** Berberine induces cell cycle arrest and apoptosis in human gastric carcinoma SNU-5 cell line. *World J Gastroenterol* **12,** 21-28.

**Lin, S. Y., Liu, J. D., Chang, H. C., Yeh, S. D., Lin, C. H. & Lee, W. S. (2002b).** Magnolol suppresses proliferation of cultured human colon and liver cancer cells by inhibiting DNA synthesis and activating apoptosis. *J Cell Biochem* **84,** 532-544.

**Liu, R. H. (2004).** Potential synergy of phytochemicals in cancer prevention: mechanism of action. *J Nutr* **134,** 3479S-3485S.

**Liu, W. K., Xu, S. X. & Che, C. T. (2000).** Anti-proliferative effect of ginseng saponins on human prostate cancer cell line. *Life Sci* **67,** 1297-1306.

**Lodish, H., Berk, A., Matsudaira, P., Kaiser, C. A., Krieger, M., Scott, M. P., Zipursky, S. L. & Darnell, J. (2004).** *Molecular Cell Biology*, 5th edn. New York: WH Freeman.

**Mantena, S. K., Sharma, S. D. & Katiyar, S. K. (2006).** Berberine, a natural product, induces G1-phase cell cycle arrest and caspase-3-dependent apoptosis in human prostate carcinoma cells. *Mol Cancer Ther* **5,** 296-308.

**Marier, J. F., Vachon, P., Gritsas, A., Zhang, J., Moreau, J. P. & Ducharme, M. P. (2002).** Metabolism and disposition of resveratrol in rats: extent of absorption, glucuronidation, and enterohepatic recirculation evidenced by a linked-rat model. *J Pharmacol Exp Ther* **302,** 369-373.

**McNeal, J. E. (1988).** Normal histology of the prostate. *Am J Surg Pathol* **12,** 619-633.

**McNeal, J. E. (1981).** The zonal anatomy of the prostate. *Prostate* **2,** 35-49.

**McNeal, J. E., Redwine, E. A., Freiha, F. S. & Stamey, T. A. (1988).** Zonal distribution of prostatic adenocarcinoma. Correlation with histologic pattern and direction of spread. *Am J Surg Pathol* **12,** 897-906.

**Meng, L. H., Zhang, H., Hayward, L., Takemura, H., Shao, R. G. & Pommier, Y. (2004).** Tetrandrine induces early G1 arrest in human colon carcinoma cells by down-regulating the activity and inducing the degradation of G1-S-specific cyclin-dependent kinases and by inducing p53 and p21Cip1. *Cancer Res* **64,** 9086-9092.

**Mitchell, J. H., Gardner, P. T., McPhail, D. B., Morrice, P. C., Collins, A. R. & Duthie, G. G. (1998).** Antioxidant efficacy of phytoestrogens in chemical and biological model systems. *Arch Biochem Biophys* **360,** 142-148.

**Miura, D., Miura, Y. & Yagasaki, K. (2003).** Hypolipidemic action of dietary resveratrol, a phytoalexin in grapes and red wine, in hepatoma-bearing rats. *Life Sci* **73,** 1393-1400.

**Morgan, D. O. (2007).** *The Cell Cycle: Principles of Control*, 1st edn. London: New Science Press.

**Mukherjee, A. K., Basu, S., Sarkar, N. & Ghosh, A. C. (2001).** Advances in cancer therapy with plant based natural products. *Curr Med Chem* **8,** 1467-1486.

**Narayanan, B. A., Narayanan, N. K., Re, G. G. & Nixon, D. W. (2003).** Differential expression of genes induced by resveratrol in LNCaP cells: P53-mediated molecular targets. *Int J Cancer* **104,** 204-212.

**Nicholson, D. W. (1999).** Caspase structure, proteolytic substrates, and function during apoptotic cell death. *Cell Death Differ* **6,** 1028-1042.

**Nishida, S., Kikuichi, S., Yoshioka, S., Tsubaki, M., Fujii, Y., Matsuda, H., Kubo, M. & Irimajiri, K. (2003).** Induction of apoptosis in HL-60 cells treated with medicinal herbs. *Am J Chin Med* **31,** 551-562.

**Oh, S. H. & Lee, B. H. (2003).** Induction of apoptosis in human hepatoblastoma cells by tetrandrine via caspase-dependent Bid cleavage and cytochrome c release. *Biochem Pharmacol* **66,** 725-731.

**Ohno, T., Nagatsu, T., Nakagawa, M., Inoue, M., Li, Y. M., Minatoguchi, S., Mizukami, H. & Fujiwara, H. (2005).** New sesquiterpene lactones from water extract of the root of Lindera strychnifolia with cytotoxicity against the human small cell lung cancer cell, SBC-3. *Tetrahedron Lett* **46,** 8657-8660.

**Orallo, F. (2006).** Comparative studies of the antioxidant effects of cis- and trans-resveratrol. *Curr Med Chem* **13,** 87-98.

**Ozmen, H., Erulas, F. A., Karatas, F., Cukurovali, A. & Yalcin, O. (2006).** Comparison of the concentration of trace metals (Ni, Zn, Co, Cu and Se), Fe, vitamins A, C and E, and lipid peroxidation in patients with prostate cancer. *Clin Chem Lab Med* **44,** 175-179.

**Pant, N. & Srivastava, S. P. (2003).** Correlation of trace mineral concentrations with fructose, gamma-glutamyl transpeptidase, and acid phosphatase in seminal plasma of different categories of infertile men. *Biol Trace Elem Res* **93,** 31-38.

**Park, K. K., Chun, K. S., Lee, J. M., Lee, S. S. & Surh, Y. J. (1998).** Inhibitory effects of [6]-gingerol, a major pungent principle of ginger, on phorbol ester-induced inflammation, epidermal ornithine decarboxylase activity and skin tumor promotion in ICR mice. *Cancer Lett* **129,** 139-144.

**Picurelli, L., Olcina, P. V., Roig, M. D. & Ferrer, J. (1991).** [Determination of Fe, Mg, Cu, and Zn in normal and pathological prostatic tissue]. *Actas Urol Esp* **15,** 344-350.

**Prasad, A. S. (1983).** Clinical, biochemical and nutritional spectrum of zinc deficiency in human subjects: an update. *Nutr Rev* **41,** 197-208.

**Reed, J. C. (1995).** Regulation of apoptosis by bcl-2 family proteins and its role in cancer and chemoresistance. *Curr Opin Oncol* **7,** 541-546.

**Renaud, S. & de, L. M. (1993).** The French paradox: dietary factors and cigarette smoking-related health risks. *Ann N Y Acad Sci* **686,** 299-309.

**Ryu, S. Y., Choi, S. U., Kim, S. K., No, Z., Lee, C. O., Ahn, J. W. & Kim, S. H. (1997).** *In vitro* antitumour activity of flavonoids from *Sophora flavescens*. *Phytother Res* **11,** 51-53.

**Sale, S., Tunstall, R. G., Ruparelia, K. C., Potter, G. A., Steward, W. P. & Gescher, A. J. (2005).** Comparison of the effects of the chemopreventive agent resveratrol and its synthetic analog trans 3,4,5,4'-tetramethoxystilbene (DMU-212) on adenoma development in the Apc(Min+) mouse and cyclooxygenase-2 in human-derived colon cancer cells. *Int J Cancer* **115,** 194-201.

**Shan, B. E., Zeki, K., Sugiura, T., Yoshida, Y. & Yamashita, U. (2000).** Chinese medicinal herb, Acanthopanax gracilistylus, extract induces cell cycle arrest of human tumor cells in vitro. *Jpn J Cancer Res* **91,** 383-389.

**Shih, R. S. M., Wong, S. H. K., Schoene, N. W. & Lei, K. Y. (2006).** Impaired G2/M cell cycle progression and marked elevation of Gadd45 protein level in zinc supplemented human bronchial epithelial cells. *Faseb Journal* **20,** A608.

**Simard, J., Dumont, M., Labuda, D. et al. (2003).** Prostate cancer susceptibility genes: lessons learned and challenges posed. *Endocr Relat Cancer* **10,** 225-259.

**Soleas, G. J., Goldberg, D. M., Grass, L., Levesque, M. & Diamandis, E. P. (2001).** Do wine polyphenols modulate p53 gene expression in human cancer cell lines? *Clin Biochem* **34,** 415-420.

**Sorensen, M. B., Stoltenberg, M., Juhl, S., Danscher, G. & Ernst, E. (1997).** Ultrastructural localization of zinc ions in the rat prostate: an autometallographic study. *Prostate* **31,** 125-130.

**Sun, M., Han, J., Duan, J. et al. (2007).** Novel antitumor activities of Kushen flavonoids in vitro and in vivo. *Phytother Res* **21,** 269-277.

**Sung, H. J., Choi, S. M., Yoon, Y. & An, K. S. (1999).** Tanshinone IIA, an ingredient of Salvia miltiorrhiza BUNGE, induces apoptosis in human leukemia cell lines through the activation of caspase-3. *Exp Mol Med* **31,** 174-178.

**Suzuki, T., Umeyama, T., Ohma, C., Yamanaka, H., Suzuki, K., Nakajima, K. & Kimura, M. (1991).** Immunohistochemical study of metallothionein in normal and benign prostatic hyperplasia of human prostate. *Prostate* **19,** 35-42.

**Tang, D. G. & Porter, A. T. (1997).** Target to apoptosis: a hopeful weapon for prostate cancer. *Prostate* **32,** 284-293.

**Tessitore, L., Davit, A., Sarotto, I. & Caderni, G. (2000).** Resveratrol depresses the growth of colorectal aberrant crypt foci by affecting bax and p21(CIP) expression. *Carcinogenesis* **21,** 1619-1622.

**Tseng, S. H., Lin, S. M., Chen, J. C., Su, Y. H., Huang, H. Y., Chen, C. K., Lin, P. Y. & Chen, Y. (2004).** Resveratrol suppresses the angiogenesis and tumor growth of gliomas in rats. *Clin Cancer Res* **10,** 2190-2202.

**Uenobe, F., Nakamura, S. & Miyazawa, M. (1997).** Antimutagenic effect of resveratrol against Trp-P-1. *Mutat Res* **373,** 197-200.

**Ukiya, M., Akihisa, T., Tokuda, H., Suzuki, H., Mukainaka, T., Ichiishi, E., Yasukawa, K., Kasahara, Y. & Nishino, H. (2002).** Constituents of Compositae plants III. Anti-tumor promoting effects and cytotoxic activity against human cancer cell lines of triterpene diols and triols from edible chrysanthemum flowers. *Cancer Lett* **177,** 7-12.

**Vallee, B. L. & Falchuk, K. H. (1993).** The biochemical basis of zinc physiology. *Physiol Rev* **73,** 79-118.

**Van, C. S. & Van Den, B. W. (2002).** Morphological and biochemical aspects of apoptosis, oncosis and necrosis. *Anat Histol Embryol* **31,** 214-223.

**Viswanathan, M., Kim, S. K., Berdichevsky, A. & Guarente, L. (2005).** A role for SIR-2.1 regulation of ER stress response genes in determining C. elegans life span. *Dev Cell* **9,** 605-615.

**Wallwork, J. C. & Sandstead, H. H. (1993).** Zinc and brain function. *Prog Clin Biol Res* **380,** 65-80.

**Wang, Y., Zhang, L., Li, Y., Hou, X. & Zeng, F. (2004).** Correlation of structure to antitumor activities of five derivatives of a beta-glucan from Poria cocos sclerotium. *Carbohydr Res* **339,** 2567-2574.

**Wood, J. G., Rogina, B., Lavu, S., Howitz, K., Helfand, S. L., Tatar, M. & Sinclair, D. (2004).** Sirtuin activators mimic caloric restriction and delay ageing in metazoans. *Nature* **430,** 686-689.

**Wu, T. S., Lin, Y. M., Haruna, M., Pan, D. J., Shingu, T., Chen, Y. P., Hsu, H. Y., Nakano, T. & Lee, K. H. (1991).** Antitumor agents, 119. Kansuiphorins A and B, two novel antileukemic diterpene esters from Euphorbia kansui. *J Nat Prod* **54,** 823-829.

**Wu, Z., Wu, L., Li, L., Tashiro, S., Onodera, S. & Ikejima, T. (2004a).** p53-mediated cell cycle arrest and apoptosis induced by shikonin via a caspase-9-dependent mechanism in human malignant melanoma A375-S2 cells. *J Pharmacol Sci* **94,** 166-176.

**Wu, Z., Wu, L. J., Li, L. H., Tashiro, S., Onodera, S. & Ikejima, T. (2004b).** Shikonin regulates HeLa cell death via caspase-3 activation and blockage of DNA synthesis. *J Asian Nat Prod Res* **6,** 155-166.

**Wyllie, A. H., Kerr, J. F. & Currie, A. R. (1980).** Cell death: the significance of apoptosis. *Int Rev Cytol* **68:251-306.,** 251-306.

**Yang, S. E., Hsieh, M. T., Tsai, T. H. & Hsu, S. L. (2003).** Effector mechanism of magnolol-induced apoptosis in human lung squamous carcinoma CH27 cells. *Br J Pharmacol* **138,** 193-201.

**Yim, D., Singh, R. P., Agarwal, C., Lee, S., Chi, H. & Agarwal, R. (2005).** A novel anticancer agent, decursin, induces G1 arrest and apoptosis in human prostate carcinoma cells. *Cancer Res* **65,** 1035-1044.

**Yin, X., Zhou, J., Jie, C., Xing, D. & Zhang, Y. (2004).** Anticancer activity and mechanism of Scutellaria barbata extract on human lung cancer cell line A549. *Life Sci* **75,** 2233-2244.

**Yoshikawa, N., Nakamura, K., Yamaguchi, Y., Kagota, S., Shinozuka, K. & Kunitomo, M. (2004).** Antitumour activity of cordycepin in mice. *Clin Exp Pharmacol Physiol* **31 Suppl 2:S51-3.,** S51-S53.

**Zaichick, V. Y., Sviridova, T. V. & Zaichick, S. V. (1997).** Zinc in the human prostate gland: normal, hyperplastic and cancerous. *Int Urol Nephrol* **29,** 565-574.

**Zhang, L. P., Jiang, J. K., Tam, J. W., Zhang, Y., Liu, X. S., Xu, X. R., Liu, B. Z. & He, Y. J. (2001).** Effects of Matrine on proliferation and differentiation in K-562 cells. *Leuk Res* **25,** 793-800.

**Zhang, M., Chiu, L. C., Cheung, P. C. & Ooi, V. E. (2006).** Growth-inhibitory effects of a beta-glucan from the mycelium of Poria cocos on human breast carcinoma MCF-7 cells: cell-cycle arrest and apoptosis induction. *Oncol Rep* **15,** 637-643.

**Zhang, Q. Y., Jiang, M., Zhao, C. Q., Yu, M., Zhang, H., Ding, Y. J. & Zhai, Y. G. (2005).** Apoptosis induced by one new podophyllotoxin glucoside in human carcinoma cells. *Toxicology* **212,** 46-53.

**Zhao, Z. Z. & Xiao, P. G. (2006).** *Encyclopedia on Contemporary Medicinal Plants*. Hong Kong: Hong Kong Jockey Club Institute of Chinese Medicine.

**Zhong, L., Qu, G., Li, P., Han, J. & Guo, D. (2003).** Induction of apoptosis and G2/M cell cycle arrest by Gleditsioside E from Gleditsia sinensis in HL-60 cells. *Planta Med* **69,** 561-563.

# CHAPTER III: ANTICANCER EFFECT OF TRIFOLIRHIZIN IN HUMAN PROSTATE CELLS

## *3.1 Abstract*

Trifolirhizin, found in the roots of *Sophora flavescens*, a traditional medicinal plant widely used in Asia, is a potent polycyclic flavonoid with anticarcinogenic effects. To elucidate the mechanisms underlying the anticancer activities of trifolirhizin, the effect of trifolirhizinon on the inhibition of cell cycle progression, induction of apoptosis and regulation of tumor suppressor gene expression was examined in human derived prostate cancer cells LNCaP and PC-3 as well as normal human prostate epithelial cells (NHPrE). The treatment of as low as 25 μM trifolirhizin in LNCaP cells for 6 days resulted in 40% inhibition of cell proliferation. Treatment of higher dosages caused the growth inhibition effect to be manifested in as early as 3 days. PC-3 cells were not affected by trifolirhizin till the very high dosage of 125 μM that resulted in more than 50 % reduction in cell proliferation after 4 to 6 days of treatment. Most importantly, for normal human prostate epithelial (NHPrE) cells, trifolirhizin was effective only at the highest concentration of 200 μM. The growth inhibition in trifolirhizin treated LNCaP and PC-3 cells was associated with cell cycle arrest at the G0/G1 and G2/M phase, respectively, in a dosage dependent manner. Moreover, the protein expression of cyclin E was unchanged but that of cyclin D1, p53 and p21 was suppressed in 50 μM trifolirhizin treated LNCaP cells, suggesting a p53 and p21 independent pathway.

## *3.2 Introduction*

### 3.2.1 Project summary

This project investigated the anticancer activity of trifolirhizin, an active component of *Sophora flavescens*, a traditional medicinal plant widely used in Asia. The effect of trifolirhizin on the inhibition of cell cycle progression, induction of apoptosis and regulation of tumor suppressor gene expression was examined in human derived prostate cancer cells LNCaP and PC-3. In response to the lack of experimental data on the effect of most natural plant products on normal cells in primary cultures, similar experiments were performed in normal human epithelial prostate cells (NHPrE). The cytotoxic effect and cell cycle progression inhibition effect of these products on different cell lines were determined by a MTS assay and flow cytometry, respectively. The expression of tumor suppressor genes under the treatment of different concentration of trifolirhizin was determined by Western blotting or flow cytometry using fluorescence labeled antibodies. Data generated from this research will contribute to the understanding of molecular mechanism(s) of the anticancer role of this plant derived natural product and specifically aid in the discovery of new effective compounds as potential anticancer chemopreventive and chemotherapeutic agents of plant origin.

### 3.2.2 Significance and rationale

For the first time, we undertook a detailed research on the sensitivity of prostate cancer cells to trifolirhizin by using an *in vitro* cell culture system including both androgen dependent, p53 widetype (LNCaP) and androgen independent, p53

null (PC-3) cells. In view of the lack of previous experimental data from corresponding normal control cells and the necessity of identifying the agents that can eradicate cancer cells without causing toxic responses in uninvolved normal cells, we also included the normal human prostate epithelial (NHPrE) cells in the present study as a control. We show that trifolirhzin exerts its antiproliferative effect against both androgen-dependent and androgen independent human prostate cancer cells at a dosage and time dependent manner and that this effect is mediated through interference of cell cycle progression without signs of apoptosis induction. Our study also sheds light on the molecular mechanism by which trifolirhizin inhibits cell cycle progression in prostate cancer cells. Under the conditions used in this study, trifolirhizin in moderately high concentrations did not affect the viability of normal prostate epithelial cells.

## *3.3 Materials and Methods*

### 3.3.1 Preparation of trifolirhizin

That pure compound, trifolirhizin was isolated, purified, identified and kindly provided by Dr. Linagli Yu's lab. Briefly, a methanol extract of the root of Sophora flavescens was separated by silica gel column chromatography (CC) and eluted with a gradient composing of CHCl3-MeOH. The fraction of CHCl3-MeOH (5:1) was further purified by repeated silica gel CC to afford a purified compound. The compound was then identified as trifolirhizin (MW 446) by $^{1}H$, $^{13}C$ NMR and ESI MS analysis, which was a known compound previously isolated from Sophora flavescens (data not shown). The powder of trifolirhizin was sealed and stored in

bottles filled with nitrogen. A stock solution of 100mM was made by dissolving trifolirhizin and in DMSO and stored at 4 $^{o}$C.

### 3.3.2 Cell culture

Human prostate carcinoma cell lines LNCaP, PC-3 were purchased from the American Type Culture Collection (Manassas, VA). The normal prostate epithelial (NHPrE) cells from a 29-year old Caucasian male were purchased from Lonza Walkersville, Inc. (Walkersville, MD). The prostate cancer cells were cultured as monolayers in RPMI 1640 supplemented with 10% heat-inactivated fetal bovine serum (Invitrogen), 100 μg/mL penicillin, and 100 μg/mL streptomycin (Invitrogen, Carlsbad, CA) and maintained in an incubator with a humidified atmosphere of 95% air and 5% $CO_2$ at 37 $^{o}$C. The normal human prostate epithelial (NHPrE) cells were cultured in Prostate Epithelial Cell Growth Medium (PrEGM) purchased from Lonza Walkersville, Inc. and maintained in an incubator under the conditions described above. In all treatments, tested drugs were dissolved in a small amount of vehicle (DMSO) with maximum concentration 0.2% (V/V). Cells treated with same amount of vehicle only were used as controls.

### 3.3.3 Cell proliferation assay

The effect of trifolirhizin or SFE on the proliferative capacity of cells was determined using the CellTiter 96 Aqueous One Solution Cell Proliferation Assay (Promega, Madison, MI), according to the procedures recommended by the manufacturer. Briefly, cells (2500 cells /well) were seeded in a flat-bottomed 96-well plate with a multichannel pipet. After overnight incubation, the medium was removed

and cells were treated with 100 µL fresh culture medium with different concentrations (0, 1, 5, 10 and 50 µg/mL for SFE or 0, 5, 10, 25, 50, 100, 200 µM for trifolirhizin) of tested candidate for 2d, 3d, 4d and 6d with 5 replicates. At the end of exposure period, 20 µL of Cell Titer 96 aqueous solution were added to each well and bioreduced by the dehydrogenase enzymes in metabolically active cells into a formazan product. After 1 h incubation in a humidified atmosphere at 37 $^{o}$C, the quantity of formazan product, which is directly proportional to the number of living cells in culture, was measured by the amount of absorbance at 490 nm. The blank was recorded by measuring the absorbance at 490 nm with wells containing medium but no cells. Results of the treatment groups were expressed as percentage of their respective control set at 100%.

### 3.3.4 Cell cycle analysis

Subconfluent cells were treated with trifolirhizin in culture medium as described above for various periods and then harvested at just below 70% confluency, washed with cold PBS and processed for cell cycle analysis. Briefly, 1 X $10^{6}$ cells were aliquoted in 50 mL polypropylene centrifuge tube, washed in 3 mL 1X in PBS (no Ca or Mg) and resuspended in 1.5 mL PBS. To these resuspended cells, 15 mL of 70% ethanol were added and mixed gently by vortex. Cells then were stored at 4 $^{o}$C for 4 h and then labeled with propidium iodide. A total of 10,000 cells were collected for DNA analyses on a FACScalibur cytometer with the CELLQuest program (Becton Dickinson, San Jose, CA) and the results were analyzed by ModFit LT (Version 3.0, Verity Software House, Topsham, ME). Calibration standards, LinearFlow Green (Molecular Probes, Carlsbad, CA) and DNA QC Particle Kit

(Becton Dickinson, San Jose, CA), were used to verify instrument performance. The DNA content of a cell population analyzed by this assay was used to determine the proportion of cells that were in G0/G1, S or G2/M phase of the cell cycle.

### 3.3.5 Protein immunodetection

Fixation and permeabilization steps were adapted from previously published methods (Chow et al., 2005; Krutzik and Nolan, 2003). Cells (2 X $10^6$) were resuspended in 300 µL of RPMI medium. Thirty µL of formaldehye (16%) were then added to give a final concentration of 1.5% and cells were fixed for 15 min at room temperature followed by centrifugation. Pellets were re-suspended by vortexing in a small volume of RPMI (less than or equal to 50 µL). One mL of ice cold methanol was added to the chilled tube while again vortexing to prevent cell clumping. Samples were capped tightly and stored at -20 $^oC$ until analysis by flow cytometry (7-10 days) using appropriate fluorescence-labeled antibody.

### 3.3.6 Statistical analysis

Data were presented as mean ± SEM. Statistical significance was examined by Student's t test between control and treated group or a one-way ANOVA followed by Tukey's test among treatment groups. A p value of $< 0.05$ was considered statistically significant.

## *3.4 Results*

### 3.4.1 The SFE is cytotoxic against NHPrE cells, while the purified compound trifolirhizin is not

We first investigated the effect of SFE on the proliferation of normal human prostate epithelial cells. As shown in **Fig. 1**, proliferation or cell growth of NHPrE cells was reduced by 30 and 90%, when treated with fairly high levels of SFE at 10 or 50 μg/ml, respectively, for 48 hours, which indicated a strong cytotoxicity in primary NHPrEs. Most importantly, the purified component trifolirhizin, prepared by column chromatography, was effective only at the very high concentration of 200 μM, which resulted in 20% and 35% reduction in cell growth after a prolonged treatment of 4 and 6 days. Lower dosages (5, 10, 25, 50 and 100 μM) and short treatment periods (2 and 3 days) were ineffective at all (**Fig. 2**).

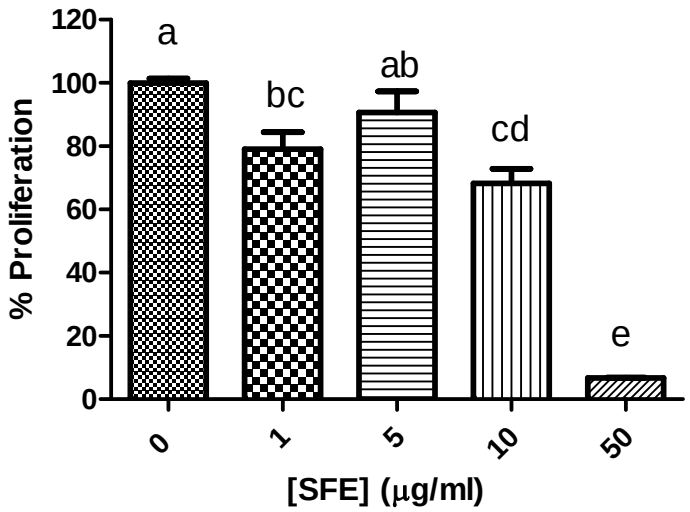


**Figure 1. The effect of methanol extract from Sophora flavescens (SFE) on the proliferation of NHPrE cells.** The NHPrE cells (5000/well) were plated in 96-well plates with different concentrations of SFE for 48 hours. Viable cell density was determined by the CellTiter 96 Aqueous One Solution Cell Proliferation Assay as described in Material and Methods. Results are expressed as percentage of control set at 100%. Values are means ± SEM from 5 separate experiments. Different letters indicate significant differences among groups ($p$<0.05); treatments with the same letter indicate no significant difference.

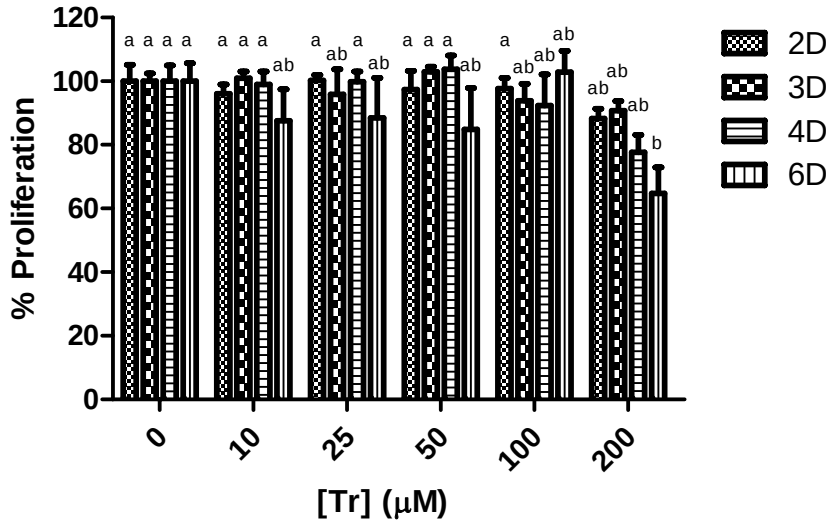


**Figure 2. The effect of trifolirhizin on the proliferation of NHPrE cells.** The NHPrE cells (2500/well) were plated in 96-well plates with different concentrations of trifolirhizin for different periods. Viable cell density was determined by the CellTiter 96 Aqueous One Solution Cell Proliferation Assay (Promega) as described in Material and Methods. Results are expressed as percentage of control set at 100%. Values are means ± SEM from 5 separate experiments. Different letters indicate significant differences among groups ($p$<0.05); treatments with the same letter indicate no significant difference.

### 3.4.2 Trifolirhizin treatment significantly inhibits the proliferation of LNCaP and PC-3 prostate cancer cells in dose and time-dependent manner

In LNCaP cells, which are androgen responsive and represent early stage prostate cancer, there was a strong dosage and time dependent response to the treatment of trifolirhizin. The lowest effective level of Trifolirhizin at 25 μM reduced cell proliferation by 40% after 6 days of treatment. Any concentration lower than that was not effective (**Fig 3A**). Thereafter, Trifolirhizin was able to reduce proliferation consistently at higher level of 50, 100 or 200 μM (**Fig. 3A**), with stronger effect at higher concentrations. The highest dosage, 200 μM was found effective as early as after 2 days of treatment, resulting in approximately 20% reduction in cell growth. Only 40% and 20% LNCaP cells could survive after treated for 6 days at 100 and 200μM trifolirhizin. On the other hand, PC-3 cells, which are androgen non-responsive, representing late stage cancer, were not affected by trifolirhizin till the very high dosage of 100 μM that resulted in an average of 15% reduction among the incubation times, a slight increase of the dose to 125 μM gave more than 40 % reduction in cell proliferation after 4 to 6 days of treatment (**Fig. 3B**). However, there was no significant difference between the 3 concentrations 125, 150 and 175 μM in each term of antiproliferative effects in each incubation period. In addition, Pc-3 cells manifested lag of 2 days in response to the treatment of trifolirhizin, , as indicated by less than 15% inhibition of proliferation after treated for 2 days regardless of the

concentration. The highest concentration 200 μM resulted in about 50% reduction in proliferation after 4 to 6 days of incubation in PC-3 cells

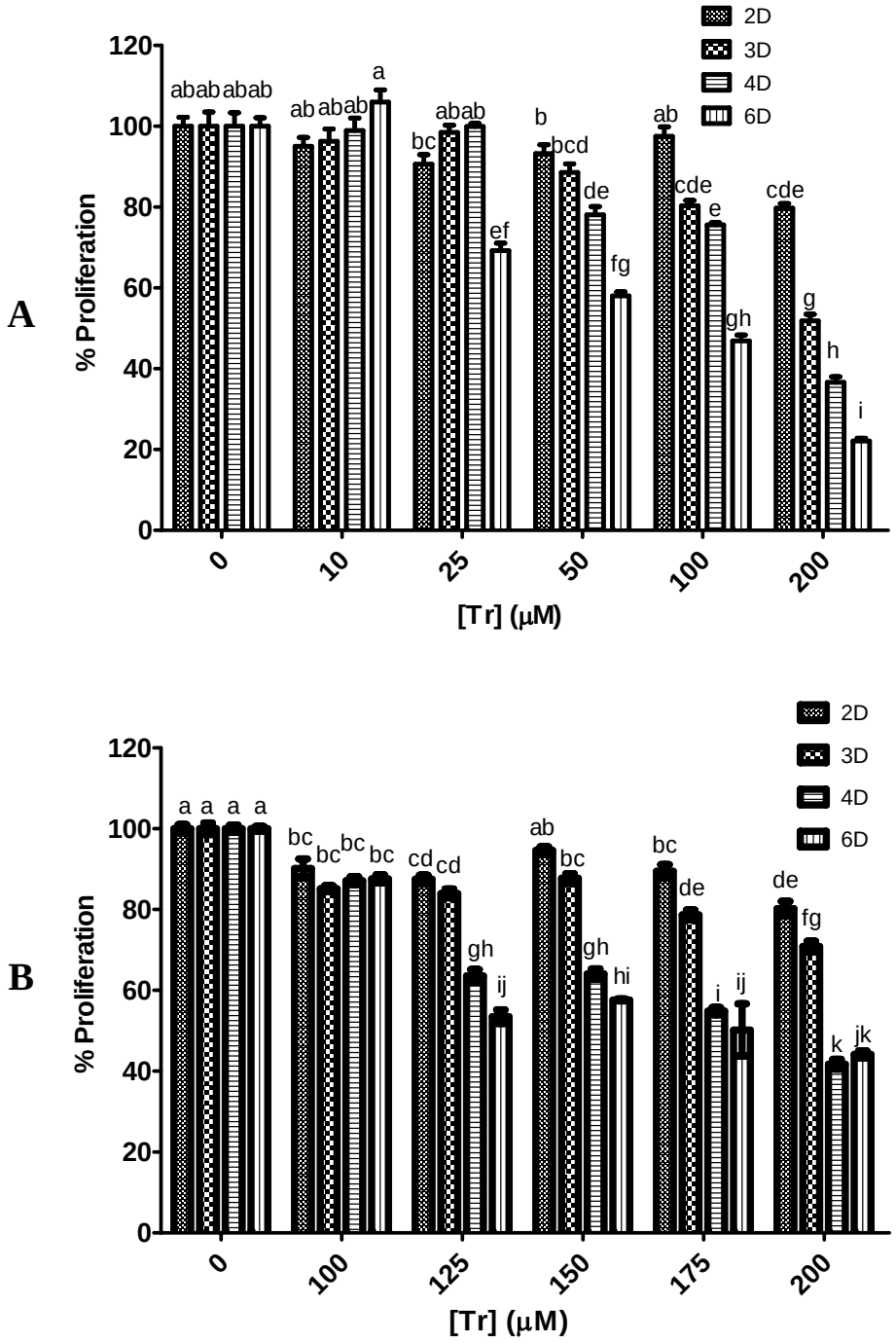


**Figure 3. The effect of trifolirhizin on the proliferation of LNCaP and PC-3 cells.** The LNCaP cells (A) and PC-3 cells (B) were plated at a density of 2500/well in 96-well plates with various concentrations of trifolirhizin for different periods. Viable cell density was determined by the CellTiter 96 Aqueous One Solution Cell

Proliferation Assay (Promega) as described in Materials and Methods. Results are expressed as percentage of control set at 100%. Values are means ± SEM from 5 separate experiments. Different letters indicate significant differences among groups ($p<0.05$); treatments with the same letter indicate no significant difference.

### 3.4.3 Trifolirhizin treatment induced cell cycle arrest at G1/G0 and G2/M stage in LNCaP and PC-3 cells, respectively

The significant antiproliferation effect of trifolirhizin led us to investigate the cell cycle distribution of trifolirhizin treated LNCaP and PC-3 cells and we observed no induction of apoptosis in both cancer cell lines. However, for the first time, our result revealed that the inhibition of proliferation in trifolirhizin treated LNCaP and PC-3 cells was associated with a cell cycle arrest at the G0/G1 starting at the treatment of 25 μM (**Fig. 4A and 4B**) and G2/M phase at that of 125 μM (**Fig. 4C and 4D**), respectively, in a dosage dependent manner. No sign of apoptosis was observed in the trifolirhizin treated LNCaP and PC-3 cells, as indicated by the little number of cells in the sub G0/G1 (Apo) region, representing hypodiploid apoptotic cells even at the highest levels (100 uM in the case of LNCaP and 175 μM in the case of PC-3), indicating that under the experimental dosages, trifolirhizin can only cause cell cycle arrest in both LNCaP and PC-3 cells, but not apoptosis.

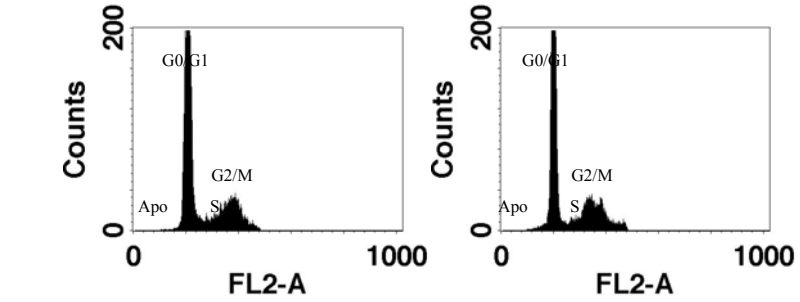
A
Counts
200
0
G0/G1
G2/M
Apo
S
0
1000
FL2-A
Control
Tr (25μM)

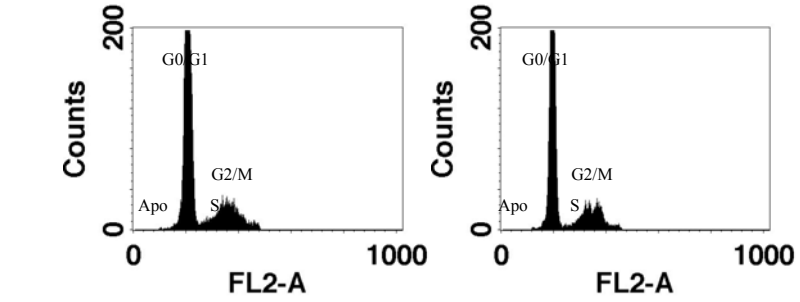
Counts
200
0
G0/G1
G2/M
Apo
S
0
1000
FL2-A
Tr (50μM)
Tr (100μM)

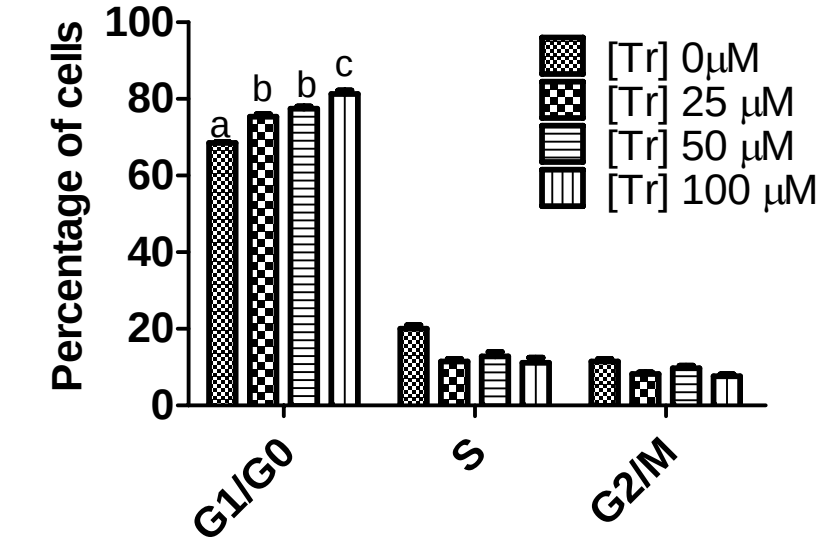
B
Percentage of cells
100
80
60
40
20
0
a
b
b
c
[Tr] 0μM
[Tr] 25 μM
[Tr] 50 μM
[Tr] 100 μM
G1/G0
S
G2/M

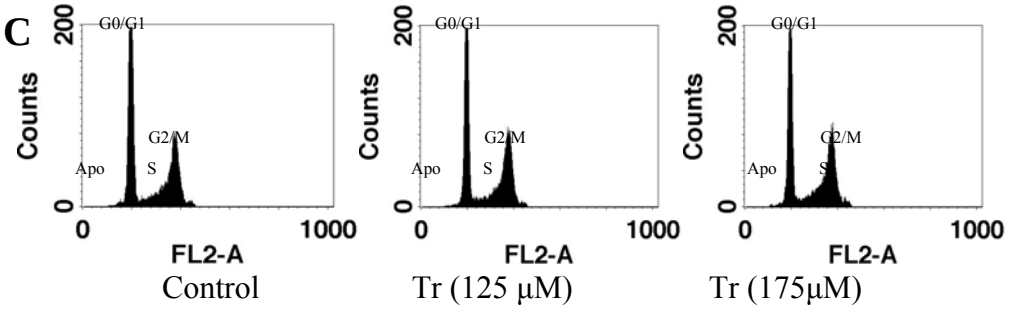
C
Counts
200
0
G0/G1
G2/M
Apo
S
0
1000
FL2-A
Control
Tr (125 μM)
Tr (175μM)

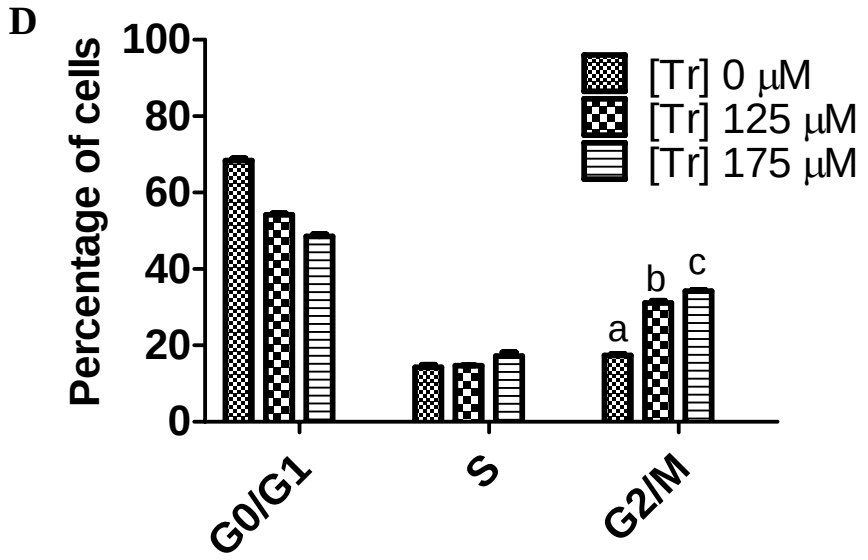


**Figure 4. The effect of trifolirhizin on cell cycle progression of LNCaP and PC-3 cells.** The LNCaP cells ($2.5X10^5$/well) (A and B) and PC-3 cells ($1.3X10^5$/well) (C and D) were plated in 6-well plates with different concentrations of trifolirhizin for 5 days. The cell cycle distribution of collected cells was determined by flow cytometry as described in Material and Methods. Open graphs (A and C) are the raw data from flow cytometry. The given result is a representative of three seperate experiments. Bar graphs (B and D) show DNA content at each phase of the cell cycle: G0/G1 phase, S phase, and G2/M phase, calculated by the computer software, CELLQuest. Values are means ± SEM from 3 separate experiments. Only the phase with an increasing trend of cell number was tested for statistical significance. Different letters indicate significant differences among groups ($p<0.05$); treatments with the same letter indicate no significant difference.

### 3.4.4 Prolonged trifolirhizin treatment depressed p53, p21 and cyclin D1 expression, induced hypophosphorylated Rb expression and kept cyclin E level constant

We further examined the molecular mechanism of trifolirhizin on cell cycle arrest by using LNCaP cells as a model. Five days (approximately one passage) of incubation time was chosen to mimick medium to long term period. The total intracellular protein levels of cyclin D1, E p53, p21 and hypophosphorylated Rb were assessed in 50 μM trifolirhizin treated LNCaP cells. A marked reduction (approximately 35%) in the expression of cyclin D1 (**Fig. 5**), while no change of cyclin E (**Fig. 5**) in trifolirhizin treated LNCaP cells was observed. Moreover, the treatment with 50 μM of trifolirhizin for 5 days suppressed p53 and p21 expression by 40% and 30% respectively and enhanced the hypophosphorylated Rb level by 50% in LNCaP cells (**Fig. 5**).

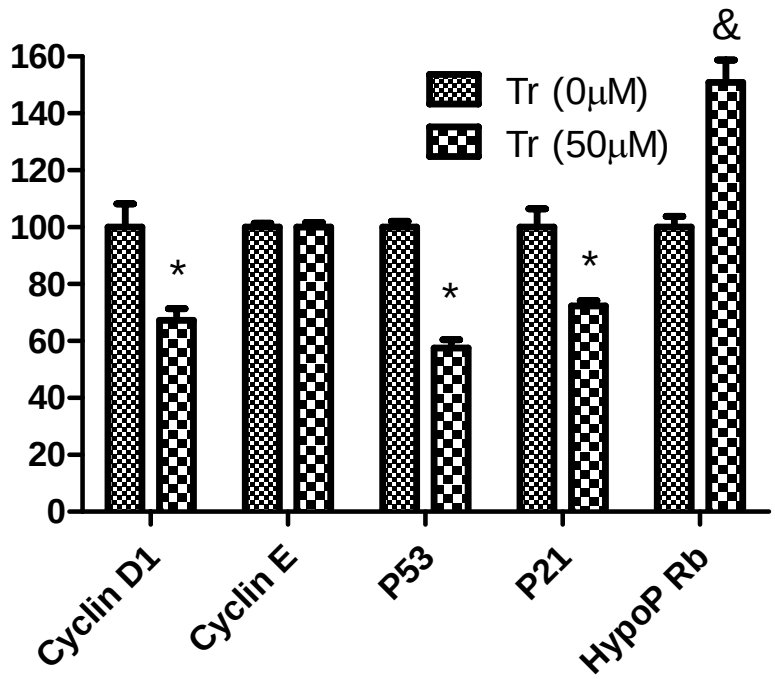


**Figure 5. The effect of trifolirhizin on Cyclin D1, E, P53, P21 and hypophospholyrated Rb expression in LNCaP cells.** The LNCaP cells ($2.5X10^5$/well) were plated in 6-well plates with 50 μM of trifolirhizin for 5 days. Collected cells were fixed in 1.6 % formaldehyde and finally resuspended in methanol before immunodetection using specific FITC labeled antibodies for each protein. Bar graph shows relative percentage of the increase in fluorescence (FL) produced by binding of the antibody specific to the protein compared to that produced by binding of the isotype control antibody. The FL increase for control was set to be 100%. Data were calculated using a gate of 10,000 events (cells) for all samples and treatments. Trifolirhizin treated cells had a modest G0/G1 block (about 10%) in each experiment. Values are means ± SEM from 3 separate experiments. *, Student's T test $p<0.05$; &, Student's T test, $p<0.01$.

## *3.5 Discussion*

Nowadays, it is still very common to screen for anticancer drugs or chemopreventive agents from candidates that are highly cytotoxic to cancer cells. However, the cytotoxic effect may not be specific for cancer cells and the side effects brought to the normal cells by these agents may be devastating as well. Thus, treatments involving the usage of these chemicals may impose detrimental effect on normal cells while inhibiting the growth of cancer cells, because the cancer cells and normal cells contain almost the same genetic background, which may be affected by these natural agents. Therefore, the search for better cancer chemotherapeutic agents with minimal side effects in normal human cells is still ongoing. In our study, a broad dosage range (25-200 μM) of trifolirhizin was found to exert anticancer activity against human prostate cancer cells (**Fig. 3**), while having little or no effect on the normal growth of healthy human prostate epithelial cells (**Fig. 2**). In 2004, Aratanechemuge et al. also reported that trifolirhizn at 270-360 μM does not induce apoptosis in normal lymphocytes prepared from healthy volunteers (Aratanechemuge et al., 2004). These data suggest that at a broad concentration range, trifolirhizin will not be harmful to healthy body tissues. In fact, many plants store important defensive chemicals in the forms of inactive glycosides and render them available quickly by hydrolysis that breaks off the sugar part from the main chain of the chemical. Maackiain, another phytochemical with one glycoside side chain less than trifolirhizin in structure, was isolated from the same extract and reported to be 5 times stronger than trifolirhizin (maackiain glycoside) in terms of growth inhibition and apoptosis induction effects in treated HL-60 cells but not harmful to normal human

lymphocytes (Aratanechemuge et al., 2004). These characteristics exhibited by maackiain makes it a promising candidate of antitumor chemopreventive agent and the effect of maackiain on prostate cancer cells LNCaP and PC-3 as well as NHPrE cells will be investigated in our lab as a separate project.

We reported cell cycle arrest at G0/G1 and G2/M stage in trifolirhizin treated LNCaP and PC-3 cells, respectively (**Fig. 4**). It is intriguing that the same compound induces cell cycle arrest at different phase in different cell type. Similarly, berberine has been documented not only induce G0/G1 cell cycle arrest in human prostate cancer DU145 cells, but also induce G2/M cell cycle arrest in human gastric carcinoma SNU-5 cells. Although in our studies, LNCaP and PC-3 are both prostate cancer cell lines, representing different states of prostate cancer, the observation of cell cycle arrest induced at different phases may be due to the interaction between the agent and the genetic background of cell lines or the different stage of cancer development.

In general, cell cycle control is a multigenic regulatory network. Therefore, we assessed the protein expression level of several target genes that might be involved in the trifolirhizin induced G0/G1 arrest in NHPrE cells. A proposed molecular mechanism of Trifolirhizin's anticancer activity in LNCaP cells is indicated in **Fig. 6**. In the trifolirhizin treated NHPrE cells with a cell cycle arrest at the G0/G1 stage, the cyclin D1 expression is expected to be repressed since cyclin D1 is the major effector that regulates the cell cycle transition from G0/G1 to S phase. In mammalian cells, two cyclin-CDK complexes, cyclin D-CDK4/6 and cyclin E-CDK2, were demonstrated to be key effectors in G1 progression and G1/S transition,

respectively (Sherr, 2000). Both cyclin D-CDK4/6 and cycln E-CDK2 complexes can successively phosphorylate retinoblastoma protein (Rb) and lead to its inactivation (Harbour and Dean, 2000), which hinders the E2F-1/Rb association necessary for the expression of E2F-1-dependent genes needed for S phase entry (Leone et al., 2001). In our study, cyclin D1 expression was repressed while cyclin E expression was not changed, suggesting the signal was exclusively transmitted through cyclin D-CDK4/6 complex. The suppressed cyclinD-CDK4/6 could no longer successively phosphorylate Rb, which leads to increased hypophosphorylated Rb level. Cyclin B is necessary for G2/M transition and for cells to enter mitosis by forming complex with Cdc-2. In trifolirhizin treated PC-3 cells with a G2/M arrest, the expression of cyclin B is very likely to be repressed as well when compared to the control. p53, a very important tumor suppressor gene, has been implicated in a variety of cellular processes, including induction of G1 arrest (Ciciarello et al., 2001) and maintenance of G2/M arrest in response to DNA damage (Bunz et al., 1998). In the cases of cell cycle arrest by plant natural product treatment, p53 upregulation was observed in both G0/G1 arrest (Chang et al., 2004; Wu et al., 2004; Meng et al., 2004; Lee et al., 1999) and G2/M arrest (Lin et al., 2006; Zhang et al., 2005), suggesting that p53 is a universal cell cycle regulator by transactivating a number of downstream genes. p21 and p27, two Cip/Kip family members of the CDK inhibiors, are the transcription targets of p53 and play an important role in mediating G1 arrest by binding to the cyclin-CDK complexes and inhibiting their activities (Waldman et al., 1995; Pavletich, 1999). An upregulation in p53 protein or mRNA level in association with cell cycle arrest and/or apoptosis induced by phytochemical treatments in various

cancer cell lines has been observed in many studies, suggesting a p53 dependent pathway (Wu et al., 2004; Lee et al., 1999; Lin et al., 2006; Zhang et al., 2005). p21, as a downstream transcription target of p53, has also been found to be elevated concomitantly with p53 (Meng et al., 2004; Chang et al., 2004). On the other hand, p21 has also been demonstrated to regulate cell cycle progression and induce apoptosis independent of p53 (Chen et al., 2004). In our study, the concomitant suppression of p53 and p21 expression (**Fig. 5**) and the G2/M arrest in trifolirhizin treated, p53 null, PC-3 cells (**Fig. 4)** suggested that the proliferation inhibition and cell cycle arrest effect caused by trifolirhizin treatment in LNCaP and PC-3 cells was probably through a p53 independent pathway. Akt, also known as Protein Kinase B (PKB), may be a potential regulator that is responsible for the concomitant downregulation of the p53 and p21 levels through the Akt-Mdm2-p53 signaling axis and Akt-p21 signaling axis. The phosphorylated form of Akt (p-Akt) has been shown to physphorylate Mdm2 at Ser 166 and 186 residues (Gottlieb et al., 2002), which are close to Mdm2's nuclear localization signal and nuclear export signal domains. The pAkt mediated physphorylation of Mdm2 (p-Mdm2) leads to its translocation from cytoplasm to nucleus and further interaction with p53 and p300, which then promotes the ubiquitin-dependent degradation of p53 (Mayo and Donner, 2001). As a result, Akt indirectly hinders p53-dependent growth suppression and apoptosis. On the other hand, the function of p21 may dichotomize depending on its cellular localization. In the nucleus, p21 acts as a CDK inhibitor that arrests the cell cycle and blocks DNA sythesis. When localized in the cytoplasm, p21 is pro-proliferative and promotes cell cycle progression by stabilizing cdk4 and cyclin D complexes. p21 translocalization

from cytoplasm to nucleus can be prevented by phosphorylation mediated by p-Akt at Thr145 residue, which lies near the nuclear localization signal (NLS) domain (Zhou et al., 2001). Thus, the cytoplasmically retained p21 can facilitate and stabilize the cyclin D-CDK4 complex (Boonstra, 2003). This may partially explain the observation that no sign of apoptosis occurred in the trifolirhizin treated LNCaP and PC-3 cells. However, more studies, such as p53 time course expression and p53 knock down in LNCaP (p53+/+) cells as well as p53 transfection in PC-3 (p53-/-) cells, need to be conducted to thoroughly investigate the p53 dependency in the trifolirhizin-induced proliferation inhibition and cell cycle arrest effect in LNCaP and PC-3 cells.

## *3.6 Conclusion*

In conclusion, these findings demonstrate that trifolirhizin exerts its antitumor activity by the inhibition of proliferation mediated by triggering cell cycle arrest at G0/G1 and G2/M stage in LNCaP and PC-3 cells, respectively. The cell cycle arrest was mediated by the depressed expression of corresponding cyclins, possibly through a p53 and p21 independent pathway (**Fig. 6**). The antitumor effect of trifolirhizin was exclusively against cancer cells LNCaP and PC-3 and under our experimental conditions trifolirhzin appeared to cause no adverse effect in NHPrE cells.

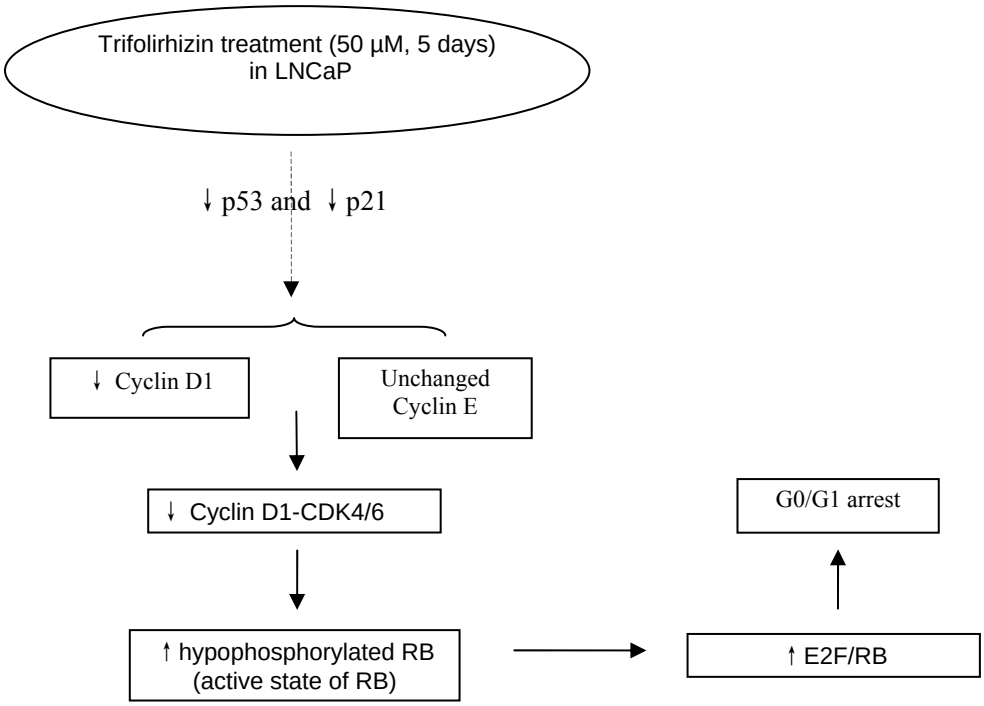


**Figure 6. Proposed molecular mechanism of Trifolirhizin's anticancer function in LNCaP cells.**

## *3.7 References*


**Aratanechemuge, Y., Hibasami, H., Katsuzaki, H., Imai, K. & Komiya, T. (2004).** Induction of apoptosis by maackiain and trifolirhizin (maackiain glycoside) isolated from sanzukon (Sophora Subprostrate Chen et T. Chen) in human promyelotic leukemia HL-60 cells. *Oncol Rep* **12,** 1183-1188.

**Boonstra, J. (2003).** Progression through the G1-phase of the on-going cell cycle. *J Cell Biochem* **90,** 244-252.

**Bunz, F., Dutriaux, A., Lengauer, C., Waldman, T., Zhou, S., Brown, J. P., Sedivy, J. M., Kinzler, K. W. & Vogelstein, B. (1998).** Requirement for p53 and p21 to sustain G2 arrest after DNA damage. *Science* **282,** 1497-1501.

**Chang, Y. C., Chou, F. P., Huang, H. P., Hsu, J. D. & Wang, C. J. (2004).** Inhibition of cell cycle progression by penta-acetyl geniposide in rat C6 glioma cells. *Toxicol Appl Pharmacol* **198,** 11-20.

**Chen, T., Turner, J., McCarthy, S., Scaltriti, M., Bettuzzi, S. & Yeatman, T. J. (2004).** Clusterin-mediated apoptosis is regulated by adenomatous polyposis coli and is p21 dependent but p53 independent. *Cancer Res* **64,** 7412-7419.

**Chow, S., Hedley, D., Grom, P., Magari, R., Jacobberger, J. W. & Shankey, T. V. (2005).** Whole blood fixation and permeabilization protocol with red blood cell lysis for flow cytometry of intracellular phosphorylated epitopes in leukocyte subpopulations. *Cytometry A* **67,** 4-17.

**Ciciarello, M., Mangiacasale, R., Casenghi, M., Zaira, L. M., D'Angelo, M., Soddu, S., Lavia, P. & Cundari, E. (2001).** p53 displacement from centrosomes and p53-mediated G1 arrest following transient inhibition of the mitotic spindle. *J Biol Chem* **276,** 19205-19213.

**Gottlieb, T. M., Leal, J. F., Seger, R., Taya, Y. & Oren, M. (2002).** Cross-talk between Akt, p53 and Mdm2: possible implications for the regulation of apoptosis. *Oncogene* **21,** 1299-1303.

**Harbour, J. W. & Dean, D. C. (2000).** Rb function in cell-cycle regulation and apoptosis. *Nat Cell Biol* **2,** E65-E67.

**Krutzik, P. O. & Nolan, G. P. (2003).** Intracellular phospho-protein staining techniques for flow cytometry: monitoring single cell signaling events. *Cytometry A* **55,** 61-70.

**Lee, I. S., Nishikawa, A., Furukawa, F., Kasahara, K. & Kim, S. U. (1999).** Effects of Selaginella tamariscina on in vitro tumor cell growth, p53 expression, G1 arrest and in vivo gastric cell proliferation. *Cancer Lett* **144,** 93-99.

**Leone, G., Sears, R., Huang, E. et al. (2001).** Myc requires distinct E2F activities to induce S phase and apoptosis. *Mol Cell* **8,** 105-113.

**Lin, J. P., Yang, J. S., Lee, J. H., Hsieh, W. T. & Chung, J. G. (2006).** Berberine induces cell cycle arrest and apoptosis in human gastric carcinoma SNU-5 cell line. *World J Gastroenterol* **12,** 21-28.

**Mayo, L. D. & Donner, D. B. (2001).** A phosphatidylinositol 3-kinase/Akt pathway promotes translocation of Mdm2 from the cytoplasm to the nucleus. *Proc Natl Acad Sci U S A* **98,** 11598-11603.

**Meng, L. H., Zhang, H., Hayward, L., Takemura, H., Shao, R. G. & Pommier, Y. (2004).** Tetrandrine induces early G1 arrest in human colon carcinoma cells by down-regulating the activity and inducing the degradation of G1-S-specific cyclin-dependent kinases and by inducing p53 and p21Cip1. *Cancer Res* **64,** 9086-9092.

**Pavletich, N. P. (1999).** Mechanisms of cyclin-dependent kinase regulation: structures of Cdks, their cyclin activators, and Cip and INK4 inhibitors. *J Mol Biol* **287,** 821-828.

**Sherr, C. J. (2000).** The Pezcoller lecture: cancer cell cycles revisited. *Cancer Res* **60,** 3689-3695.

**Waldman, T., Kinzler, K. W. & Vogelstein, B. (1995).** p21 is necessary for the p53-mediated G1 arrest in human cancer cells. *Cancer Res* **55,** 5187-5190.

**Wu, Z., Wu, L., Li, L., Tashiro, S., Onodera, S. & Ikejima, T. (2004).** p53-mediated cell cycle arrest and apoptosis induced by shikonin via a caspase-9-dependent mechanism in human malignant melanoma A375-S2 cells. *J Pharmacol Sci* **94,** 166-176.

**Zhang, Q. Y., Jiang, M., Zhao, C. Q., Yu, M., Zhang, H., Ding, Y. J. & Zhai, Y. G. (2005).** Apoptosis induced by one new podophyllotoxin glucoside in human carcinoma cells. *Toxicology* **212,** 46-53.

**Zhou, B. P., Liao, Y., Xia, W., Zou, Y., Spohn, B. & Hung, M. C. (2001).** HER-2/neu induces p53 ubiquitination via Akt-mediated MDM2 phosphorylation. *Nat Cell Biol* **3,** 973-982.

# CHAPTER IV: THE EFFECT OF RESVERATROL AND ZINC ON INTRACELLULAR ZINC STATUS IN NHPrE CELLS

## *4.1 Abstract*

To evaluate the influence of resveratrol on cellular zinc status, normal human prostate epithelial (NHPrE) cells and human hepetoblastoma (HepG2) cells were treated in 6 levels of resveratrol (0, 0.5, 1, 2.5, 5 and 10 μM) and 4 levels of zinc [0, 4, 16 and 32 μM or zinc deficient (ZD), zinc normal (ZN), zinc adequate (ZA) and zinc supplemented (ZS), respectively]. Among each zinc treatment, a progressive reduction in cell growth or increase in cellular total zinc was observed with increases of resveratrol from 2.5, 5 and 10 μM or from 5 and 10 μM, respectively. Moreover, in ZS cells, a much higher increase in cellular total zinc was observed as early as 1 μM resveratrol. In contrast, resveratrol exerted no effect on cell growth and cellular zinc level in HepG2 cells. A flow cytometry study revealed that the resveratrol (10 μM) induced G2/M arrest was responsible for the depressed cell growth in NHPrE cells. Data from an *in vitro* experiment using zinquin, as an indicator of intracellular free Zn(II) status, demonstrated possible complex formation between resveratrol and zinc ion. Zinquin ethyl ester fluorescence spectrofluorimetry and microscope imaging revealed that intracellular labile free zinc tended to be decreased in ZD and ZN NHPrE cells but increased in high zinc (ZA and ZS) cells. In addition, the abundance of metallothionein (MT) mRNA was markedly elevated only in ZS cells, with or without resveratrol treatment, but the response was independent of metal-responsive

transcription factor-1 (MTF-1) mRNA abundance. Furthermore, increases in cellular zinc status induced enhanced levels of reactive oxygen species (ROS) as well as senescenece detected by morphological and histochemical changes in cells treated with 2.5 or 10 μM resveratrol, especially in ZA and ZS cells. These findings support the contention that the reduction in cell growth and G2/M arrest induced by resveratrol treatment may be modulated by the marked increase in intracellular total zinc and free labile zinc, which in turn mediated the increases in ROS formation and senescence.

## *4.2 Introduction*

### 4.2.1 Project summary

Resveratrol has been shown to chelate divalent cations. We hypothesize that at low mineral status, resveratrol enhances zinc, copper (Cu), and selenium (Se) status by increasing their cellular uptake. However, at high mineral status, high resveratrol intake may cause excessive mineral deposition. We aim to evaluate the interrelationships of resveratrol with zinc, Cu, and Se in a mouse model and in normal human cells in culture. As part of my dissertation, my work was mainly focused on the in vitro studies designed to determine the interrelationship of resveratrol with zinc in NHPrE cells. NHPrE cells were cultured in six levels of resveratrol and four levels of metals (from none for resveratrol, or deficient for zinc, to the high end of plasma levels attainable by oral consumption in humans), in a 6X4 factorial design to assess: 1) cell growth, cell cycle progression, apoptosis; 2) cellular total zinc and free labile zinc levels; and 3) in vitro possible interaction between zinc and resvervatrol.

### 4.2.2 Significance and rationale

Resveratrol is widely reported to have health promoting properties: cardiovascular, anti-inflammatory (Jang et al., 1997), antimutagenic (Uenobe et al., 1997), antioxidant, and pro-oxidant activities (Azmi et al., 2006) as well as chemopreventive against various stages of chemically induced carcinogenesis (Jang et al., 1997). In the US and Europe, resveratrol is commercially available as a nutraceutical, ranging from 50 μg to 100 mg per dosage. However, detailed animal

and cell culture studies, as well as human long term studies, using dose response approaches to aid in the establishment of upper limits of intake are lacking. Thus, data generated by the cell-based studies will aid in establishing the effective minimum dose for certain biological activities and contribute to the setting of upper limits for resveratrol. Data generated may support the need to revise the upper limit for zinc if excessive zinc deposition is detected in NHPrE cells.

In recent studies, resveratrol was established to exert its pro-oxidant activity of oxidative DNA breakage for its anticancer properties (Azmi et al., 2006). In addition, resveratrol was shown to be a potent chelator of Cu but it did not chelate Fe (Belguendouz et al., 1997). Moreover, resveratrol administration has been shown to markedly increase plasma zinc and Cu in adult rats (Kavas et al., 2007). Furthermore, our preliminary NHPrE cell culture studies demonstrated that resveratrol is capable of inhibiting cell proliferation and markedly enhancing cellular zinc level in normal human prostate epithelial cells maintained under various zinc status. Thus, resveratrol may alter the metabolism and requirement of these trace minerals. In this project, the impact of resveratrol and zinc as well as the interactions of resveratrol with zinc were examined in NHPrE cells. Data generated in this study will contribute to the development of biomarkers for the measurement of health outcomes for the bioactive resveratrol, together with its nutritional interactions with zinc, and aid in the setting of dietary reference intakes and tolerable upper limits for resveratrol and zinc, as well as in the design of clinical studies for further exploration of the interaction between resveratrol and zinc in human subjects. More importantly, this study involving NHPrE in primary culture will serve as a pioneering example for further exploration

of the impact of the interaction between other trace minerals such as Cu and Se and bioactive resveratrol in normal human cells derived from a wide range of human tissues, e.g. normal human bronchial epithelial cells (NHBE), normal human aortic epithelial cells (NHAE), which may behave differently due to tissue specificity.

## *4.3 Materials and Methods*

### 4.3.1 Materials

Resveratrol, $ZnSO_4$ (1 M) solution, zinquin and zinquin ethyl ester were purchased from Sigma-Aldrich Co. (St. Louis, Mo). Resveratrol, zinquin and zinquin ethyl ester were dissolved in dimethyl sulphoxide (DMSO) at a concentration of 20 mM, 25 mM and 25 mM, respectively, and stored at -20 $^{o}$C.

### 4.3.2 Experimental design

A factorial design involving six (6) levels of trans-resveratrol (0, 0.5, 1, 2.5, 5 and 10 μM; from none to the high end of plasma levels attainable by oral consumption in humans) and four (4) levels of zinc [<0.4, 4, 16 and 32 μM, which represent deficient (ZD); as in most culture medium (ZN); normal plasma level (ZA); and the high end of plasma level attainable by oral consumption in humans (ZS), respectively] were used in the investigation of the effect of zinc and resveratrol on the proliferation and intracellular total zinc level of NHPrE and HepG2 cells. A simplified experimental design involving 4 levels of zinc and 2 or 3 levels of resveratrol was used in intracellular free labile zinc assay as well as Real-time PCR.

### 4.3.3 Cell culture

NHPrE cells from two different donors (21-year old and 29-year old male Caucasian) were purchased from Lonza Walkersville, Inc. (Walkersville, MD). The NHPrE cells used in the experiments in this dissertation are from the 29-year old male Caucasian for consistency except otherwise indicated. NHPrE cells were plated at 2,500 cells/$cm^2$ in tissue culture dishes containing prostate epithelial cell growth medium (PREGM), supplemented with 0.5 μg/mL epinephrine, 10 μg/mL transferrin, 5 μg/mL insulin, 0.1 ng/mL retinoic acid, 52 μg/mL bovine pituitary extract, 0.5 μg/mL hydrocortisone, 0.5 pg/mL human recombinant epidermal growth factor, and 6.5 ng/mL triiodothyronine (as growth supplements) without antibiotics, and cultured at 37°C in a 5% $CO_2$ incubator. Endotoxin-free medium were used (<0.005 endotoxin units/mL). The medium were changed at day 1 and subsequently every 48 h. Cells were grown to 80% confluence for 6 days, and subcultured using trypsin-EDTA at a ratio of 1: 8 at passage 3 for experimental treatment. A zinc-free Prostate Epithelial Basal Medium (PREBM w/o zinc), in which the manufacturer had omitted the addition of $ZnSO_4$, were used as the zinc-depleted medium after supplemented with necessary growth components and contains residual amounts of zinc (<1 μM), as detected by flame atomic absorption spectrophotometry. For the other zinc treatment groups, zinc was added to the media in the form of $ZnSO_4$ so that the only difference between these media was the zinc concentration. The zinc-normal (ZN), the zinc-adequate (ZA), and the zinc-supplemented (ZS) medium, will contain 4 μM, 16 μM, and 32 μM $ZnSO_4$, respectively. The ZA treatment was used as a representative of human plasma zinc levels, and the ZS group was used to represent the high end of

plasma zinc levels attainable by oral supplementation in humans (Fanzo et al., 2001). Resveratrol in 0.05% DMSO was added to each level of zinc medium to generate the 0, 0.5, 1, 2.5, 5 and 10 μM of resveratrol. The ZN medium without resveratrol was used as the control group for comparison with other treatments. Cells were cultured overnight in normal PREGM before changing to their respective treatment medium.

The HepG2 cells purchased from the American Type Culture Collection (Manassas, VA) were cultured at 25000 cells/$cm^2$ in DMEM supplemented with 10% FBS and appropriated antibiotics. Chelex 100 ion exchange resin (Bio-Rad, Hercules, CA) was used to deplete zinc from FBS. Briefly, the resin was first neutralized to physiological pH with 0.25 M HEPES, pH 7.4 before mixed with FBS at a ratio 1:4 at 4 $^oC$ for 2h. The Chelex 100 resin was then separated from FBS by centrifugation followed by fitration through a 0.22 μm filter for sterilization and removal of residual Chelex 100 resin. Chelated FBS has a zinc concentration < 1.0 μM, as determined by flame atomic absorption spectrophotometry (Hitachi, San Jose, CA). The basal DMEM medium with 10% chelated FBS containing < 0.1 μM zinc was termed zinc-deficient (ZD) medium. For the other zinc treatment groups (ZN, ZA and ZS), zinc was added to the media in the form of $ZnSO_4$ as described in the previous paragraph. Resveratrol in DMSO was added to each level of zinc medium to generate the 0, 0.5, 1, 2.5, 5 and 10 μM of resveratrol. The ZN medium without resveratrol was used as the control group for comparison with other treatments. Cells were cultured overnight in normal DMEM before changing to their respective treatment.

### 4.3.4 Cell proliferation and total intracellular zinc assay

An aliquot (100 μL) of the collected samples was used for total cell count determination by the NucleoCounter using the Nucleocassette Kit and NucleoView software (New Brunswick Scientific, Edison, New Jersey), according to the manufacturer protocol. Briefly, all cells were lysed and stabilized in the same volume of lysing and stablzing buffer and then 50 μL of lysed sample were sucked into a Nucleocassette and then scanned by the NucleoCounter, which features an integrated fluorescence microscope designed to detect signals from a fluorescent dye, propidium iodide, that intercalates to DNA in the nuclei of the lyzed cells. The rest of cells were then resuspended in 1.5 mL PBS and sonicated for two 30-second intervals on ice. Cellular zinc content was measured by flame atomic absorption spectrophotometry (Model 5000, Perkin Elmer, Norwalk, CT) using standard curves of 0.05-1.0 ppm generated with certified zinc reference solutions (Fisher Scientific, Fair Lawn, NJ) as previously described (Reaves et al., 2000). Furthermore, the certified zinc solutions were compared to Bovine Liver Standard Reference (US Department of Commerce, National Insitute of Standards, Gaithersburg, MD). Appropriate blanks were employed for all measurements. Cellular zinc was calculated as ng per million cells.

### 4.3.5 Cell cycle analysis

Subconfluent cells were treated in different culture media as described above for 3 days and then harvested at just below 70% confluency, washed with cold PBS and processed for cell cycle analysis. Briefly, 1.5 X $10^6$ cells were aliquoted in 50 mL polypropylene centrifuge tube, washed in 3 mL 1X in PBS (no Ca or Mg) and

resuspended in 1.5 mL PBS. To these resuspended cells, 15 mL of 70% ethanol was added and mixed gently by vortex with cap on tube. Cells will then be stored at 4 $^{o}$C for 2 to 4 h or overnight and then labeled with propidium iodide. A total of 10,000 cells were collected for DNA analyses on a FACScalibur cytometer with CELLQuest program (Becton Dickinson, San Jose, CA) and the results were analyzed by ModFit LT (Version 3.0, Verity Software House, Topsham, ME). Calibration standards, LinearFlow Green (Molecular Probes, Carlsbad, CA) and DNA QC Particle Kit (Becton Dickinson, San Jose, CA), were used to verify instrument performance. The DNA content of a cell population analyzed by this assay was used to determine the proportion of cells that are in G0/G1, S or G2/M phase of the cell cycle.

### 4.3.6 *In vitro* assay for zinc and resveratrol interaction

Experiment 1: 100 μL of PBS, containing the full combination of different concentrations of zinc (0, 2, 4, 6, 8, 16, 24, or 32 μM) in the form of $ZnSO_4$ and resveratrol (0, 5, 10 or 20 μM), were aliquoted into a 96-well plate in triplicates and then mixed with 25 μM zinquin.

Experiment 2: 100 μL of PBS, containing the full combination of different concentration of zinc (0, 2, 4, 6, 8, 16, 24, or 32 μM, final concentration) and zinquin (5 or 25 μM) were aliquoted into a 96-well plate in triplicates and then mixed with (10 μM) or without resveratrol.

The plates were incubated in 37 $^{o}$C for 5 min before the fluorescence signal from each well was quantitated at an excitation wavelength of 340 nm and emission wavelength of 460 nm using a Genios Pro spectrophotometer (Tecan Group Ltd., Männedorf, Switzerland).

### 4.3.7 Determination of labile level of free intracellular zinc

Free intracellular zinc was measured to see if increases in resveratrol in the medium would lead to elevations in free intracellular Zn(II), which has been suggested to depress cell proliferation but not induce apoptosis in normal cells. Zinquin ethyl ester was used to quantify labile level of free intracellular Zn(II) by spectrofluorimetry using a method adopted from Zalewaki et al. (1993) and Coyle et al. (1994) with slight modification. At the end of treatment, 100 µL suspended cells at a concentration of 1 X $10^6$ /mL were transferred to a 96-well optical plate (Nunc A/S). Zinquin was added to cells at a final concentration of 25 µM in PBS and incubated for 30 min before the fluorescence readings were measured at an excitation wavelength of 340 nm and emission wavelength of 460 nm in a Genios Pro spectrophotometer (Tecan Group Ltd., Männedorf, Switzerland). Fluorescence of unloaded cells (caused by autofluoresence and light scattering) was subtracted from the readings to provide the zinquin-dependent fluorescence.

### 4.3.8 Quantitative real time PCR (Q-RT PCR)

Treated cells were washed in PBS for 3 times before being lysed in the plate with TRIzol reagent (Invitrogen Corp. Carlsbad, CA) for RNA extraction according to the manufacturer's instruction. The isolated total RNA were quantitated by spectrophotometry using a SPECTRAmax Plus spectrophotometer (Molecular Devices, Sunnyvale, CA) and 1 µg of total RNA was used for cDNA synthesis in a 20 µL system with an AffinityScript Multiple Temperature cDNA synthesis Kit (Stratagene, La Jolla, CA) according to the manufacturer's instruction. A sample of

0.5 μL of the 20 μL cDNA product was used in a 25 μL RT-PCR reaction system as template and amplified by *Taqman* PCR Master Mix (Applied Biosystems, Foster City, CA) according to manufacturer's instruction. Primers and probe sets for RT PCR for MTF-1 (Assay ID Hs00232306_m1) and GAPDH (Assay ID Hs99999905_m1) were purchased from the *TaqMan* Gene Expression Assays of Applied Biosystems (Foster City, CA) and the assays were carried out according to the manufacturer's instruction. The Primers and probes sets for detecting total MT were synthesized by Applied biosystems (Foster City, CA) as a custom order because no single common amplicon region was found for all the 8 MT isoforms, MT1H, -1H-like, -1G, -1L, -1E, -1A, and MT2, most highly expressed in human mononuclear cells (Cousins et al., 2003). A combination of two forward primers, two reverse primers and two *Taqman* probes was used to amplify all the 8 MT isoforms in one single assay. For this assay, the concentration for the four primers was at 450nM each, and that for the two probes was each at 125 nM. The Primer/probes for MTF-1, Total MT and GAPDH are shown in **Table 1**. Q-RTPCR was performed with a polymerase-activating step of 95 $^{o}$C for 10 min, followed by 40 cycles of 95 $^{o}$C for 15 s and 60 $^{o}$C for 1 min, and 95 $^{o}$C for 15 s. The real-time fluorescent signal was detected and quantitated by an ABI PRISM 7000 Sequence Detection System (Applied Biosystems, Foster City, CA).

**Table 1. Sequences of primers and probes for quantitative RT-PCR**

| Name | Sequences |
|---|---|
| hMT1, 2 | Forward: 5’ GCACCTCCTGCAAGAAAAGCT 3’ |
| | Probe 5’ FAM CACAGCCCACAGGGCAGCAGG BHQ1 3’ |
| | Reverse: 5’ GCAGCCTTGGGCACACTT 3’ |
| hMT1, 2 Alt | Forward: 5’ GCACCTCCTGCAAGAAGAGCT 3’ |
| | Probe: 5’ FAM CACAGCCCACAGGACAGCAGG BHQ1 3’ |
| | Reverse: 5’ GCAGCCCTGGGCACACTT 3’ |
| GAPDH | Forward: 5’ Assay ID Hs99999905_m* |
| | Probe: 5’ FAM GGAAAAGCCATTTCGGTGCGATCAC NFQ 3’ |
| | Reverse: 5’ Assay ID Hs99999905_m* |
| MTF-1 | Forward: 5’ Assay ID Hs00232306_m1* |
| | Probe: 5’ FAM TTGGGCGCCTGGTCACCAGGGCTGC NFQ 3’ |
| | Reverse: 5’ Assay ID Hs00232306_m1* |

*Primer sequences for the Taqman Gene Expression Assays are confidential information of ABI. The assay ID numbers are listed.

### 4.3.9 Cell morphology and fluorescence microscopic imaging

Cells were cultured in Nunc Lab-Tek II Chamber Slide (8 wells) and treated accordingly as described above for 3 days. Morphological pictures of live cells were taken under a microscope before further experimental procedures. Cells were then washed three times in PBS, before fixation by the addition of 3.7% formaldehyde to each well for 30 min at 37 $^{o}$C. The fixed cells were washed three times with PBS, incubated with 25 μM of zinquin ethyl ester in PBS for 30 min at 37 $^{o}$C, and then washed 3 times with PBS. A coverglass was mounted on top of the slide and Vaseline was used to seal the edge of the coverglasses to prevent evaporation. The slides were then placed under a Zeiss AxioObserver 100 fluorescence microscope for image acquisition. Fluorescence of individual cells was observed by using the filter cube set 49 for DAPI (ex. 365nm, FT 395nm, em. 445nm). Photomicrographs for each treatment were taken using the same magnification scale (200X), exposure time (2s) within 10 min to avoid errors from the autofading of the fluorescence signal.

### 4.3.10 Reactive Oxygen Species (ROS) assay

NHPrE cells were cultured in Nunc Lab-Tek II Chamber Slide (8 wells) at 7500 cells/well and treated accordingly as described above for 24 hours. A dye named 5-(and-6)-chloromethyl-2', 7'-dichlorodihydrofluorescein diacetate, acetyl ester (CM-$H_2$DCFDA), a cell-permeant indicator for reactive oxygen species, was added into the medium at a final concentration of 10 μM. After incubation in 37 $^{o}$C incubator for 30 min, the chamber was then placed under a Zeiss AxioObserver 100 fluorescence microscope for image acquisition. Fluorescence of individual cells was observed by

using the filter cube set 43 for GFP (ex. 470nm/40nm, FT 495nm, em. 525/50nm). Photomicrographs for each treatment were taken using the same magnification scale (100X), exposure time (6ms) within 10 min to avoid errors from the autofading of the fluorescence signal.

### 4.3.11 Senescence assay

Senescence assay was conducted using a Senescence Detection Kit (MBL Co. Ltd., Woburn, MA) according to the manufacturer's instruction. Briefly, NHPrE cells were cultured in 24-well plates with a density of 6000 cells/well and treated for 3 days. The culture medium was removed and the cells were washed once with PBS. The cells were then fixed in 0.25 mL of Fixative Solution at room temperature for 10 min. After another wash with PBS, the cells were stained in 250 μL 1X staining solution containing 1mg/mL X-gal and 1X staining supplement for 12 hours. Cells were then overlayed with 70% glycerol and stored at 4 $^{o}$C for storage or observed under a microscope for development of blue color.

### 4.3.12 Statistical analysis

Data were analyzed with SAS 9.1.3 windows software (SAS Institute Inc., Cary, NC) and presented as mean ± SEM. Student's t test between control and treated group was employed in the cell cycle distribution analysis. A one-way ANOVA followed by least significant differences (LSD) was used to determine the statistical significance among treated groups and controls in other experiments. The level of statistical significance is set at $p < 0.05$.

## *4.4 Results*

### 4.4.1 Resveratrol is the major factor that inhibits the proliferation of NHPrE cells

NHPrE cells were cultured in 6-well plates and treated in a 6X4 factorial design as described in Materials and Methods section 4.3.2 for 3 days before being collected and the total cell count was determined by the NucleoCounter using the Nucleocassette Kit and NucleoView software (New Brunswick Scientific, Edison, New Jersey), according to the manufacturer's protocol. Cell growth of NHPrE cells, as determined by total cell number per plate, was markedly depressed by resveratrol but to lesser extent by zinc (**Fig. 1A**). After 3 days of culture, resveratrol treatement exerted little or no reduction in cell growth until the concentration reached 2.5 μM, which resulted in an average of 30 % reduction, as compared to no addition of resveratrol among all zinc treatments (**Fig. 1A**). Thereafter, a progressive reduction in cell growth was observed with the increase in resvertrol concentration to 5 and 10 μM among each zinc treatment. In general, there was little or no change in the pattern in cell growth reduction among zinc treatments, with the exception of lower cell growth in ZD and ZS cells as compared to ZN and ZA cells treated with no or 05 μM resveratrol. Similarly, Han (2007) has observed lower cell growth in ZD and ZS than ZN NHPrE cells not treated with resveratrol.

### 4.4.2 Resvertrol significantly enhances total zinc level in NHPrE cells

Total intracellular zinc content was measured using atomic absorption spectrophometry as described in Materials and Methods and then normalized with the cell number as the denominator. Resveratrol exerted little or no increase in cellular zinc level until 5 μM, as compared to no addition of resveratrol, among all zinc treatments. A further marked increase in cellular zinc level was observed with 10 μM resveratrol in each zinc treatment. In the ZD, ZN and ZA cells, a similar pattern of little or no change in cellular zinc status was observed among the no or low resveratrol treatments (0, 0.5, and 1 μM). However, in the ZS cells, as the resveratrol concentration was increased to 1, 2.5, 5 or 10 μM, dramatic increases of total cellular zinc by 2-, 3-, 5-, and 7.5- fold were observed, respectively (**Fig. 1B**).

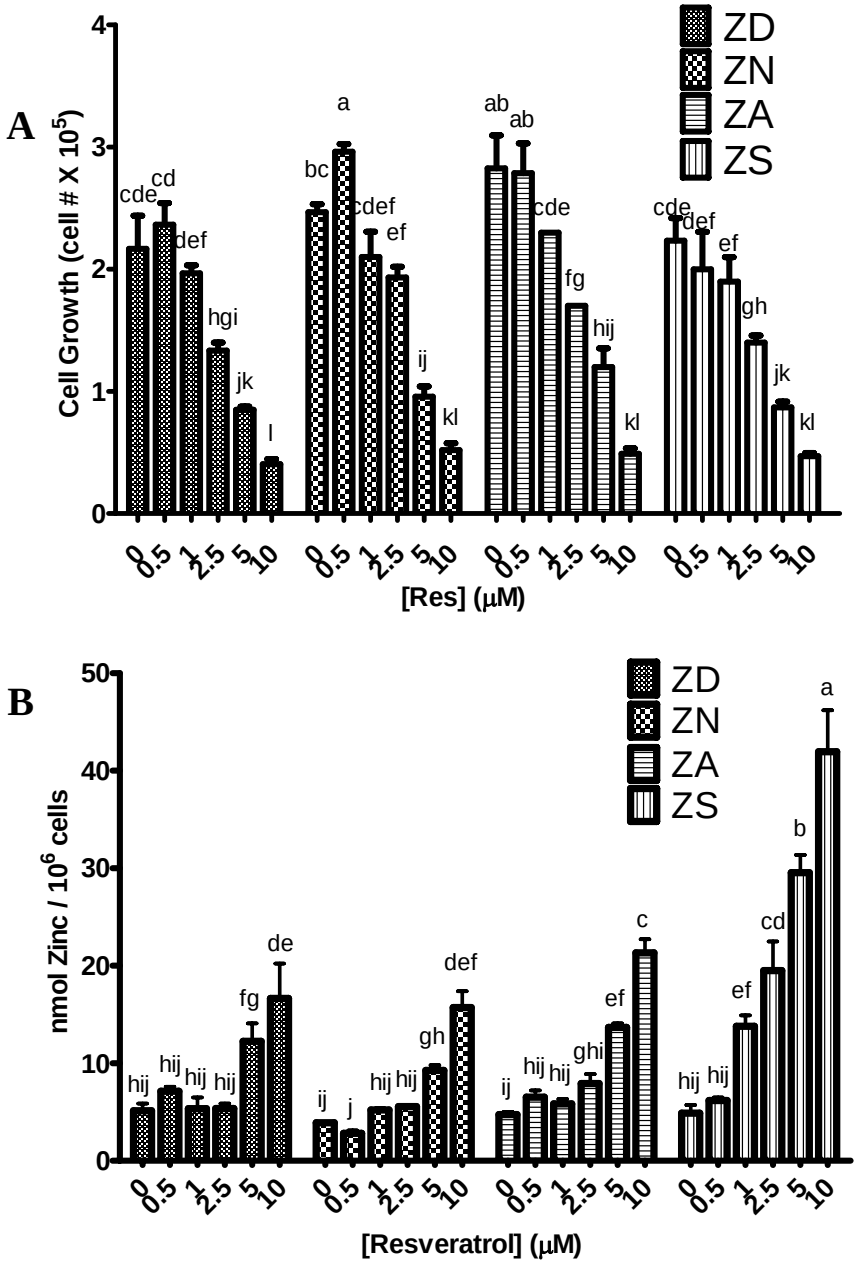


**Figure 1. The effect of resveratral and zinc on the proliferation (A) and the total intracellular zinc level (B) of NHPrE cells**. The NHPrE cells (25,000/well) were plated in 6-well plates and treated by 6 levels of resveratrol (0, 0.5, 1, 2.5, 5 and 10 μM) and 4 levels of zinc (ZD, ZN, ZA and ZS) for 3 days before being harvested. The total cell count for each sample was attained by the NucleoCounter using the

Nucleocassette Kit and NucleoView software (New Brunswick Scientific, Edison, New Jersey), according to the manufacturer's protocol. Cellular zinc status was determined by atomic absorption spectrophotometry. Nanogram of zinc per million cells was expressed to account for any differences in cell numbers between samples. Values are means ± SEM from 3 separate experiments. Different letters indicate significant differences among groups ($p<0.05$); treatments with the same letter indicate no significant difference. Similar results were observed using NHPrE cells from another donor with the same experimental design.

### 4.4.3 Resveratrol does not affect the proliferation and intracellular zinc level of HepG2 cells, but zinc does

Since the liver is an important organ responsible for heavy metal metabolism and storage, a similar experiment was carried out in HepG2 cells as in the NHPrE cells to investigate if resveratrol and zinc would affect the proliferation and intracellular zinc content in HepG2 cells. Zinc was found to be the only factor that actually affected the proliferation of HepG2 cells significantly, with about 20% cell number reduction in ZD cells and no change in ZA and ZS cells as compared to ZN cells (**Fig. 2A**). This observation confirmed previous findings from our lab (Wong et al., 2007). In addition, intracellular total zinc level in HepG2 cells increased progressively as the zinc level of the media increased from ZD to ZS, as observed in the past (Wong et al., 2007). Resveratrol appeared to have no overall effect on cell proliferation and intracellular zinc content in HepG2 cells, since in each zinc group, the resveratrol treatments did not alter cell number and total zinc content. However, high levels of resvertraol (5 and 10 μM) tended to depress intracellular total zinc by about 20 % in ZD cells, but not in ZN, ZA and ZS cells (**Fig. 2B**).

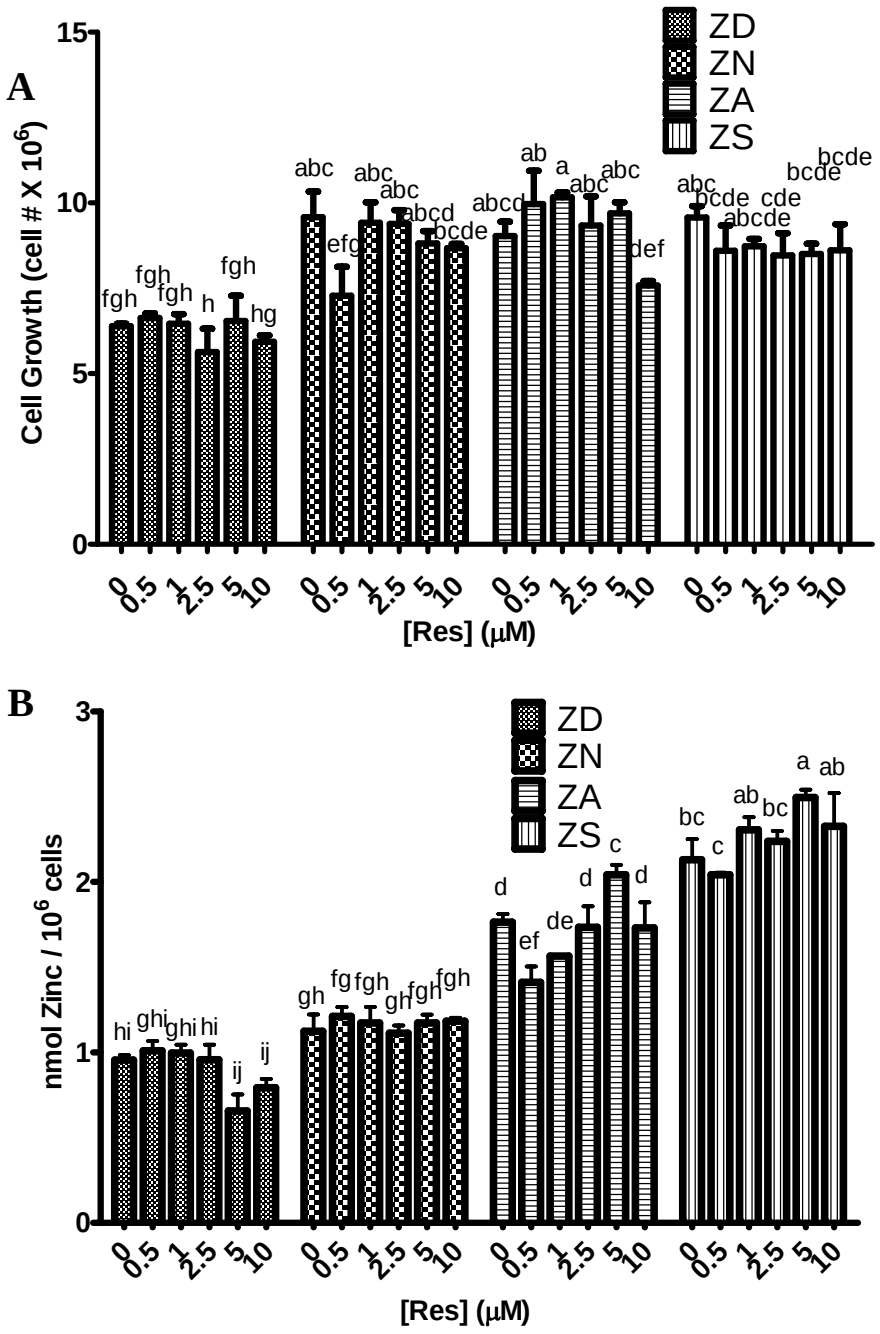


**Figure 2. The effect of resveratral and zinc on the proliferation (A) and the total intracellular zinc level (B) of HepG2 cells**. The HepG2 cells (250,000/well) were plated in 6-well plates and treated by 6 levels of resveratrol (0, 0.5, 1, 2.5, 5 and 10 μM) and 4 levels of zinc (ZD, ZN, ZA and ZS) for 3 days before being harvested. The total cell count for each sample was attained by the NucleoCounter using the

Nucleocassette Kit and NucleoView software (New Brunswick Scientific, Edison, New Jersey), according to the manufacturer protocol. Cellular zinc status was determined by atomic absorption spectrophotometry. Nanogram of zinc per million cells was expressed to account for any differences in cell numbers between samples. Values are means ± SEM from 3 separate experiments. Different letters indicate significant differences among groups ($p<0.05$); treatments with the same letter indicate no significant difference.

### 4.4.4 Resveratrol inhibits the proliferation of NHPrE cells by causing cell cycle arrest at G2/M stage, but not apoptosis

We were very interested in the resveratrol-dependent inhibition of proliferation in NHPrE cells. Therefore, a cell cycle distribution study was perfomed to examine the influence of resveratrol (with or without 10 μM) in the ZN NHPrE cells. Treatment with 10μM of resveratrol caused 1.5-fold increase of the percentage of cells in G2/M phase (from 12% to 30%) compared to the controls, indicating an obvious G2/M arrest (**Fig. 3B**). No sign of apoptosis was detected in the control cells or cells treated with 10 μM resveratrol, as indicated by the clean Apo region observed in **Fig. 3A**.

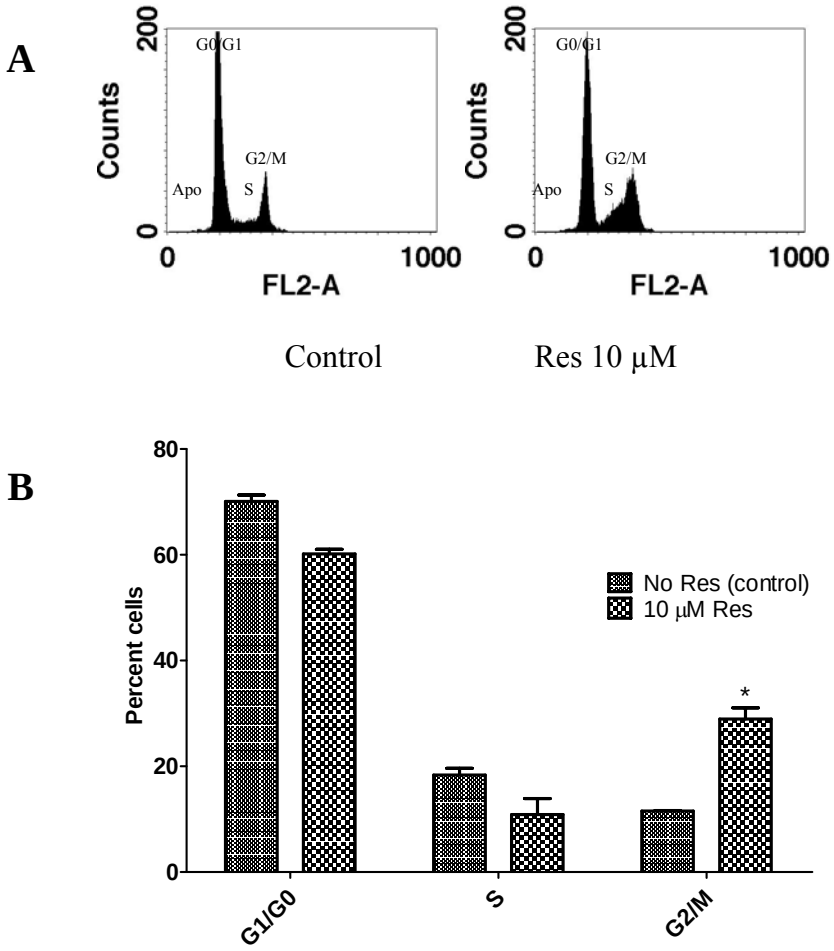


**Figure 3. The effect of resveratrol on cell cycle progression of NHPrE cells.** The NHPrE cells (25,000/well) were plated in 6-well plates with (10 μM) or without resveratrol under ZN condition for 3 days. The cell cycle distribution of collected cells was determined by flow cytometry as described in Material and Methods. Open graphs (A) are the raw data from flow cytometry. The given results are a representative of three seperate experiments. Bar graphs (B) show the percentage of cells at each phase of the cell cycle: G0/G1 phase, S phase, and G2/M phase, calculated by the computer software, CELLQuest. Values are means ± SEM from 3 separate experiments. * depicts a significant increase in the percentage of cells in G2/M as analyzed by the Student's *t* test ($p<0.05$).

### 4.4.5 Resveratrol chelates zinc *in vitro*

In the present study, the marked enhancement of total intracellular zinc content, especially in ZA and ZS cells suggests that resveratrol may form a complex with Zn(II) at with Cu(II)and it is the complex that brings in most of zinc through a separate channel which is different from free zinc ion trafficking. Thus, to address this issue, an *in vitro* experimental system was designed to include 7 levels of Zn(II) (0, 2, 4, 8, 16, 24 and 32 μM), in the form of $ZnSO_4$, and 4 levels of resveratrol (0, 5, 10 and 20 μM) in a 100 μL PBS. With the addition of zinquin, a membrane-permeant fluorophore specific for Zn(II), the amount of free Zn(II) in the system was detected by the amount of fluorescence given out by the zinquin-Zn(II) complex. By keeping zinquin concentration constant at 25 μM, a dose-dependent decrease of fluorescence was observed along with increased concentration of resveratrol at 4, 8, 16, 24 and 32 μM Zn(II) (**Fig. 4A**). In addition, with different concentration of zinquin (5 or 25 μM), there was a significant decrease of fluorescent signal in treatment Res10 (resveratrol at 10 μM) compared to control Res0 (resveratrol at 0 μM) at 4, 8, 14, 24 and 32 μM Zn(II) (**Fig. 4B**).

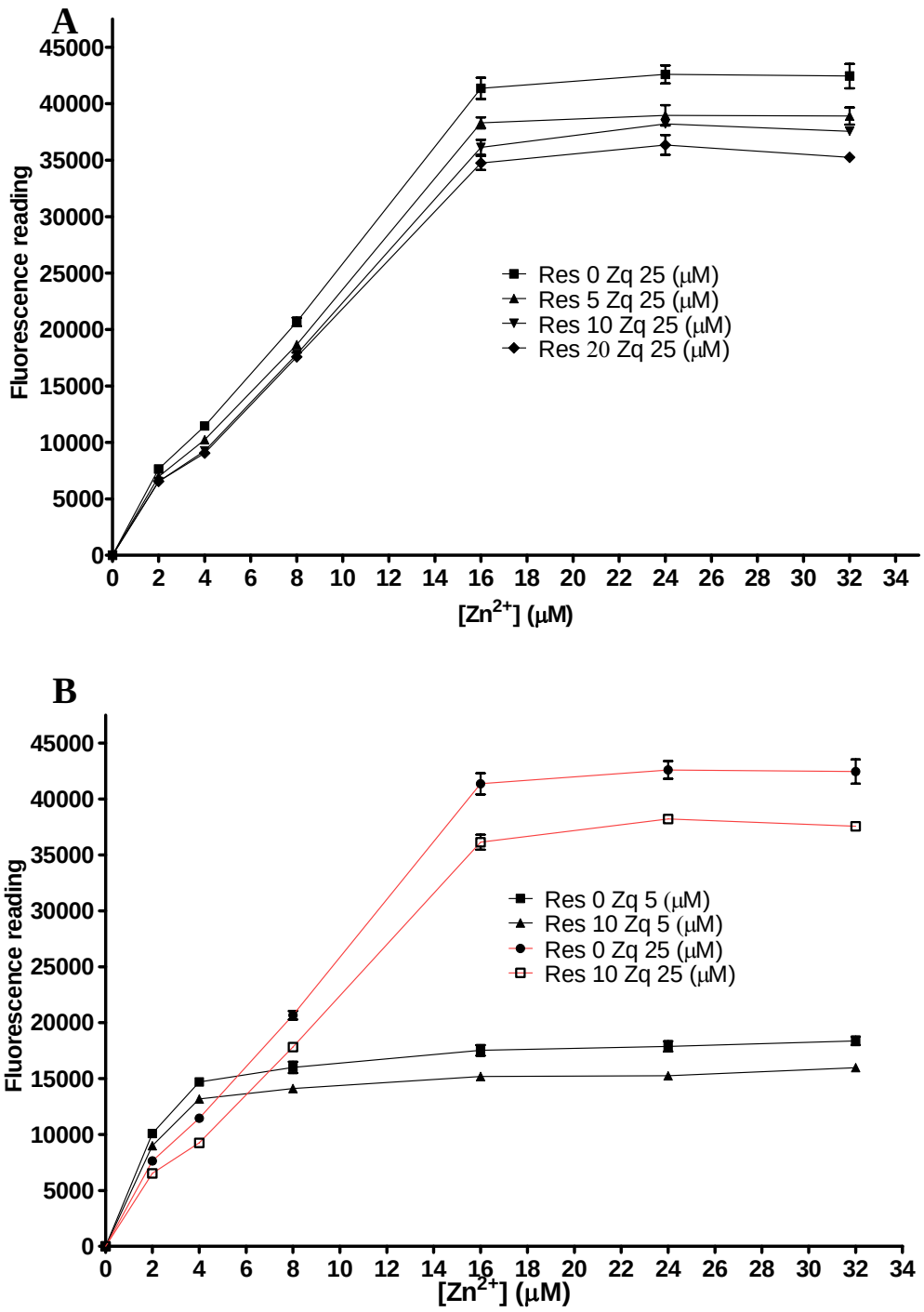


**Figure 4. The chelating effect of resveratrol for zinc**. The experiments were carried out in a 100 μL PBS system with indicated concentration of components. The plate was incubated at 37 $^{o}$C for 5 min before fluorescent signal was quantitated at an

excitation wavelength of 340 nm and emission wavelength of 460 nm.Values are the direct reading of fluorescent signal, represented by means ± SEM from 3 separate experiments.

### 4.4.6 Resveratrol enhances the effect of zinc supplementation on intracellular free labile zinc level

Labile pool of intracellular zinc plays an important role in many cell activities. To investigate the effect of resveratrol on the intracellular labile zinc level, we used zinquin ethyl ester, which emitts much stronger fluorescent signal than zinquin (**Fig. 6**), to visualize the free labile zinc pool under a fluorescence microscope as well as to quantitate free labile zinc level using spectrofluorimetry (**Fig. 5**). Zinquin-Zn(II) associated fluorescence was found to be deposited mainly in the secretary granules in the cytoplasm. Clear dark zone in the center of cells representing nuclei can be identified easily until loss of nuclear membrane (**Fig. 6**).

Resveratrol treatment at 10 μM markedly increased intracellular free labile zinc status as measured by spectrofluorimetry in ZA and ZS cells by 52% and 49%, respectively, as compared to their corresponding controls with no resveratrol (**Fig. 5**). In contrast, resveratrol treatment at 2.5 μM resulted in no increase in intracellular free labile zinc level in ZA and ZS cells (**Fig. 5**). Moreover, in ZD and ZN cells, resveratrol treatment at 2.5 or 10 μM exerted no effect on intracellular free zinc level (**Fig. 5**).

The fluorescence microscopic results (**Fig. 7**) revealed a clear ascending trend of fuorescent signal for the ZD, ZN, ZA and ZS cells without the treatment of resveratrol (**Fig. 7**), indicating that the mediam zinc concentration and total intracellular zinc status positively affected intracellular free labile zinc level. As to the effect of resveratrol on the free labile zinc, increased fluorescent signal was observed in the ZA and ZS cells treated with 10 μM resveratrol, as compared to their

corresponding controls treated without resveratrol. In addition, no difference in fluorescent signal was identified in ZD and ZN cells among the 0, 2.5 and 10 μM resveratrol treatments (**Fig. 7**). The fluorescence microscopic imaging results appeared to substantiate those derived from spectrofluorimetry (**Fig. 5 and 7**).

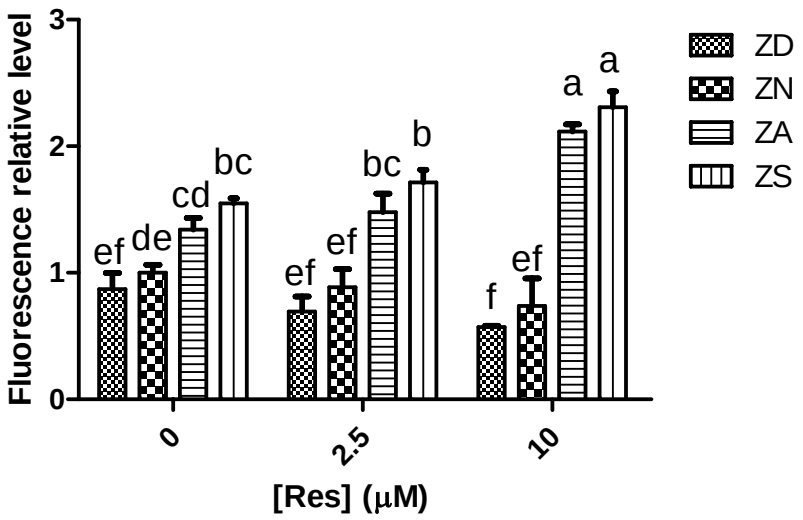


**Figure 5. The effect of resveratrol and zinc on intracellular free labile zinc status (by spectrofluorimetry)**. NHPrE cells were cultured in 6-well plates and treated by 3 levels of resveratrol (0, 2.5 and 10 μM) and 4 levels of zinc (ZD, ZN, ZA and ZS) for 3 days before being collected. The total cell count for each sample was attained by the NucleoCounter using the Nucleocassette Kit and NucleoView software (New Brunswick Scientific, Edison, New Jersey), according to the manufacturer's protocol. The final cell density of each sample was set to be 1 X $10^6$/mL. An aliquot of 100 μL of each sample was transferred to a 96-well plate in triplicates and 25 μM of zinquin ethyl ester were added into each well. The fluorescent signal in each sample was normalized according to its own cell number and the one from ZNR0 was set to be 1. Values are means ± SEM from 3 separate experiments.

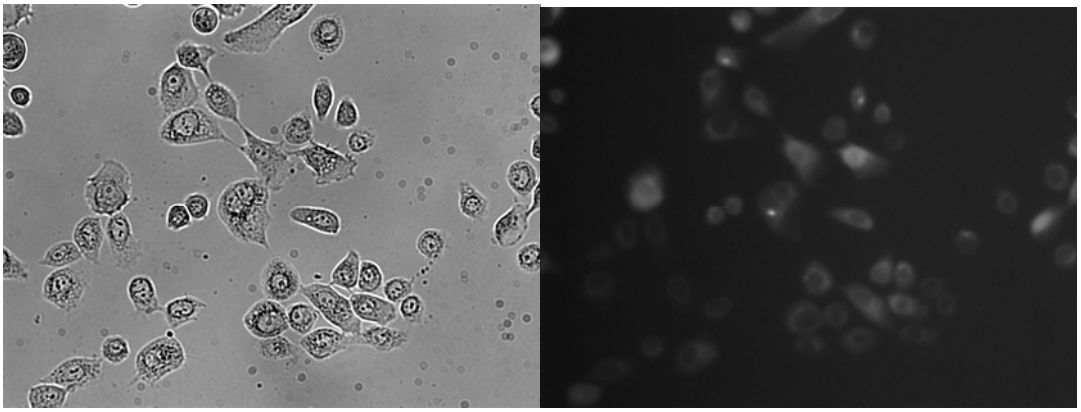

**A**

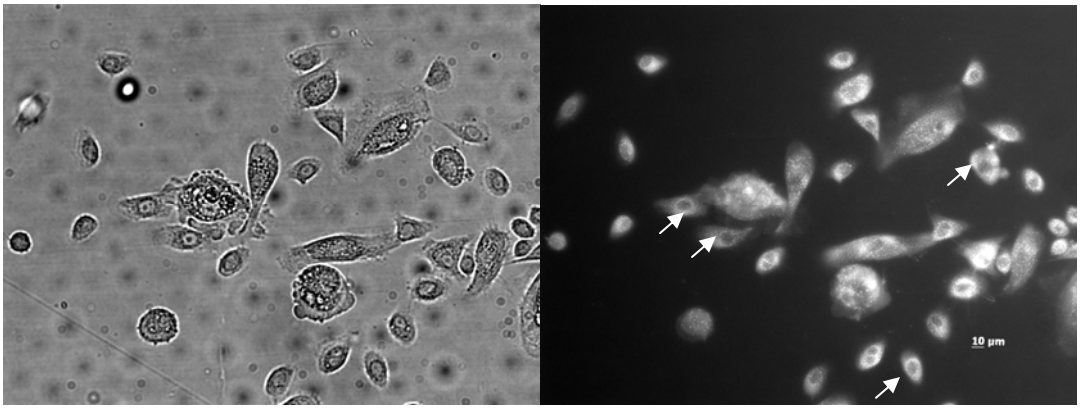


**B**

**Figure 6. Comparison of cellular fluorescent signal by zinquin (A) and zinquin ethyl ester (B)**. NHPrE cells were cultured in ZN condition for 3 days in Nunc Lab-Tek II Chamber Slide (8-well) before being fixed by 3.7% formaldehyde and stained by 25 µM zinquin or zinquin ethyl ester. After that, cells were observed under a fluorescent microscope with excitation wavelength at 365 nm, emission wavelength at 445 nm and magnification at 200X. Pictures on the left column show the cells under normal setting (no fluorescence), while pictures on the right show the cells under fluorescence settings (with fluorescence). Arrows indicate the location of nuclei. Shown image is the representative of 3 seperate experiments.

Fig. 7

**ZD**

[Res]: 0 μM

[Res]: 2.5 μM

[Res]: 10 μM

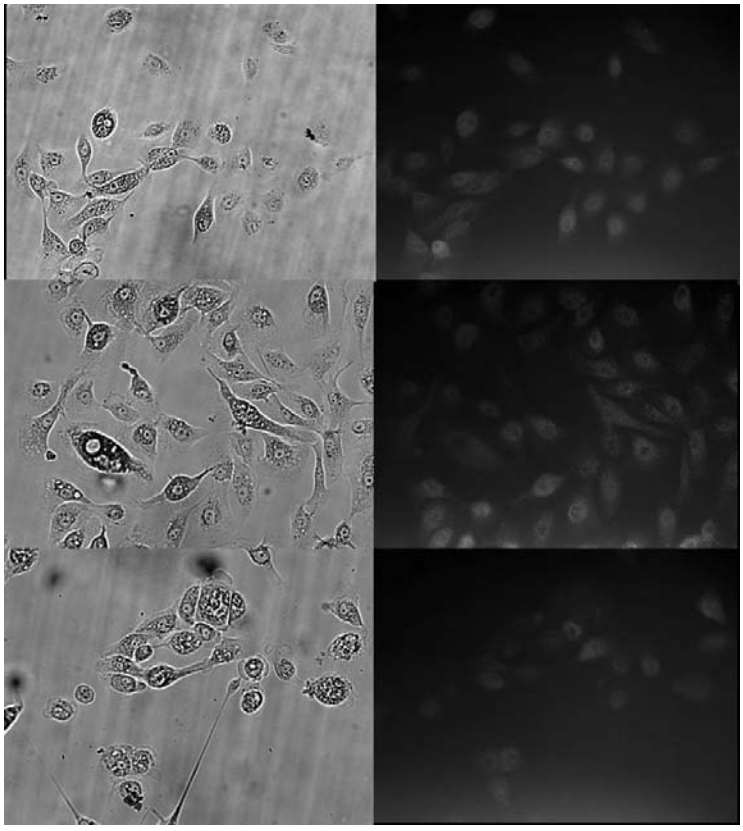

**ZN**

[Res]: 0 μM

[Res]: 2.5 μM

[Res]: 10 μM

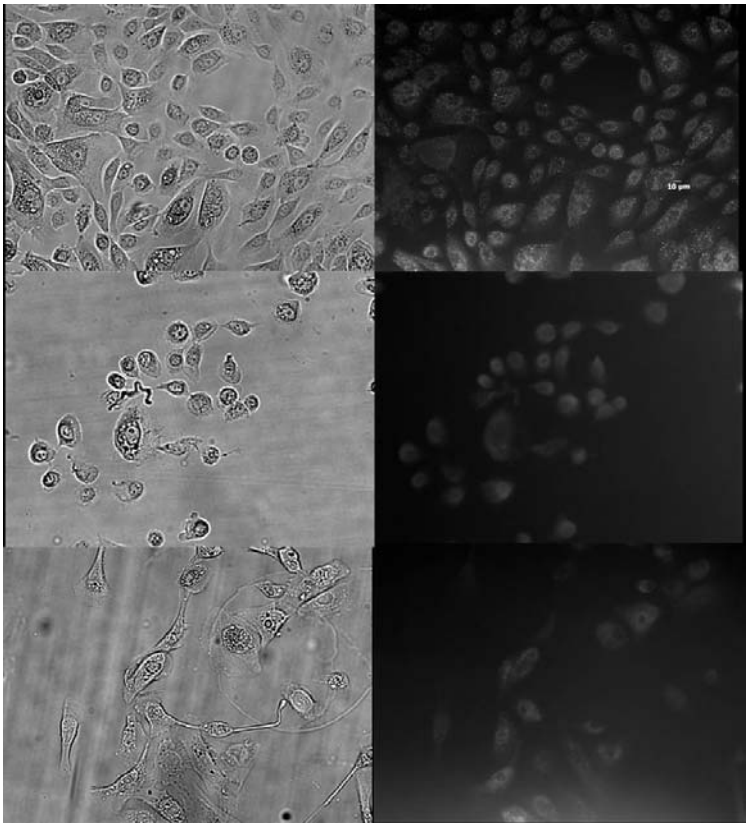

Fig. 7

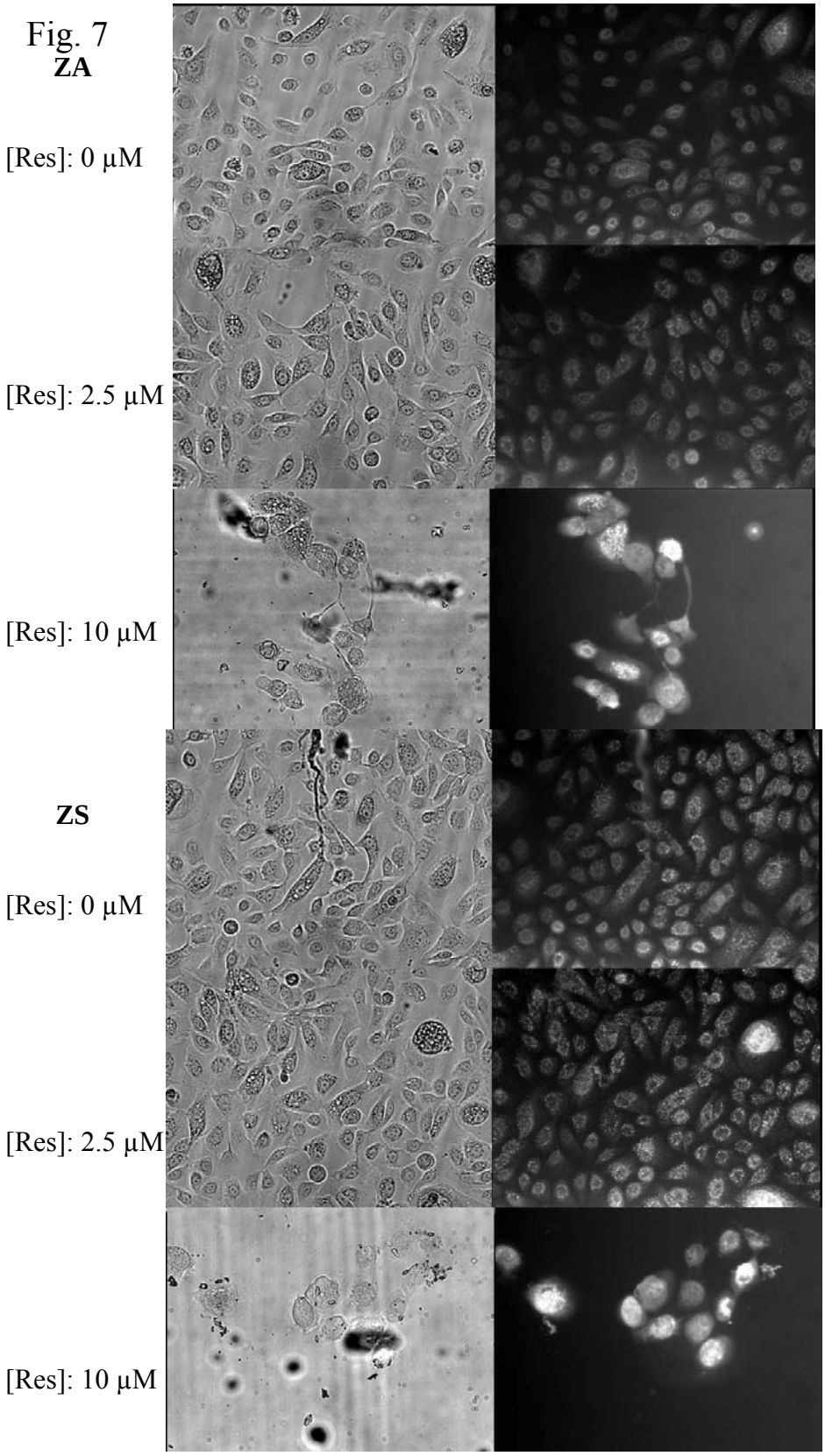

**Figure 7. The effect of resveratrol and zinc on intracellular free labile zinc status (by fluorescence microscopic imaging)**. NHPrE cells were cultured in Nunc Lab-Tek II Chamber Slide (8 wells) and treated by 3 levels of resveratrol (0, 2.5 and 10 μM) and 4 levels of zinc (ZD, ZN, ZA and ZS) for 3 days being fixed by 3.7% formaldehyde and stained by 25 μM zinquin ethyl ester for 30 min at 37 $^{o}$C. After that, cells were observed under a fluorescent microscope with excitation wavelength at 365 nm, emission wavelength at 445 nm and magnification at 200X. Pictures on the left column show the cells under normal setting (no fluorescence), while pictures on the right show the cells under fluorescence settings (with fluorescence). Shown images are the representatives from 3 seperate experiments.

### 4.4.7 The effect of zinc and resveratrol on the MT and MTF-1 mRNA abundance

Metallothionein (MT), the major labile zinc bind protein, has been reported to be upregulated by zinc supplementation and positively correlated with the total and labile free intracellular zinc level under a range of zinc status from deficient to adequate. In view of the marked increase in total cellular zinc by resveratrol treatment, the abundance of MT and MTF-1 mRNA was measured to determine if they are affected by resveratrol treatment. Interestingly, MT mRNA level was only affected by cellular zinc status, and not by resveratrol (**Fig. 8A**). Without resveratrol treatment, the MT mRNA level of ZS cells was higher than ZD and ZN cells (Fig. 8A). With 10 μM resveratrol treatment, the abundance of MT mRNA of ZS cells was higher than ZD, ZN and ZA cells. Moreover, there were no significant difference of MT mRNA abundance between the – Res and + Res treatment in all 4 zinc groups. In addition, both resveratrol and zinc treatment appeared to have little or no significant effect on the abundance of MTF-1 mRNA in NHPrE cells (**Fig. 8B**).

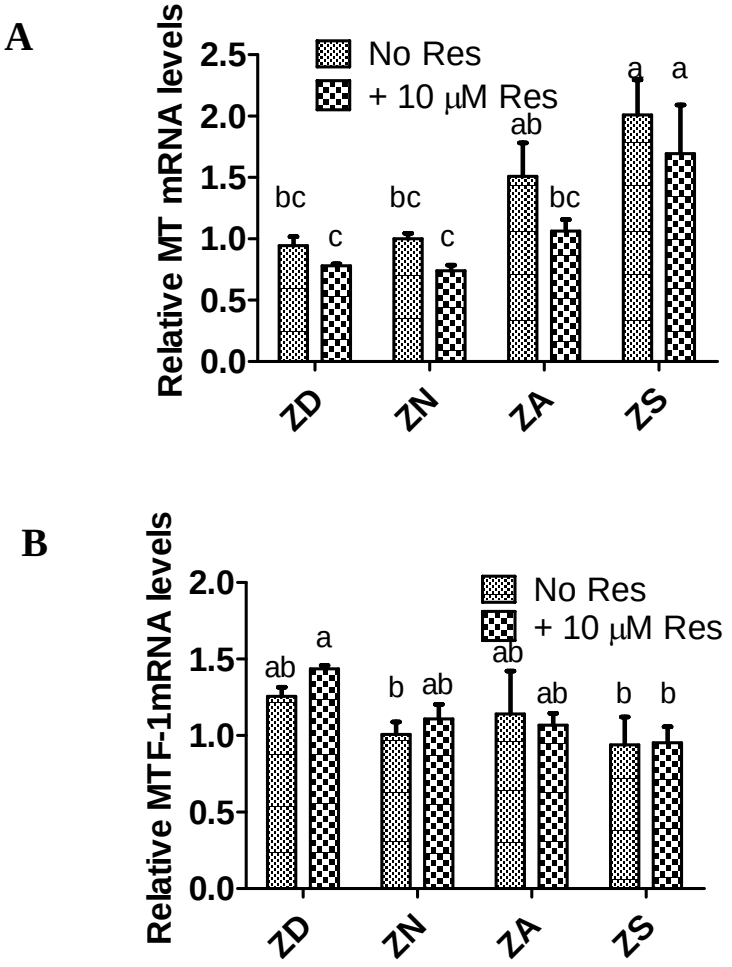


**Figure 8. The effect of resveratrol and zinc on the total MT (A) and MTF-1 (B) mRNA abundance.** NHPrE cells were cultured in 6-well plates and treated by 2 levels of resveratrol (0 and 10 μM) and 4 levels of zinc (ZD, ZN, ZA and ZS) for 3 days before being collected. Total RNA were extracted from these cell samples and 1 μg of extracted total RNA were reversely transcribed into cDNA. Q-RTPCR analyses were performed in triplicates. Relative quantity was established by using GAPDH as the endogenous normalization control. The mRNA level of ZN without resveratrol cells was set as 1. Values are means ± SEM from 3 separate experiments.

### 4.4.8 Resveratrol induces senescence in NHPrE cells through ROS generation

Althought the NHPrE cells treated with resveratrol and zinc were not apoptotic, they all exhibited impaired proliferation, especially in 10 μM resveratrol treated cells at all zinc levels with only one population doubling in 3 days (**Fig. 1A**). The proliferation inhibition, but not apoptosis induction effect of resveratrol was highly likely to be mediated by the enhanced Reactive Oxygen Species (ROS) generation as a byproduct from the interaction between the resveratrol and transition metals, especially Zn(II). Therefore, the ROS levels of NHPrE cells treated with 3 levels of resveratrol (0, 2.5 and 10 μM) and 4 levels of zinc status (ZD, ZN, ZA and ZS) were determined using a dye named 5-(and-6)-chloromethyl-2', 7'-dichlorodihydrofluorescein diacetate, acetyl ester (CM-$H_2$DCFDA), a cell-permeant indicator for ROS. The increase of resveratrol concentration in culture medium significantly enhanced cellular ROS level of NHPrE cells, starting from 2.5 μM and reaching the highest at 10 μM, at each zinc level after one day of incubation, as indicated by the resveratrol dose dependent increase of fluorescent signal (**Fig. 9**). In ZA and ZS cells, ROS levels appared to be higher than ZD and ZN NHPrE cells treated with resveratrol.

Morphological changes such as flatten shape, larger volume, larger nuclei and wide spread of cell body were observed in resveratrol treated NHPrE cells, especially in the ZA and ZS cells (**Fig. 10**). Moreover, these treated cells were not as tolerable as the controls to the sub-optimal culturing environment. Exposure of the NHPrE cells treated with 10 μM resveratrol outside the incubator at room

temperature for 15 min resulted in the cells becoming dismembered and could not recover as the control cells (data not shown).

Since the observed morphological changes of NHPrE cells match the description of those detected in cells undergoing senescence, senescent NHPrE cells in the same experimental design as in the ROS assay were detected by a senescence detection kit designed to histochemically detect senescence-associated expression of β-galactosidase (SA-β-Gal) activity by x-gal in cultured cells. The percentage of senescent cells increased following the resveratrol concentration ladder in all 4 zinc treatements. Increased zinc concentration appeared to induce enhanced senescence when cells were treated with 2.5 or 10 μM resveratrol (**Fig. 11**). The strongest effect was observed in the ZA and ZS cells, with about 10% and 70% cells undergoing senescence when treated with 2.5 and 10 μM resveratrol, respectively.

**Fig. 9**

**ZD**

[Res]: 0 μM

[Res]: 2.5 μM

[Res]: 10 μM

**ZN**

[Res]: 0 μM

[Res]: 2.5 μM

[Res]: 10 μM

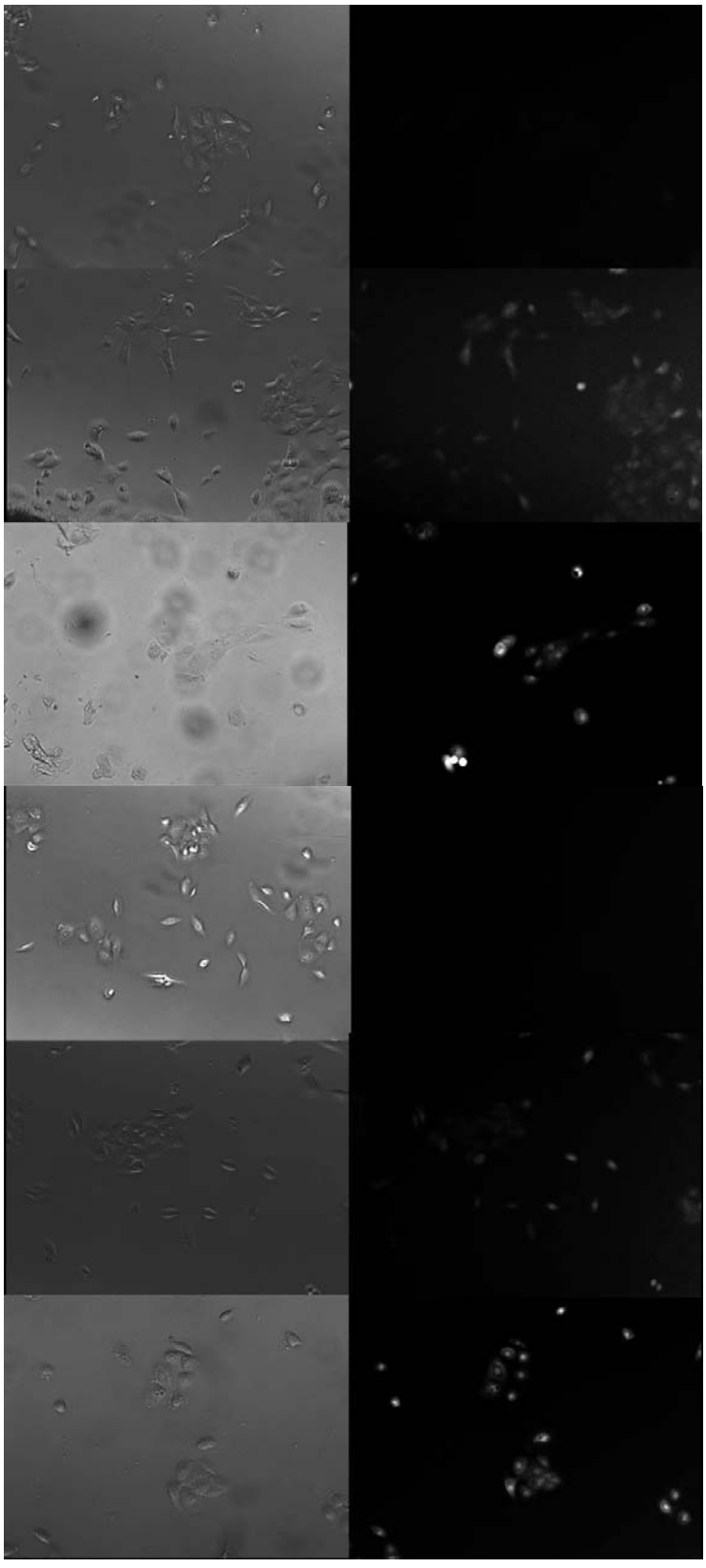

**Fig. 9**

**ZA**

[Res]: 0 μM

[Res]: 2.5 μM

[Res]: 10 μM

**ZS**

[Res]: 0 μM

[Res]: 2.5 μM

[Res]: 10 μM

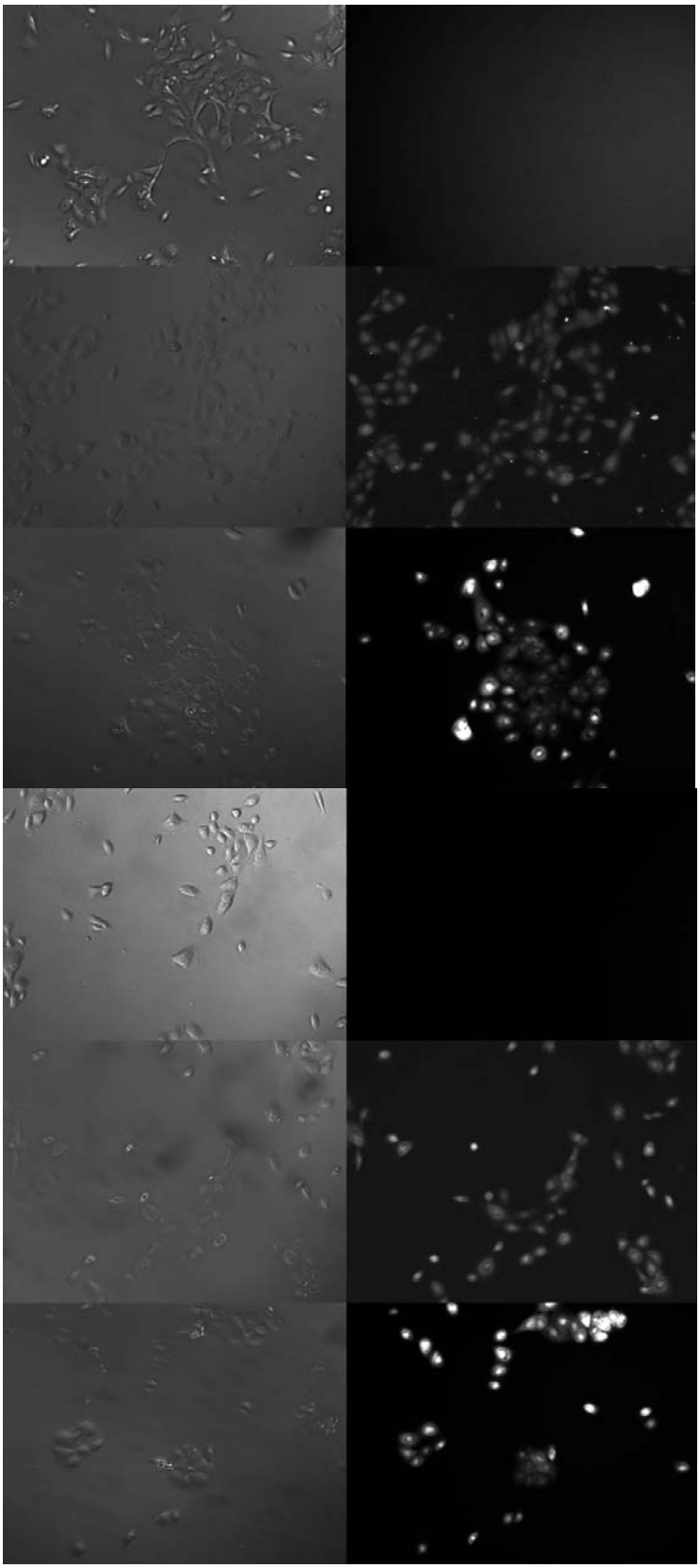

**Figure 9. The effect of resveratrol and zinc on reactive oxygen species (ROS) generation in NHPrE cells**. NHPrE cells were cultured in Nunc Lab-Tek II Chamber Slide (8 wells) and treated by 3 levels of resveratrol (0, 2.5 and 10 μM) and 4 levels of zinc (ZD, ZN, ZA and ZS) for 24 hours before being stained by 10 μM 5-(and-6)-chloromethyl-2', 7'-dichlorodihydrofluorescein diacetate, acetyl ester (CM-H2DCFDA), a cell-permeant indicator for ROS for 30 min at 37 $^{o}$C. After that, cells were observed under a fluorescent microscope with excitation wavelength at 470 nm, emission wavelength at 525 nm and magnification at 100X. Pictures on the left column show the cells under normal setting (no fluorescence), while pictures on the right show the cells under fluorescence settings (with fluorescence). Shown image is the representative of 3 seperate experiments.

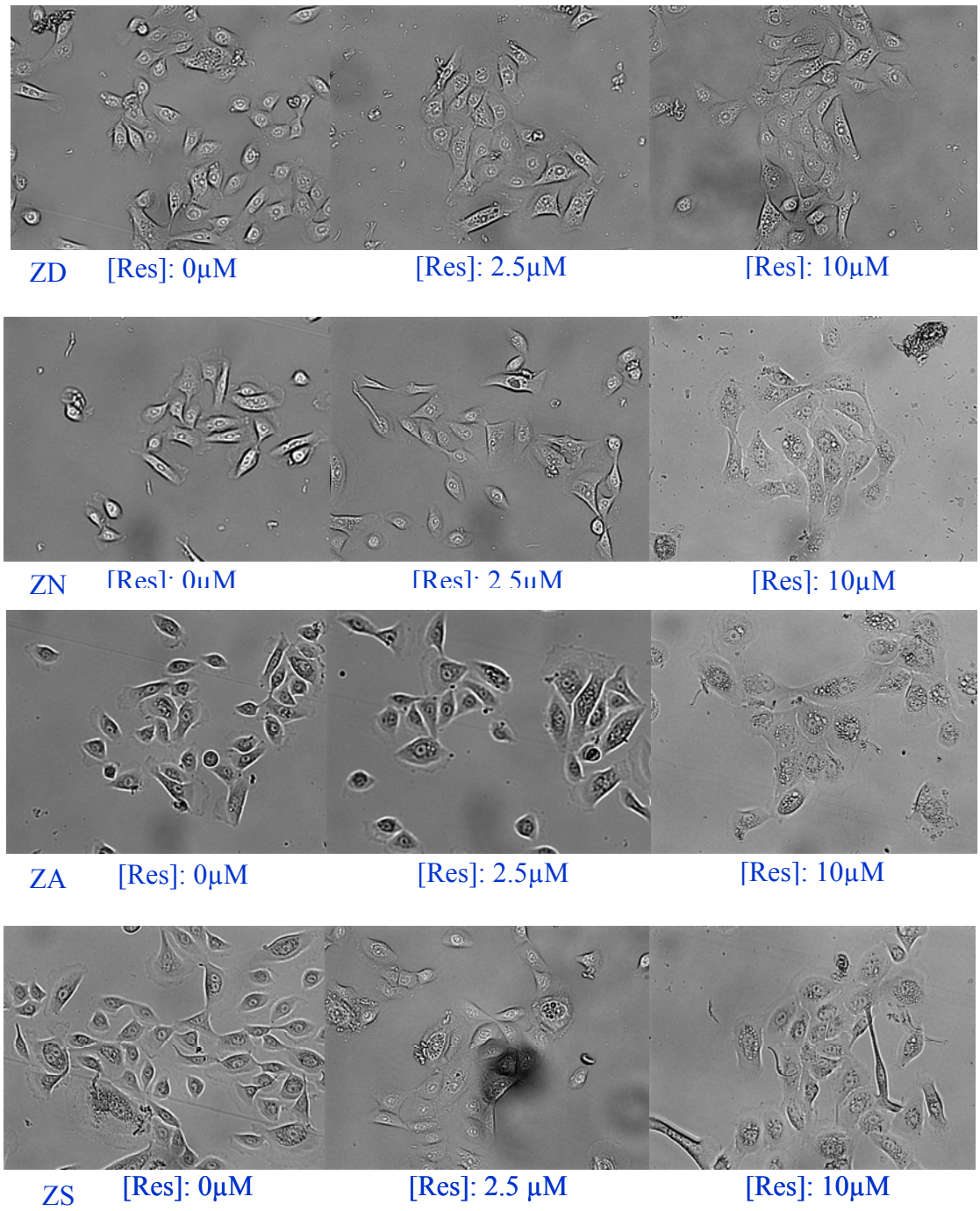


**Figure 10. Morphological change caused by resveratrol and zinc treatment in NHPrE cells**. NHPrE cells were cultured in Nunc Lab-Tek II Chamber Slide (8 wells) and treated by 3 levels of resveratrol (0, 2.5 and 10 μM) and 4 levels of zinc (ZD, ZN,

ZA and ZS) for 3 days before being examined under a microscope at a magnification of 200X. Shown images are the representative findings of 3 seperate experiments.

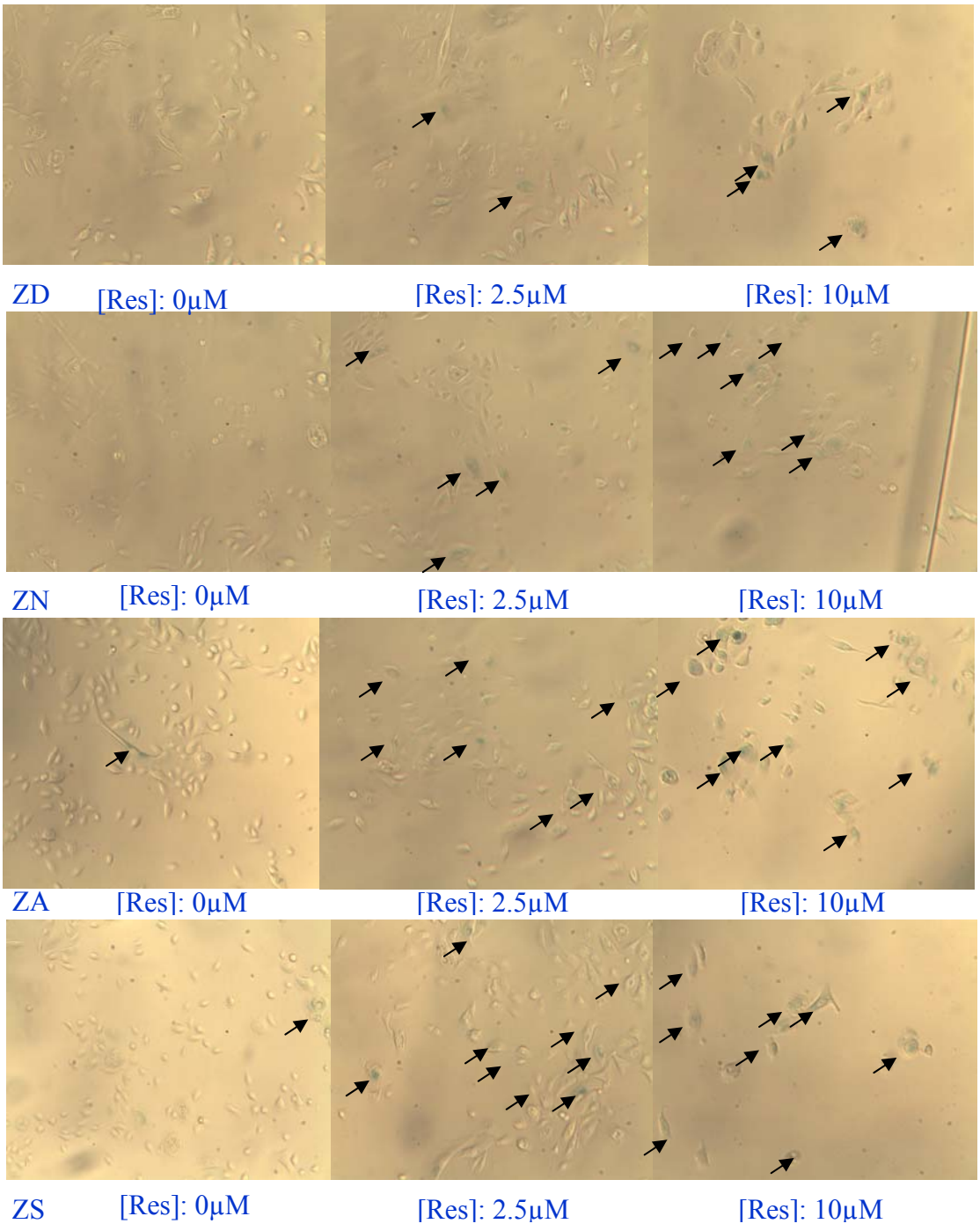


**Figure11. The effect of reserveratrol on senescence in NHPrE cells**. NHPrE cells were cultured in 24-well plates and treated by 3 levels of resveratrol (0, 2.5 and 10 μM) and 4 levels of zinc (ZD, ZN, ZA and ZS) for 3 days before being fixed and stained for β-galactosidase activity by 1mg/mL X-gal. After that, cells were layed

over with 70% glycerol and observed under a microscope at a magnification of 100X. Black arrows point to the cells that are undergoing senescence (blue color indicating x-gal stain positive). Shown image is the representative of 3 seperate experiments.

## *4.5 Discussion*

There have been a large volume of reports on the anticancer activity, antioxidant activity and pro-longevity activity of the health-promoting phytochemical, resveratrol. In the US market, resveratrol has been commercially available in the form of neutraceutical supplements. However, there are only very few studies tackling the undesired aspect of resveratrol such as its prooxidant activity. No previous study has ever used a cell-based approach to examine resveratrol supplementation in the context of nutrient interaction between phytochemicals and trace minerals, specifically, with resveratrol and zinc. Our study was designed to address this issue by using resveratrol and zinc as an example to build a feasible and efficient model to investigate the interaction between phytochemical supplements and trace mineral. NHPrE cells were selected as our cell model system because they represent normal prostate tissue and they accumulate high levels of zinc. Human hepatoblastoma HepG2 cells was used to represent the liver cells, as no normal human liver cells are commercially available.

Strong cell growth is normal for low passage normal human prostate cells but would decline drastically in high passage cells. This was demonstrated by the usage of low passage cells in the present study. NHPrE cells in the control group (R0 cells treated without resveratrol) from all zinc treatments had doubled more than 3 times at the end of 3 days of culture. Cell growth of NHPrE cells was significantly affected by the treatment of resveratrol, with more that 80% reduction with 10 μM resveratrol after 3 days of culture (**Fig. 1A**). In another study, which used the same NHPrE cells, resveratrol was found to exert no significant effect on NHPrE cell

proliferation after 3 days of incubation (Hudson et al., 2007). The very low growth rate of cell doubling (less than once in the last 2 days of a 3-day-culture) may indicate that high passage cells were used and may explain for the lack of inhibition of proliferation in resveratrol treated NHPrE cells reported by Hudson et al. (2007).

In the present study, zinc status only slightly inhibited cell growth of ZD and ZS NHPrE cells (**Fig. 1A**), which partially confirmed the results from Han (2007) in our lab that found 39% cell growth reduction in the ZD cells using exactly the same cells without resveratrol treatment. Most importantly, a slight 20% enhancement of cell growth with low dosage of resveratrol treatment (0.5 μM) was observed in the ZN cells (**Fig. 1A)**. These results suggest that low dosage of resveratrol might help improve cell proliferation and promote longevity, as reflected by the 'French paradox' in a bigger picture (Renaud and de, 1993).

The resveratrol induced dramatic increase of total cellular zinc level in NHPrE cells suggests possible intereaction between resveratrol and zinc. Since the liver is a very important organ responsible for heavy metal metabolism and storage, we wondered if the liver cells have the same response to resveratrol treatment as prostate cells do. To our surprise, the HepG2 cells used in our system to represent liver were not affected by resveratrol treatment in cell proliferation and total cellular zinc content. Zinc deficiency (ZD) exerted a modest inhibition (~20%) on the proliferation of HepG2 cells (**Fig. 2A**), just as reported by previous studies in our lab (Wong et al., 2007). In addition, intracellular zinc content in HepG2 cells did not vary much between different zinc levels ranging from 1-2.3 nmol/million cells. When we compared the intracellular zinc level between the HepG2 cells and the

NHPrE cells, we found only 3 fold difference in the control group ZNR0 (4 μM zinc, 0 μM resveratrol), but more than 10 fold difference in ZNR10 (4 μM zinc, 10 μM resveratrol) or ZSR10 (32 μM zinc, 0 μM resveratrol) group. These results again confirmed the ability of prostate cells to accumulate 10-fold higher zinc as compared to cells from other organs, e.g. liver and kidney (Suzuki et al., 1991; Costello et al., 2004) and suggested that the cell proliferation inhibition observed in resveratrol treated NHPrE cells may be related to the increase of total cellular zinc content.

Under normal circumstatnce, zinc uptake into the cells and its transport into and out of the intracellular organelles are accomplished by its transporters, which span the membranes and facilitates the movement of zinc (Eide, 2006). However, in our present study, in view of the marked increase of total intracellular zinc with the addition of resveratrol starting from 5 μM in ZD, ZN and ZA cells and 1 μM in ZS cells, the zinc uptake may not only rely on the zinc transporters that are located on the cell membrane under resveratrol treatment. Other channels may be activated by resveratrol treatment and let extra zinc in. Since resveratrol has been shown to be able to form resveratrol-Cu(II) complex with Cu(II) resulting in the reduction of Cu ions and the formation of reactive oxygen species (Ahmad et al., 2000), the similarity between the atomic structure of zinc and copper leads us to the hypothesis that resveratrol may chelate zinc to form a complex, which passes the cell membrane through a channel specific for resveratrol.

The direct way to address this hypothesis is to isolate and measure the formation of resveratrol-Zn(II) complex inside the cells, which is very difficult. However, with the usage of the zinquin and zinquin ethyl ester, we were able to

establish the existence of the complex by showing the resveratrol dose dependent quenching of the fluorescent signal emitted by the complex formed by zinquin and Zn(II) (**Fig. 4**) . These results clearly indicated that resveratrol was able to compete for Zn(II) with zinquin, leading to less Zn(II)-zinquin complex formation that emits less fluorescence. The only possible explanation for this chelating effect of resveratrol for zinc is that resveratrol is able to form complex with Zn(II), just as with Cu(II), which was accompanied by the generation of hydroxyl-radical (·OH) as established by Electron Paramagnetic Resonance (EPR) (Burkitt and Duncan, 2000). This complex forming and prooxidant property of resveratrol with copper was later established to be hydroxyl group dependent, since *trans*-stilbene without the hydroxyl groups was found inactive in Cu(II) dependent, resveratrol promoting DNA breakage (Azmi et al., 2005).

Most of the total cellular zinc detected by atomic absorption spectrophometry is very tightly bound to MT or other cellular proteins for various functions and essentially non exchangeable (Zalewski et al., 1993; Coyle et al., 1994). The other pool of intracellular zinc, which is a very small fraction, remains labile and is dynamically exchangeable with tightly bound and extracellular zinc pools. The intracellular labile zinc pool is metabolically important because it responds to zinc deprivation or supplementation by decreasing or increasing its content, respectively (Zalewski et al., 1993). As resveratrol is able to increase total intracellular zinc dramatically, the intracellular free labile zinc content may be altered by the interaction of resveratrol and zinc in our cell system. Two methods were employed to address this issue: spectrofluorimetry and fluorescent microscopic imaging. Both

methods utilized the same chemical: zinquin ethyl ester, a membrane–permeant fluorophore specific for Zn(II), and are based on the same principle: the content of labile free zinc is proportional to the fluorescent signal emitted by the complex formed by zinquin ethyl ester and Zn(II). Zinquin ethyl ester, instead of zinquin, was chosen due to an ethyl ester in place of the 6-mehtoxy group of toluenesulphonamidoquinoline in the molecular structure of zinquin ethyl ester, which facilitates its retention in living cells and enhances its fluorescent signal. With the usage of zinquin ethyl ester, we were able the identify the subcellular localization of free labile Zn(II) in extranuclear secretary granule, which is consistent with the findings of two previous reports (Smith et al., 2008; Truong-Tran et al., 2000). Results from both methods indicated that free labile zinc increases along with the extracellular zinc concentration while resveratrol tends to increase free labile zinc level in ZA and ZS group but decrease free labile zinc level in ZN and ZD group (**Fig. 5 and 7**). These findings suggest that resveratrol may enhance the effect of total intracellular zinc on intracellular free labile zinc content. As a matter of fact, the positive correlation of extracellular zinc, total cellular zinc, intracellular free zinc as well as MT mRNA (**Fig. 1B, 8, 5 and 7**) observed in the present study was also reported in a rat hepatocytes study using both methods (Coyle et al., 1994), which provided supportive evidence to the results of our study.

Since all of our experimental results favor the contention that resveratrol enhances zinc uptake by complex formation, we then asked the question: are these extra intracellular Zn(II) bound to MT, converted to free labile zinc or remained coupled with resveratrol? To answer this question, we assessed the MT transcript

levels in NHPrE cells treated with zinc and resveratrol using a highly sensitive and reproducible method, Quantitative RT-PCR. Total MT mRNA levels were found to be elevated by two-fold in ZS cells but unchanged in ZD cells in our system (**Fig. 8A**) A 13-fold induction and onefold suppression of MT-1 mRNA by 40 μM of zinc supplementation and 10μM TPEN depletion was detected by Q-RTPCR and reported by Cousins et al. (Cousins et al., 2003). To facilitate the better understanding of our result, we need to indicate that MT-1 is only part of the targets of our MT probes and primers which were designed to detect the transcript level of 8 MT isoforms: MT1H, MT-1H-like, MT-1G, MT-1L, MT-1E, MT-1A, and MT2, which are the most abundantly expressed in human mononuclear cells. In fact, another study that used the same MT probes reported only 2-fold induction of total MT mRNA level by modest oral zinc supplementation (15 mg of Zn as $ZnSO_4$ / day) for 10 days in leukocytes from human subjects (Aydemir et al., 2006). Since this result was achieved under physiological condition just as in our experimental system, it is reasonable to believe that the expression of total MT mRNA is fairly stable and does not fluctuate much regardless of zinc status under physiological condition, although some isoforms of the MT family do, such as MT-1. We also investigated the expression of metal-regulated transcription factor-1 (MTF-1) mRNA, an upstream regulator of MT, under the influence of zinc and resveratrol. To our surprise, there was little or no change in the mRNA level of MTF-1 among the treatments. However, the MTF-1 mRNA abundance in the ZD cells treated with 10 μM resveratrol was significantly higher than that in the ZN and ZS cells not treated with resveratrol, as well as the ZS cells treated with 10 μM resveratrol (**Fig. 8B**). A

3-fold induction of MTF-1 mRNA was reported in 10 μM PTEN induced zinc-deficient human THP-1 mononuclear cells (Cousins et al., 2003). Comparing the fold difference of induction, it is not difficult to note that zinc deficiency induction by medium zinc depletion is not as severe as by TPEN chelation. However, more importantly, the latter is not clinically practical and feasible.

On the other hand, the positive results of the senescence assay (**Fig. 11**) gave strong support to the hypothesis that resveratrol enhances zinc uptake by complex formation, because the formation of resveratrol-Zn(II) complex is very likely to generate reactive oxygen species that could cause DNA damage inside the cells. Senescence is one way for the cells to choose to prevent ROS-induced carcinogenesis if they do not become apoptotic, which was established by the clean apo zone in the histograms of cell cycle analysis (**Fig. 3**). The increased percentage of cells undergoing senescence along with increased zinc and resveratrol concentration may be explained by more ROS generation as the result of enhanced complex formation, as supported by the strong positive association between the percentage of senescent cells and the quantity of ROS generated within the cells (**Fig. 9**).

In sum, the results of this study suggest the possible existence of interaction between Zn(II) and resveratrol. Due to the 3 parallel hydroxy groups in the molecular structure of resveratrol, Zn(II) and resveratrol are able to form complex at a 1:1 or up to 3:2 ratio in a dynamic equilibrium depending on the availability of Zn(II) and resveratrol. In ZD and ZN cells, intracellular zinc concentration is relatively low, the resveratrol-ZN(II) complex is formed mainly as a ratio of 1:1 and

the binding capacity of resveratrol for Zn(II) is not saturated yet. However, in ZA and ZS cells, the chelating capacity of resveratrol for Zn(II) has been saturated due to increased availability of Zn(II). When the complexes formed by Zn(II) and resveratrol pass through cell membrane and remain in the coupled form in the senescent, metabolically inactive cells, the unsaturated resveratrol under ZD and ZN condition keeps chelating the Zn(II) from the free labile zinc pool, which causes a decreasing trend of labile free zinc. On the contrary, in ZA and ZS cells with an elevated level of total cellular zinc, a small portion of Zn(II) bound to the saturated resveratrol starts to dissociate from the complex to join the free labile zinc pool, resulting in a modest increase of free labile zinc in the presence of a dramatic increase of total cellular zinc (**Fig. 12**).

## *4.6 Conclusion*

In conclusion, resvertrol significantly inhibits the growth of NHPrE cells through induction of cell cycle arrest at G2/M stage as well as senescence, but has no effect on the proliferation of HepG2 cells. In NHPrE cells, the intracellular total zinc enhancement effect of resveratrol was established to be through possible complex formation with Zn(II) and was accompanied by ROS generation. However, resveratrol treatment exerted little or no effect on the mRNA abundance of total MT mRNA and MTF-1 mRNA. Moreover, resveratrol tended to decrease intracellular free labile zinc of NHPrE cells cultured in normal (ZN) or low zinc (ZD) environment but increase intracellular free labile zinc of NHPrE cells cultured in high zinc (ZA) and (ZS) environment. All of the results can be explained by the dynamic equilibrium theory (**Fig. 12**) described in the discussion section.

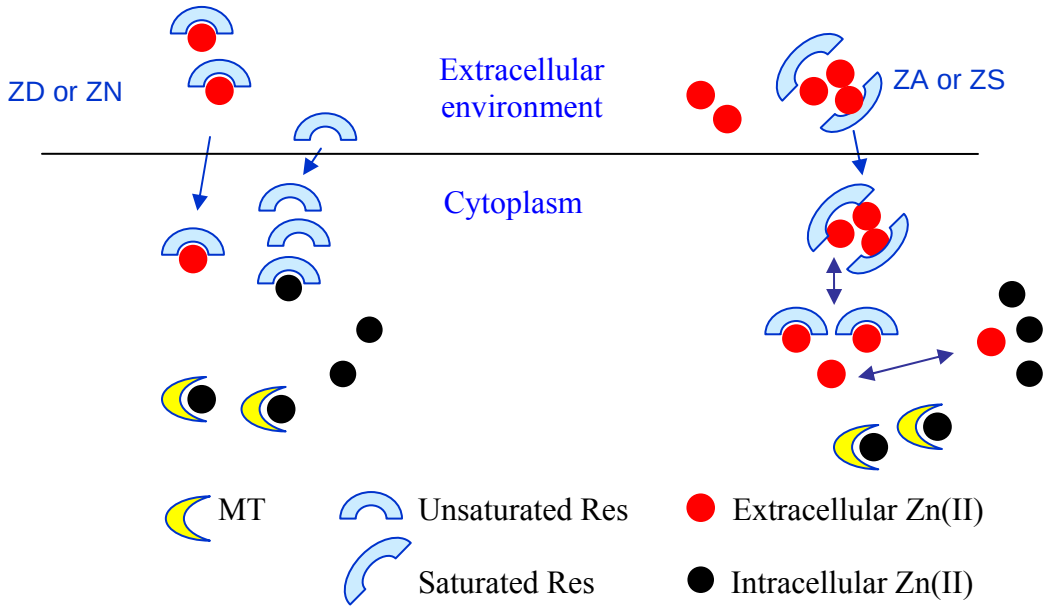


**Figure 12. Proposed dynamic equilibrium theory for the interaction of resveratrol and zinc in NHPrE cells.** Whithout zinc supplementation (ZD and ZN), resveratrol binds Zn(II) tightly due to lower zinc availability, enters the NHPrE cells as a complex and remains coupled with Zn(II) intracellularly. On the contrary, with zinc supplementation (ZA and ZS), resveartrol's binding capacity for zinc is mitigated by increased zinc availability. As more and more resveratrol-Zn(II) complexes enter the NHPrE cells, a small portion of Zn(II) dissociates from the complex and joins the intracellular labile free zinc pool. The dissociation of resvertrol-Zn(II) complex is a reversible process under the control of dynamic balance.

## *4.7 References*

**Ahmad, A., Farhan, A. S., Singh, S. & Hadi, S. M. (2000).** DNA breakage by resveratrol and Cu(II): reaction mechanism and bacteriophage inactivation. *Cancer Lett* **154,** 29-37.

**Aydemir, T. B., Blanchard, R. K. & Cousins, R. J. (2006).** Zinc supplementation of young men alters metallothionein, zinc transporter, and cytokine gene expression in leukocyte populations. *Proc Natl Acad Sci U S A* **103,** 1699-1704.

**Azmi, A. S., Bhat, S. H. & Hadi, S. M. (2005).** Resveratrol-Cu(II) induced DNA breakage in human peripheral lymphocytes: implications for anticancer properties. *FEBS Lett* **579,** 3131-3135.

**Azmi, A. S., Bhat, S. H., Hanif, S. & Hadi, S. M. (2006).** Plant polyphenols mobilize endogenous copper in human peripheral lymphocytes leading to oxidative DNA breakage: a putative mechanism for anticancer properties. *FEBS Lett* **580,** 533-538.

**Belguendouz, L., Fremont, L. & Linard, A. (1997).** Resveratrol inhibits metal ion-dependent and independent peroxidation of porcine low-density lipoproteins. *Biochem Pharmacol* **53,** 1347-1355.

**Burkitt, M. J. & Duncan, J. (2000).** Effects of trans-resveratrol on copper-dependent hydroxyl-radical formation and DNA damage: evidence for hydroxyl-radical scavenging and a novel, glutathione-sparing mechanism of action. *Arch Biochem Biophys* **381,** 253-263.

**Costello, L. C., Feng, P., Milon, B., Tan, M. & Franklin, R. B. (2004).** Role of zinc in the pathogenesis and treatment of prostate cancer: critical issues to resolve. *Prostate Cancer Prostatic Dis* **7,** 111-117.

**Cousins, R. J., Blanchard, R. K., Popp, M. P., Liu, L., Cao, J., Moore, J. B. & Green, C. L. (2003).** A global view of the selectivity of zinc deprivation and excess on genes expressed in human THP-1 mononuclear cells. *Proc Natl Acad Sci U S A* **100,** 6952-6957.

**Coyle, P., Zalewski, P. D., Philcox, J. C., Forbes, I. J., Ward, A. D., Lincoln, S. F., Mahadevan, I. & Rofe, A. M. (1994).** Measurement of zinc in hepatocytes by using

a fluorescent probe, zinquin: relationship to metallothionein and intracellular zinc. *Biochem J* **303 ( Pt 3),** 781-786.

**Eide, D. J. (2006).** Zinc transporters and the cellular trafficking of zinc. *Biochim Biophys Acta* **1763,** 711-722.

**Fanzo, J. C., Reaves, S. K., Cui, L., Zhu, L., Wu, J. Y., Wang, Y. R. & Lei, K. Y. (2001).** Zinc status affects p53, gadd45, and c-fos expression and caspase-3 activity in human bronchial epithelial cells. *Am J Physiol Cell Physiol* **281,** C751-C757.

**Hudson, T. S., Hartle, D. K., Hursting, S. D., Nunez, N. P., Wang, T. T., Young, H. A., Arany, P. & Green, J. E. (2007).** Inhibition of prostate cancer growth by muscadine grape skin extract and resveratrol through distinct mechanisms. *Cancer Res* **67,** 8396-8405.

**Jang, M., Cai, L., Udeani, G. O. et al. (1997).** Cancer chemopreventive activity of resveratrol, a natural product derived from grapes. *Science* **275,** 218-220.

**Kavas, G. O., ribal-Kocaturk, P. & Buyukkagnici, D. I. (2007).** Resveratrol: is there any effect on healthy subject? *Biol Trace Elem Res* **118,** 250-254.

**Mukherjee, A. K., Basu, S., Sarkar, N. & Ghosh, A. C. (2001).** Advances in cancer therapy with plant based natural products. *Curr Med Chem* **8,** 1467-1486.

**Reaves, S. K., Fanzo, J. C., Arima, K., Wu, J. Y., Wang, Y. R. & Lei, K. Y. (2000).** Expression of the p53 tumor suppressor gene is up-regulated by depletion of intracellular zinc in HepG2 cells. *J Nutr* **130,** 1688-1694.

**Renaud, S. & de, L. M. (1993).** The French paradox: dietary factors and cigarette smoking-related health risks. *Ann N Y Acad Sci* **686,** 299-309.

**Smith, P. J., Wiltshire, M., Furon, E., Beattie, J. H. & Errington, R. J. (2008).** Impact of overexpression of metallothionein-1 on cell cycle progression and zinc toxicity. *Am J Physiol Cell Physiol*.

**Suzuki, T., Umeyama, T., Ohma, C., Yamanaka, H., Suzuki, K., Nakajima, K. & Kimura, M. (1991).** Immunohistochemical study of metallothionein in normal and benign prostatic hyperplasia of human prostate. *Prostate* **19,** 35-42.

**Truong-Tran, A. Q., Ruffin, R. E. & Zalewski, P. D. (2000).** Visualization of labile zinc and its role in apoptosis of primary airway epithelial cells and cell lines. *Am J Physiol Lung Cell Mol Physiol* **279,** L1172-L1183.

**Uenobe, F., Nakamura, S. & Miyazawa, M. (1997).** Antimutagenic effect of resveratrol against Trp-P-1. *Mutat Res* **373,** 197-200.

**Wong, S. H., Zhao, Y., Schoene, N. W., Han, C. T., Shih, R. S. & Lei, K. Y. (2007).** Zinc deficiency depresses p21 gene expression: Inhibition of cell cycle progression is independent of the decrease in p21 protein level in HepG2 cells. *Am J Physiol Cell Physiol* **.**.

**Zalewski, P. D., Forbes, I. J. & Betts, W. H. (1993).** Correlation of apoptosis with change in intracellular labile Zn(II) using zinquin [(2-methyl-8-p-toluenesulphonamido-6-quinolyloxy)acetic acid], a new specific fluorescent probe for Zn(II). *Biochem J* **296 ( Pt 2),** 403-408.